AN ABSTRACT OF THE THESIS OF

Dawn Marie McDaniel for the degree of Master of Science in Chemistry presented on December 13, 1983.

Title: Chemical Analysis for Boron in Nuclear Reactor Coolant Water

Abstract approved: Signature redacted for privacy.
John C. Westall

Two chemical methods for the determination of boron in aqueous solution have been investigated: 1) a potentiometric titration of a boron/mannitol complex, and 2) a spectrophotometric determination of a boron/azomethine H complex.

Potentiometric titrations are a rapid, simple, and reliable method for the determination of boron in aqueous samples. Because boric acid is a weak acid, the endpoint of the titration is difficult to detect. Mannitol is added to solutions of boric acid to improve the clarity of the titration endpoint. The conditions of the boric acid/mannitol titration have been investigated to develop an understanding of all the equilibria in the system.

Azomethine H has been employed in the quantitative determination of boron in aqueous samples. Equilibrated aqueous solutions of azomethine, A, and boron, B, contain species of stoichiometry A, B, A_2, AB and A_2B. The stability constants and molar absorptivities of the

boron/azomethine complexes have been determined. They are: $K_{AB} = 7.9$, $\beta_{A_2B} = 1.2 \times 10^5$, $\varepsilon_{AB} = 6.7 \times 10^3$ A.U. cm^{-1} M^{-1}, $\varepsilon_{A_2B} = 2.0 \times 10^4$ A.U. $cm^{-1} M^{-1}$. The formation of the AB and A_2B complexes have been described with the following rate laws

$$\frac{d[AB]}{dt} = k_{f1}\,[A][B] - k_{b1}\,[AB]$$

$$\frac{d[A_2B]}{dt} = k_{f2}\,[A]^2[B] - k_{b2}[A_2B]$$

Values for the forward rate constants have been determined from interpretation of initial rate data $k_{f1} = 1.8 \times 10^{-3}$ s^{-1} M^{-1}, $k_{f2} = 4.7$ s^{-1} M^{-2}. Values for the backward rate constants have been determined from the equilibrium stability constants; $k_{b1} = 2.3 \times 10^{-4} s^{-1}$ $k_{b2} = 4.0 \times 10^{-5}$ s^{-1}. It is shown that the determined constants represent the data very well over the concentration range considered. The applicability of three different modes of analysis: stopped flow, continuous flow, and flow injection is discussed.

Both the potentiometric titration method and the spectrophotometric method have been evaluated for determination of boron concentration in nuclear reactor coolant water. The purpose of the evaluation was to test the chemical methods and associated equipment under experimental conditions representative of those in nuclear power plants.

Chemical Analysis for Boron in Nuclear Reactor Coolant Water

by

Dawn Marie McDaniel

A THESIS

submitted to

Oregon State University

in partial fulfillment of
the requirements for the
degree of

Master of Science

Completed December 13, 1983

Commencement June 1984

APPROVED:

Signature redacted for privacy.

Professor of Chemistry in charge of major

Signature redacted for privacy.

Chairman of Department of Chemistry

Signature redacted for privacy.

Dean of Graduate School

Date thesis is presented December 13, 1983

Typed by A β S Wordprocessing for Dawn Marie McDaniel

ACKNOWLEDGEMENT

I wish to acknowledge the advice and help received during my graduate career from my major professor, Dr. J.C. Westall. In addition, I wish to acknowledge the advice received from other faculty members especially Dr. J.D. Ingle, and from fellow graduate students, whose aid and suggestions were invaluable. Finally, I wish to recognize the grant received from the Electric Power Research Institute, the summer support received from the Tartar Fellowship, and the grant received from the Oregon State University Computer Center.

DEDICATION

To my family without whose support and aid I could not have accomplished this. In particular to the joys of my life, my husband Dave and my cat Traci.

TABLE OF CONTENTS

LIST OF FIGURES

Figure

LIST OF TABLES

CHEMICAL ANALYSIS FOR BORON IN NUCLEAR REACTOR COOLANT WATER

INTRODUCTION

Two chemical methods for the determination of boron in nuclear reactor coolant water have been investigated and are presented: 1) the potentiometric titration of a boron/mannitol complex, and 2) the spectrophotometric determination of a boron/azomethine H complex.

Potentiometric titrations can provide rapid and reliable results. Mannitol is used to improve the clarity of the endpoint of a titration of boric acid. The reactions of borate and mannitol in aqueous solution have been interpreted in terms of 1:1, 2:1, and 1:2 complexes in various degrees of protonation (1-3). The values of the stability constants of these complexes are available (4). The goal of the studies presented here was to develop a complete understanding of all the equilibria in the system, and the stoichiometry of all of the species and their stability constants.

The spectrophometric method using azomethine H as the color producing reagent has been previously developed for use in the 0.10-10 mg/L concentration range (5). The studies presented here focus on determining the stability constants and molar absorptivities for each species and

the rate constants for each chemical reaction. Determination of these values enabled calculation of the absorbance signal for any set of boric acid concentration, azomethine H concentration, and time conditions. A flow system has been designed and tested for the determination of boric acid concentration. The flow system was under the control of a microprocessor to increase the ease and accuracy of the analysis.

Both the potentiometric titration method and the spectrophotometric method have been evaluated for determination of boron concentration in nuclear reactor coolant water. The research in this thesis is related to a project, the purpose of which was to test the chemical methods and associated equipment under experimental conditions representative of those in nuclear power plants. A chemical method must work satisfactorily under controlled laboratory conditions before it can be considered for application in process monitoring. The criteria which were considered in the evaulation of the chemical methods, plus a brief review of the reactor operations are provided in Appendix A.

The results in this thesis are divided into two sections, those pertaining to potentiometry and those pertaining to spectrophotometry. Each section is developed independently with an introduction, theoretical,

experimental, and discussion section. A general conclusion covering both the potentiometric and spectrophotometric experiments as they apply to the monitoring of boron in nuclear reactor coolant water is included in the final section of this thesis.

POTENTIOMETRIC TITRATION

Introduction

Boric acid is a weak acid (pK_a=9). When a solution of a weak acid is titrated, it is often difficult to observe a titration endpoint at low acid concentrations. In the mid 1800's it was reported that the addition of sugars or other polyhydroxyl compounds caused boric acid solutions to become more acidic. In the years following many workers tested series of compounds and determined that the complexes formed between boric acid and the polyhydroxyl compounds were more acidic than boric acid (lower pK_a values). When a solution of these complexes is titrated, the titration endpoint is more distinct, allowing for accurate titrations to be performed at lower boric acid concentrations. Mannitol ($C_6H_{14}O_6$) is a readily available polyhydroxyl compound. Titration of the boric acid/mannitol complex is a common method for the determination of boron. In solution mannitol reacts with borate to yield complexes with borate to mannitol ratios of 1:1, 2:1, and 1:2, in various degrees of protonation (1-3). Values of the formation constants of these complexes are available (4).

Initial studies focused on developing a complete understanding of all the equilibria in the system, and the

stoichiometry of all of the species and their stability constants. In each case, after the stoichiometry and equilibria were confirmed, a theoretical potentiometric titration curve was computed for comparison with the experimental data.

Final potentiometry studies focused on the application of the method for the determination of boron concentration. The method of analysis currently employed by the nuclear industry was evaluated and found to be suitable for determining boric acid in the range specified.

Theory

In the following sections the theories applied in the interpretation of the experimental data are discussed.

Potentiometry

The theory behind potentiometry can be found in numerous texts (6-9). An attempt is made here to describe briefly the principles according to which the ion selective electrode functions.

In potentiometry the electrical potential which develops between two reversible electrodes is measured. One electrode is selectively sensitive to the species of interest and the other is at a fixed potential, providing

a stable reproducible reference potential. The potential developed between the two electrodes is related to the concentration of the ion x (C_x), to which the indicator electrode is selective, by a form of the Nernst equation:

$$E = E^o + s \log(C_x) \qquad (1)$$

where E is the measured cell potential, and E^o and s are the calibration constants which ideally remain constant with time. One can measure a series of standard samples for which C_x is known and determine the value for E^o and s for a particular electrode pair.

A glass membrane indicating electrode selective for the hydrogen ion, H^+, with an Ag/AgCl internal reference and a double junction Ag/AgCl external reference electrode were employed in this study. The electrochemical cell can be represented by:

external reference electrode		sample	internal reference electrode
$Ag;AgCl\|K^+,Cl^-$	$\|K^+,NO_3^-\|$	H^+	$\|H^+,Cl^-\|AgCl;Ag$
	↖ liquid junctions ↗		↑ ion-selective membrane

In the schematic representation above, each vertical line indicates an electrode-solution interface across which an electrical potential exists. The potential indicated by a voltmeter, E_{cell}, is the sum of these potentials:

$$E_{cell} = E_{int} + E_m + E_{1j} - E_{ext} \quad (2)$$

where each of the potentials is given by (symbols described in Table I):

- internal reference electrode potential:

$$E_{int} = E^{\circ}_{AgCl/Ag} - \frac{RT}{F} \ln (a_{Cl^-(internal)}) \quad (3)$$

- ion-selective membrane potential:

$$E_m = \frac{RT}{F} \ln \frac{(a_{H^+}\ (sample))}{(a_{H^+}\ (internal))} \quad (4)$$

- liquid junction potentials,
  approximated by a form of the Henderson equation (6):

$$E_{1j} = \frac{RT}{F} \frac{(U_1 - V_1) - (U_2 - V_2)}{(U'_1 + V'_1) - (U'_2 + V'_2)} \ln\left(\frac{U'_1 + V'_1}{U'_2 + V'_2}\right) \quad (5)$$

where the subscripts 1 and 2 indicate the right and left boundary solutions respectively.

$$U = \Sigma\ C_i \lambda^{\circ}_i, \text{ cations}$$

$$V = \Sigma\ C_i \lambda^{\circ}_i, \text{ anions}$$

$$U' = \Sigma\ C_i \lambda^{\circ}_i |z_i|, \text{ cations}$$

$$V' = \Sigma\ C_i \lambda^{\circ}_i |z_i|, \text{ anions}$$

E_{1j} is a function of the concentration and the mobilities

Table I. Description of Symbols.

Symbol	Units	Description
R	8.314 V C K^{-1} mol^{-1}	gas constant
F	96,487 C mol^{-1}	Faraday constant
T	K	absolute temperature
E^o	V	standard potential of a particular electrode, E^o is a function of temperature $E^o_{AgCl/Ag}$ = 0.222 V at 298K
a_i	M	activity of the ion i
C_i	M	concentration of the ion i
λ^o	$cm^2 \Omega^{-1} eq^{-1}$	mobilities of the ion at infinite dilution
z_i		charge of the ion i

of ions in both bulk solutions. In Equation 5 the ionic mobilities have been taken as equal to the mobilities at infinite dilution. In practice the liquid junction potential is on the order of two millivolts for these solutions.

- external reference electrode potential:

$$E_{ext} = E^{o}_{Ag/AgCl} - \frac{RT}{F} \ln (a_{Cl^-}\ (external)) \qquad (6)$$

Equation 1 can be rewritten as:

$$E_{cell} = E^{o'}_{cell} + s \log a_{H^+}\ (sample) \qquad (7)$$

where the theoretical expressions for the calibration constants $E^{o'}_{cell}$ and s are:

$$E^{o'}_{cell} = E_{int} + E_{lj} - E_{ext} - \frac{RT}{F} \ln a_{H^+}(internal) \qquad (8)$$

$$s = \frac{RT}{F} \ln 10 = 0.05916 \text{ volts at } 25^{o}C \qquad (9)$$

The empirical calibration, Equation 1, is similar to Equation 7 with C_x substituted for a_{H^+}. The activity is the effective concentration. The relationship between activity and concentration is given by

$$a_i = \gamma_i C_i \qquad (10)$$

where γ_i is the activity coefficient. The activity coefficient can be estimated from the Debye-Hückel expression (6):

$$\log \gamma_i = \frac{-Az_i^2(I)^{1/2}}{1 + Ba(I)^{1/2}} \qquad (11)$$

where $I = 1/2 \sum z_i^2 C_i$ (12)

i ; all ions i in the solution

z_i = the charge of the ion i

C_i = the concentration of the ion i

A = 0.5115 at 25°C

B = 0.3291 at 25°C

a = ion size parameter (set equal to 9 for all ions)

Any electrode responds to the activity of the ion to which it is selective. The glass electrode responds to a_{H^+}. The pH is defined as $-\log a_{H^+}$. From Equation 8 it is seen that the term $E^{\circ'}_{cell}$ includes the potentials of the reference electrode and of the liquid junctions between the reference half cell and the sample solution. The value of $E^{\circ'}_{cell}$ may change for one of the following reasons:

(i) intrusion of sample solution into the reference half cell, diluting the reference electrolyte;

(ii) clogging of the porous frit of the liquid junction of the reference electrode creating erroneous liquid junction potentials;

(iii) mechanical damage to the glass membrane;

(iv) particularly high liquid junction potentials

developed on account of highly concentrated sample solutions;

(v) changes in solution temperature.

The first three reasons are primarily mechanical in nature and the effects can be minimized with proper maintenance of the electrodes. The last two effects can be minimized by knowledge of the sample and proper control over analysis conditions. The theoretical response slope from Equation 9 is 59.16 mV at 25°C, but in practice may be 2 to 3 mV less than the theoretical value. The slope varies with the condition of the active surface of the glass electrode and temperature.

A potentiometric titration involves sequential additions of the titrant to the sample solution. The cell potential is measured and recorded after each addition. Sufficient time must be allowed for the attainment of equilibrium after each addition of titrant. The titration is ordinarily carried well beyond the endpoint by additions of excess titrant.

Two methods for endpoint detection have been considered: (i) the sample solution is titrated to a fixed potential, and (ii) the first or second derivative is taken in the region of the steeply changing portion of the curve to determine the location of the inflection point. The first method requires reproducible endpoint

potentials for all solutions within the necessary range. The latter method requires a relatively noise free signal.

Chemical Equilibrium

Graphical representation of chemical information has found wide application in the interpretation of chemical equilibrium. From a graph, quick insight into the chemical equilibria can be gained. These insights include: how the distribution of all species in the system change when the concentration of one species is changed, which species in the system are predominant in the material balance equations, and which species in the system are negligible. The graph used frequently to illustrate chemical equilibria is obtained by plotting the logarithm of the concentration of every species against the logarithm of the concentration of the hydrogen ion. Such a diagram is called a master variable diagram.

The chemical equilibrium problems considered in this section have been solved with the Basic computer program MICROQL (10). Chemical equilibrium problems are expressed mathematically in the following way. Species are defined as every chemical entity to be considered in the problem. A set of components is defined in such a way that every species can be written as the product of a reaction

involving only the components. No component can be written as the product of a reaction involving other components. While the set of components is not unique, once it has been defined the representation of the species in terms of components is unique. Associated with each component is a material balance equation

$$Y_j = \sum_i a_{ij} C_i - T_j \qquad (13)$$

and with each species is a mass law equation

$$\log C_i = \log K_i + \sum_j a_{ij} \log X_j \qquad (15)$$

where

i ; a species i in solution

j ; a component j in solution

C_i = concentration of species i

K_i = stability constant of species i

T_j = total concentration of component j

a_{ij} = stoichiometry of species i in terms of component j

X_j = equilibrium concentration of component j

Y_j = the error, or remainder in the material balance equation for component j

These two sets of equations define the chemical equilibrium problem. To solve the problem the Newton-Raphson method, an iterative technique, is used. First,

an initial estimate of the concentration of each component is made, and the concentration of each species is computed. Second, the error in the material balance equation is computed. The value of each equilibrium component concentration is improved such that the error, Y_j, decreases. The problem is solved when $Y_j = 0$. Once the equilibrium concentration of each component is determined, the free concentrations of each species is calculated.

The procedure above calculates the free concentration of each species from the total concentration of each component. The computing of the equilibrium speciation of a solution at a fixed pH requires a small modification to allow for calculation of the total hydrogen ion concentration from the free hydrogen ion concentration.

In the previous discussion activity coefficients are assumed to be constant. This assumption is valid in very dilute electrolyte solutions or in solutions with a constant ionic strength. In the potentiometric titration being considered the assumption of constant activity coefficients is not valid. The changing ionic strength affects the apparent stability constant. This conditional stability constant can be calculated from

$$\log K_i = \log K^o_i + \log G_i \qquad (15)$$

where G_i is a correction factor defined by:

$$\log G_i = \sum_j a_{ij} \log \gamma_j - \log \gamma_i \qquad (16)$$

j ; a component j in the solution

i ; a species i in the solution

K_i^o = the stability constant of species i at infinite dilution

K_i = the apparent stability constant of species i dependent upon the ionic strength of the solution

γ = the activity coefficient calculated from Equation 11.

The value calculated for K_i is used as the stability constant of species i in computing the equilibrium concentration of species i.

Boric Acid/Borate Equilibrium System

Before an attempt is made to discuss the interaction of mannitol with boric acid, it is useful to consider the boric acid/borate equilibria by itself. Boric acid is a weak acid. In solution boric acid is in equilibrium with the borate anion and many polyborate species.

The question is, at what concentration do the polyborate species become significant. The species which have been considered in the equilibrium problem and the literature values of their stability constants are

provided in Table II. MICROQL was used to solve the equilibrium problem. The results are presented as master variable diagrams in Figures 1-4. The log of the concentration of each species is plotted versus the log of the hydrogen ion concentration log C_{H^+}, for solutions of 0.0010, 0.010, 0.10, and 0.93 M total borate, TB. (0.93 M is the solubility of boric acid at 25°C) (11). The diagrams illustrate the relative concentration change of the different species at varying log C_{H^+} values. Of major interest is the relative concentrations of the polyborate species with respect to the monomeric borate and boric acid species. The maximum concentration for the polymeric species occurs around log C_{H^+} = -9. This is not surprising because there is the largest amount of both borate and boric acid present. As the total borate concentration increases, the equilibrium concentration of the polyborate species increase. In the 0.0010 M solution the polymeric concentrations are always five orders of magnitude less than the monomeric species. At the maximum in the 0.010 M solution three orders of magnitude difference is observed, and one order of magnitude difference in the 0.10 M solution. High concentrations of all borate species are expected at the solubility limit around a log C_{H^+} of -9. From these diagrams, inclusion of all species is necessary at total borate concentrations

Table II. Components and Species Considered in the $B(OH)_3/B(OH)_4^-$ Equilibrium Problem (4).

Components: $B(OH)_4^-$ and H^+

Reaction	Species	Symbol	log K[c]
$B(OH)_4^-$	$= B(OH)_4^-$	B^-	
H^+	$= H^+$	H^+	
$-H^+ + H_2O$	$= OH^-$	OH^-	-14.00[a]
$3\ B(OH)_4^- + 2\ H^+ - 5\ H_2O$	$= B_3O_3(OH)_4^-$	$H_2B_3^-$	20.07[b]
$3\ B(OH)_4^- + H^+ - 4\ H_2O$	$= B_3O_3(OH)_5^{2-}$	HB_3^{2-}	10.4[b]
$4\ B(OH)_4^- + 2\ H^+ - 7\ H_2O$	$= B_4O_5(OH)_4^{2-}$	$H_2B_4^{2-}$	20.9[b]
$5\ B(OH)_4^- + 4\ H^+ - 10\ H_2O$	$= B_5O_6(OH)_4^-$	$H_5B_6^-$	38.2[b]
$B(OH)_4^- + H^+ - H_2O$	$= B(OH)_3$	HB	8.97[b]

[a] T = 298K, I = 0.0. [b] T = 298K, I = 3.0.

[c] For computations at I = 3.0 M the constants were used as shown in the table. For computations at other ionic strengths, Equation 11 and 15 were used to correct the constants for the activity coefficients, although it is recognized that use of Equation 11 is unjustified up to I = 3.0 M.

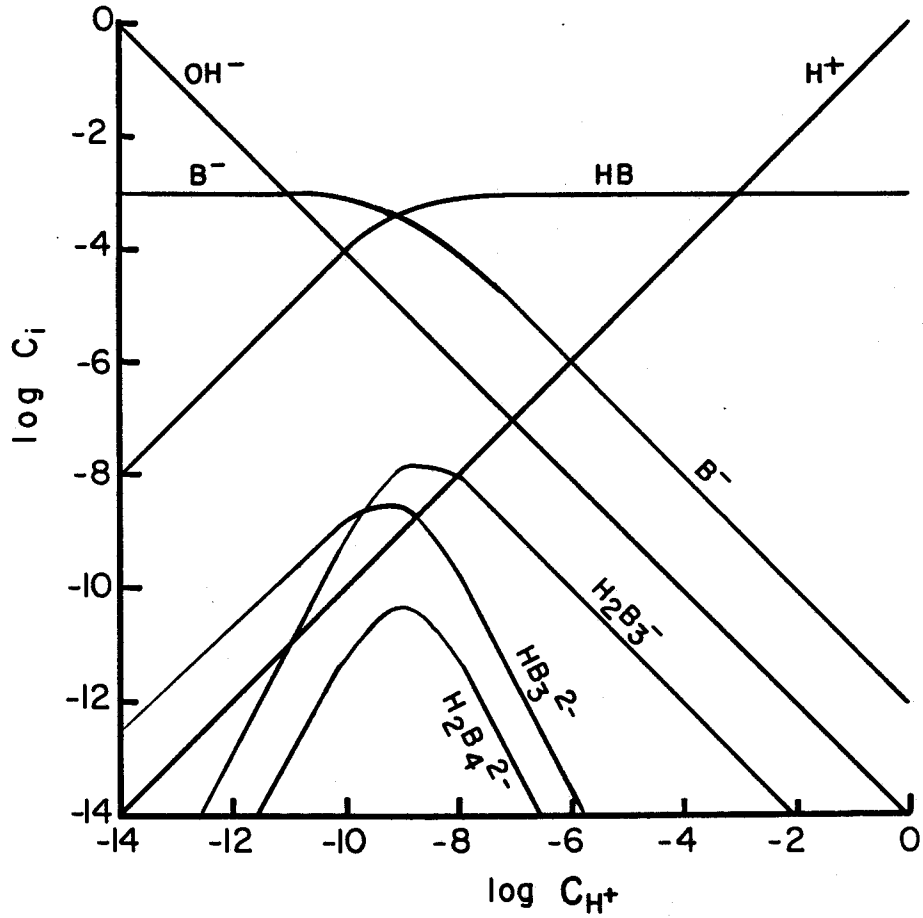

Figure 1. Master Variable Diagram for the $B(OH)_3$ System with TB = 0.0010 M. T = 25°C, I = 3.0. The equilibrium system is defined in Table II.

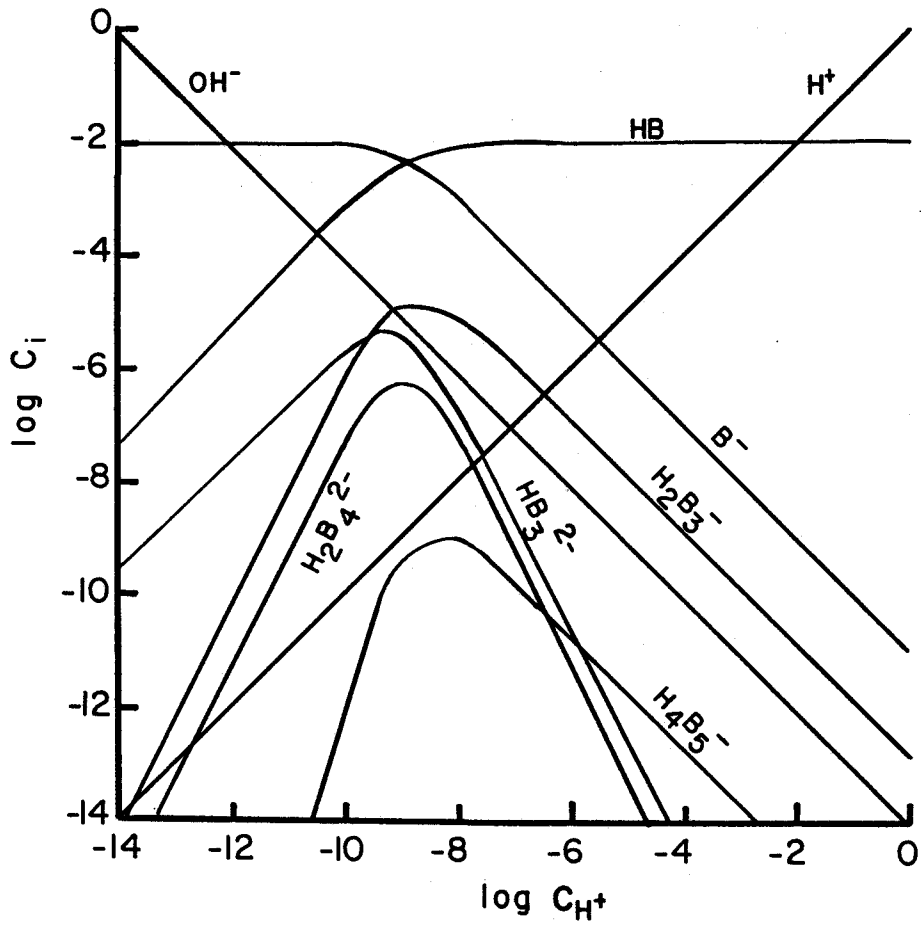

Figure 2. Master Variable Diagram for the $B(OH)_3$ System with TB = 0.010 M. T = 25°C, I = 3.0. The equilibrium system is defined in Table II.

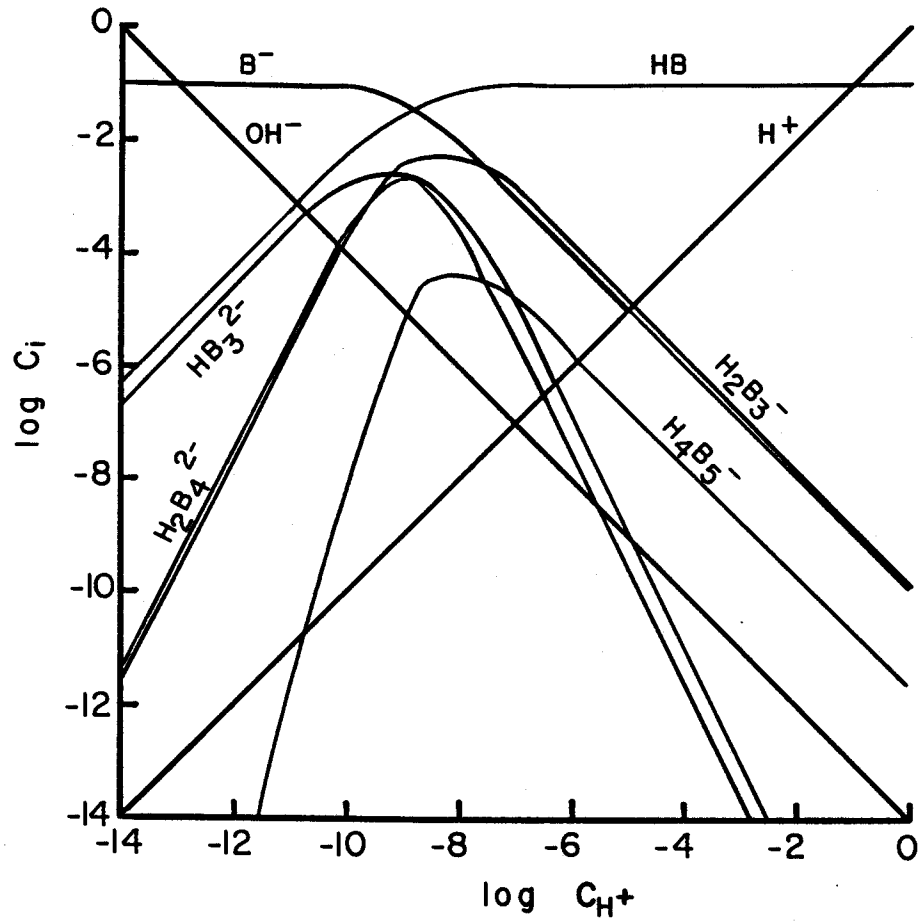

Figure 3. Master Variable Diagram for the $B(OH)_3$ System with TB = 0.10 M. T = 25°C, I = 3.0. The equilibrium system is defined in Table II.

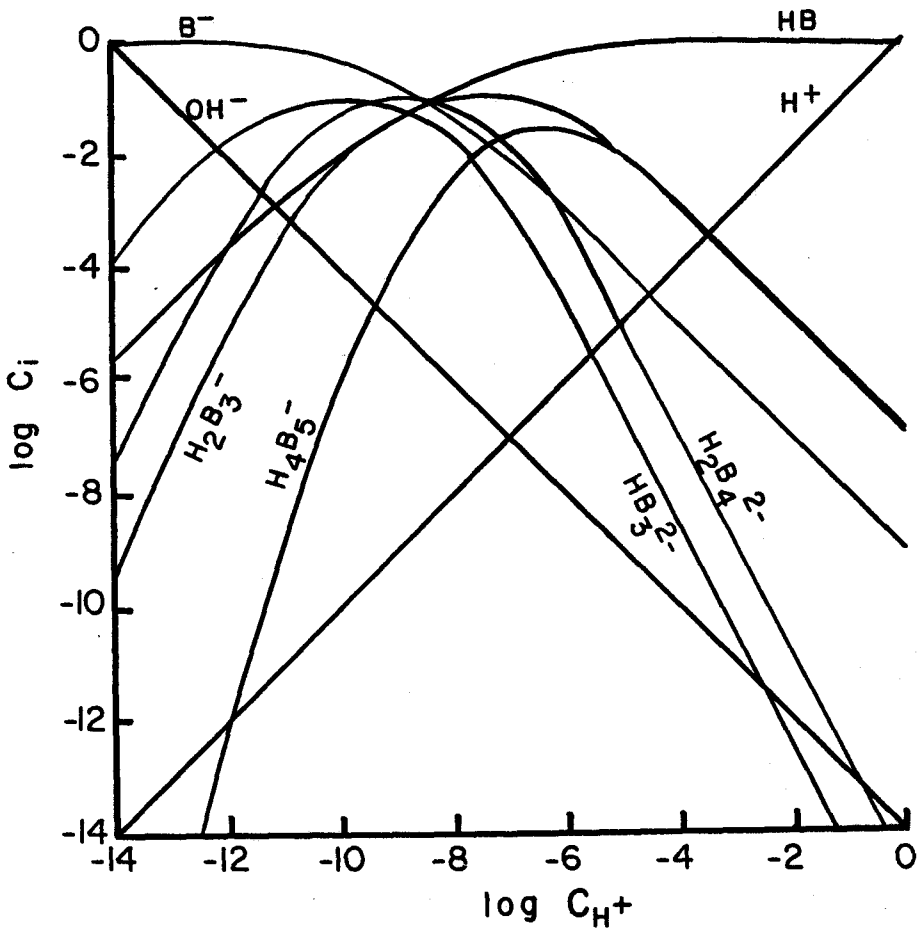

Figure 4. Master Variable Diagram for the $B(OH)_3$ System with TB = 0.93 M. T = 25°C, I = 3.0. The equilibrium system is defined in Table II.

greater than 0.01 M for equilibrium calculations. For consistency of calculating, however, all species have been included at all concentrations.

Figure 5 provides the computed titration curves, plotted as the log of the hydrogen ion activity versus the fraction titrated, of successively dilute boric acid solutions. The fraction titrated represents moles of base added per mole of acid. As the solution becomes less concentrated the titration endpoint becomes less distinct, until the titration curve appears as a straight line. The titration curves indicate that solution concentrations greater than 0.10M $B(OH)_3$ are necessary for observance of an endpoint.

Boric Acid/Mannitol Equilibrium System

Mannitol is used to improve the clarity of the endpoint of a titration of boric acid. Mannitol is readily available, inexpensive, and the stability constants for its complexes with boric acid and borate are available (1). The reaction of borate and mannitol in aqueous solution has been interpreted in terms of 1:1, 2:1, and 1:2 complexes (Table III) in various degrees of protonation.

The question is, what is the effect of increasing mannitol concentrations on the boric acid equilibria. The

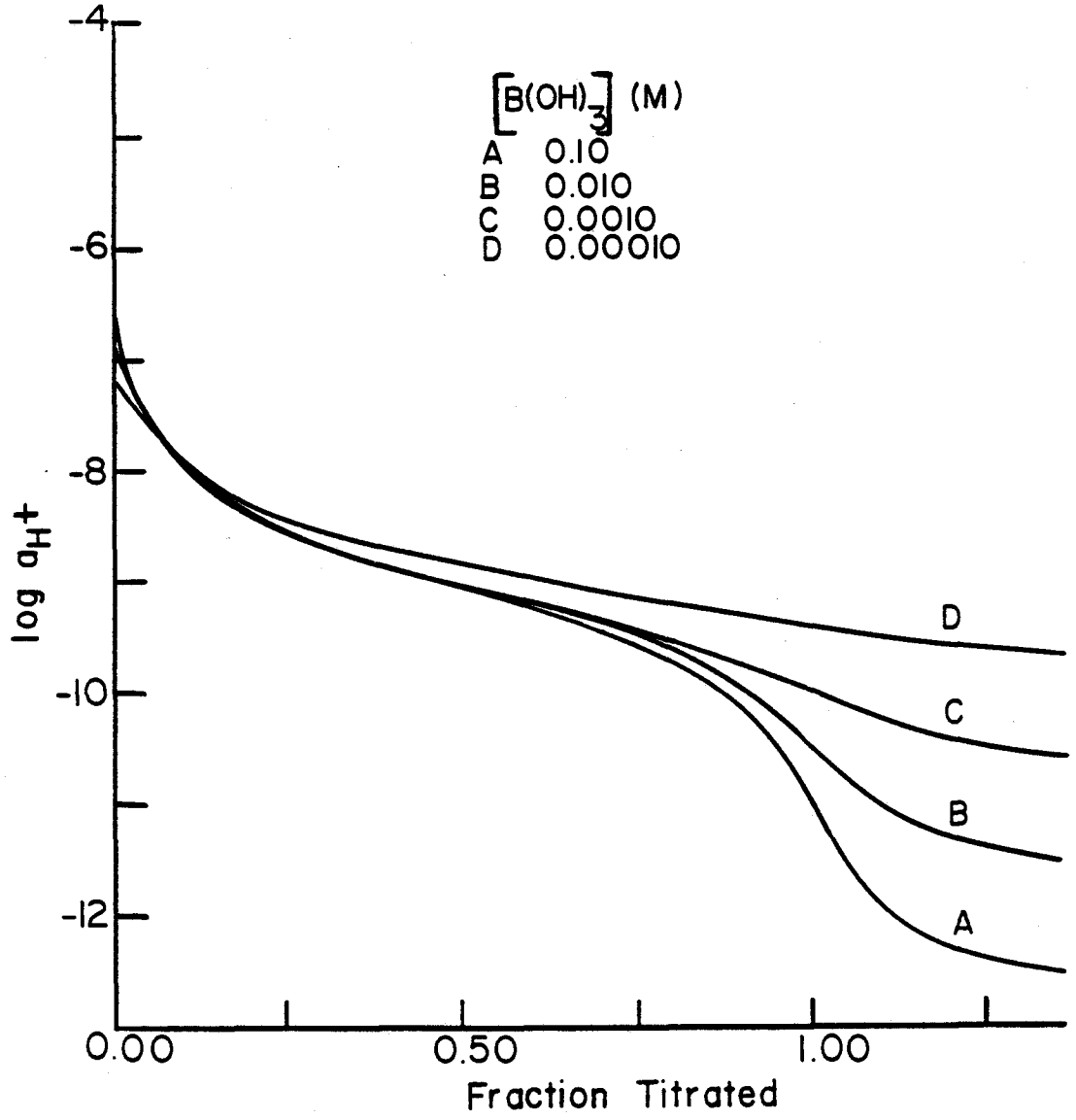

Figure 5. Theoretical Titration of $B(OH)_3$ with LiOH. T = 25°C, I = 3.0. Fraction titrated represents moles of base added per mole of acid. The equilibrium system is defined in Table II.

Table III. Reactions and Configurations of the Borate/Mannitol Complexes.

$$x\ B(OH)_4^- + y\ C_6H_{14}O_6 \rightarrow complex^{-x} + z\ H_2O$$

Ratio	x	y	z	Configuration	
1:1	1	1	2	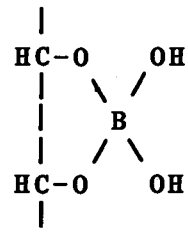	-
1:2	1	2	4	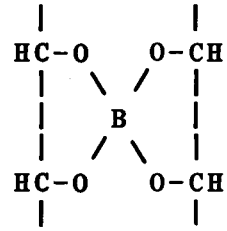	-
2:1	2	1	4	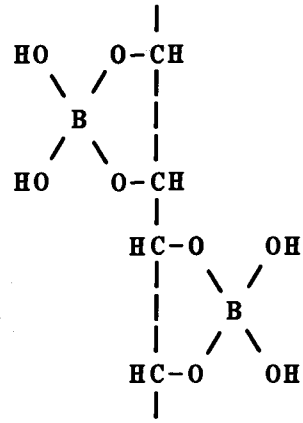	2-

species which have been considered in the equilibrium problem and the literature values of their stability constants are provided in Table II and Table IV. Computed master variable diagrams of 1, 10, and 100 millimolar concentration of mannitol with a 1 mM total borate concentration are shown in Figures 6 - 8. Figure 9 illustrates the effect of the concentration of mannitol upon the titration curve of 0.0010 M boric acid. A change in the order of the predominant species occurs with increases in the concentration of mannitol. With equal concentrations of mannitol and borate the order of species predominance in the basic domain is $B^- \simeq MB^- \geq M_2B^-$ and the order of species predominance in the acidic domain is $HB > M(HB) > M(HB)_2 > M_2(HB)$. With a 10 fold excess of mannitol the order of species predominance in the basic domain changes to $M_2B^- \simeq MB^- > B^-$, with no change in the order of species predominance in the acidic domain. With a 100 fold excess of mannitol the order of species predominance changes to $M_2B^- > MB^- > B^-$ and $HB > M(HB) > M(HB)_2 \simeq M_2(HB)$. As the concentration of mannitol increases the clarity of the titration endpoint improves and the inflection point shifts to lower log C_{H^+} values. The figures illustrate that a factor of 100 excess mannitol to total borate is necessary to accurately determine low concentrations of boron.

Table IV. Components and Species Considered in the $B(OH)_3$/Mannitol Equilibrium Problem. (1)

Components: $B(OH)_4^-$, Mannitol (LH_4), and H^+

Reaction	Species	Symbol	$\log K^a$
$LH_4 =$	LH_4	M	
$B(OH)_4^- + LH_4 - 2\,H_2O =$	$LH_2B(OH)_2^-$	MB^-	2.99
$B(OH)_4^- + 2LH_4 - 4\,H_2O =$	$(LH_2)_2B^-$	M_2B^-	5.07
$2B(OH)_4^- + LH_4 - 4\,H_2O =$	$L(B(OH)_2)_2^{2-}$	MB_2^{2-}	4.41
$2B(OH)_4^- + LH_4 + 2\,H^+ - 6\,H_2O =$	$L(B(OH))_2$	$M(HB)_2$	20
$B(OH)_4^- + LH_4 + H^+ - 3\,H_2O =$	$LH_2B(OH)$	M(HB)	8.79
$B(OH)_4^- + 2LH_4 + H^+ - 4\,H_2O =$	$(LH_2)(LH_3)B$	M_2(HB)	8.77
$2B(OH)_4^- + LH_4 + H^+ - 5\,H_2O =$	$L(B(OH)_2)(B(OH))^-$	$MB(HB)^-$	7.2

[a] T = 298K, I = 3.0 M. For computations at I = 3.0 M the constants were used as shown in the table. For computations at other ionic strengths, Equations 11 and 15 were used to correct the constants for the activity coefficients, although it is recognized that use of Equation 11 is unjustified up to I = 3.0 M.

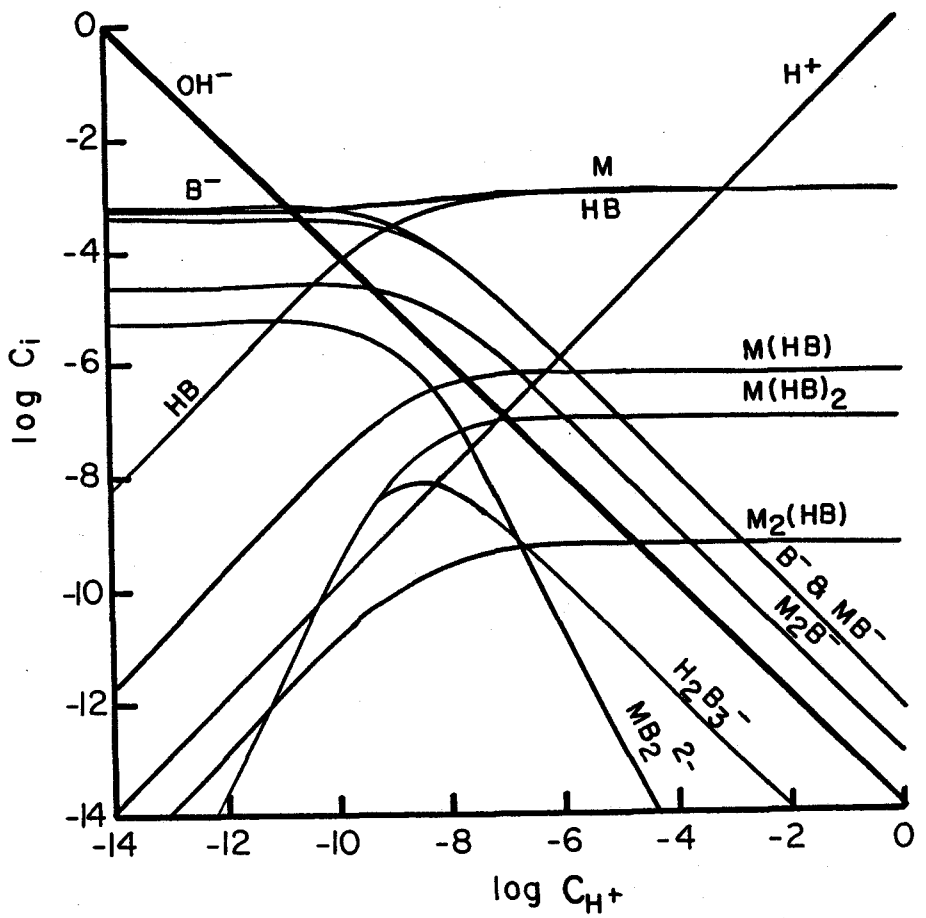

Figure 6. Master Variable Diagram for the $B(OH)_3$/Mannitol System with TB = 0.0010 M, TM = 0.0010 M. T = 25°C, I = 3.0. The equilibrium system is defined in Table IV and Table II.

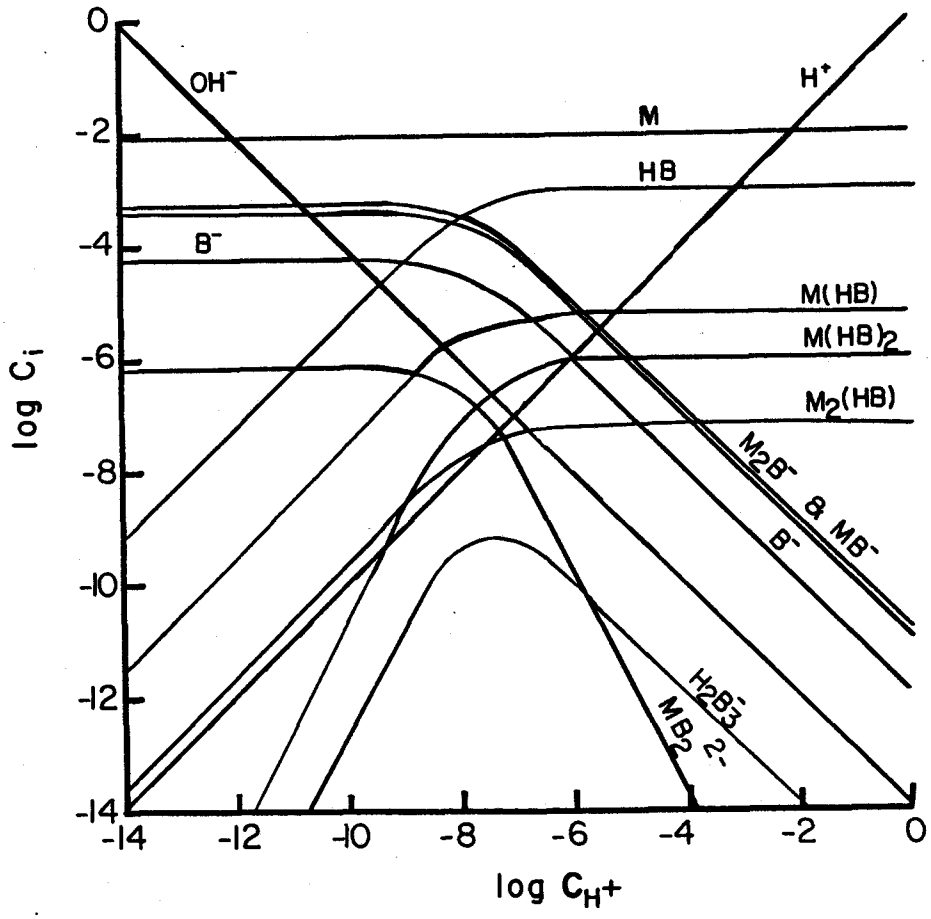

Figure 7. Master Variable Diagram for the $B(OH)_3$/Mannitol System with TB = 0.0010 M, TM = 0.010 M. T = 25°C, I = 3.0. The equilibrium system is defined in Table IV and Table II.

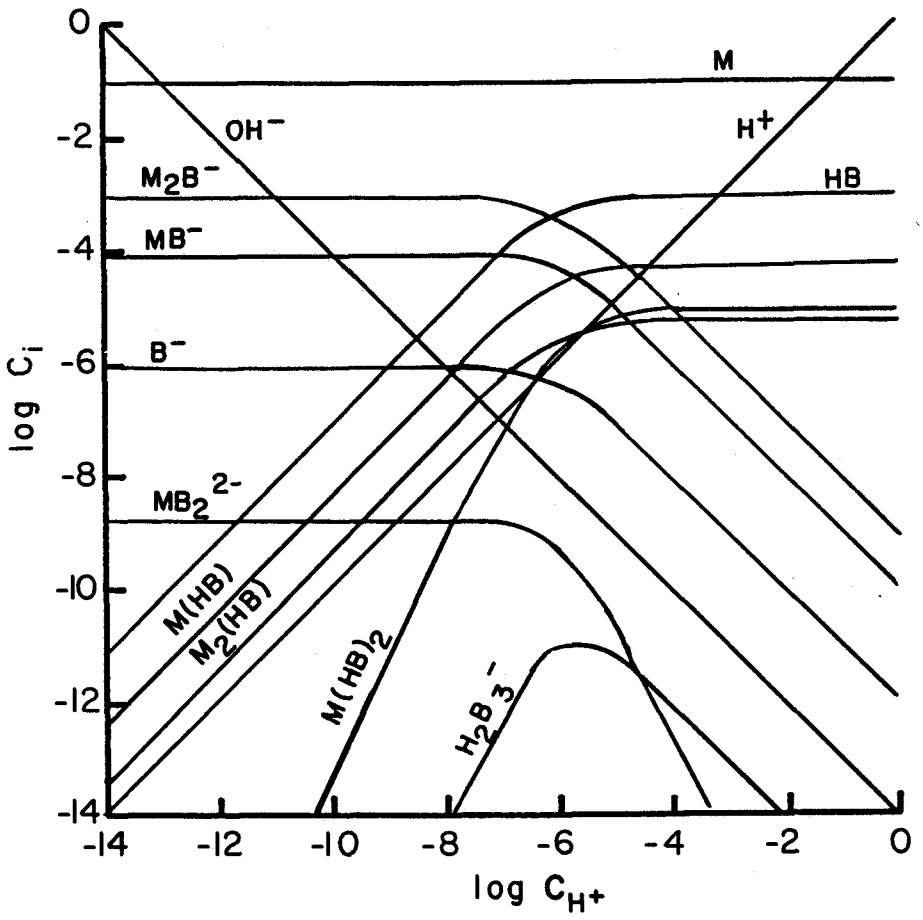

Figure 8. Master Variable Diagram for the $B(OH)_3$/Mannitol System with TB = 0.0010 M, TM = 0.10 M. T = 25°C, I = 3.0. The equilibrium system is defined in Table IV and Table II.

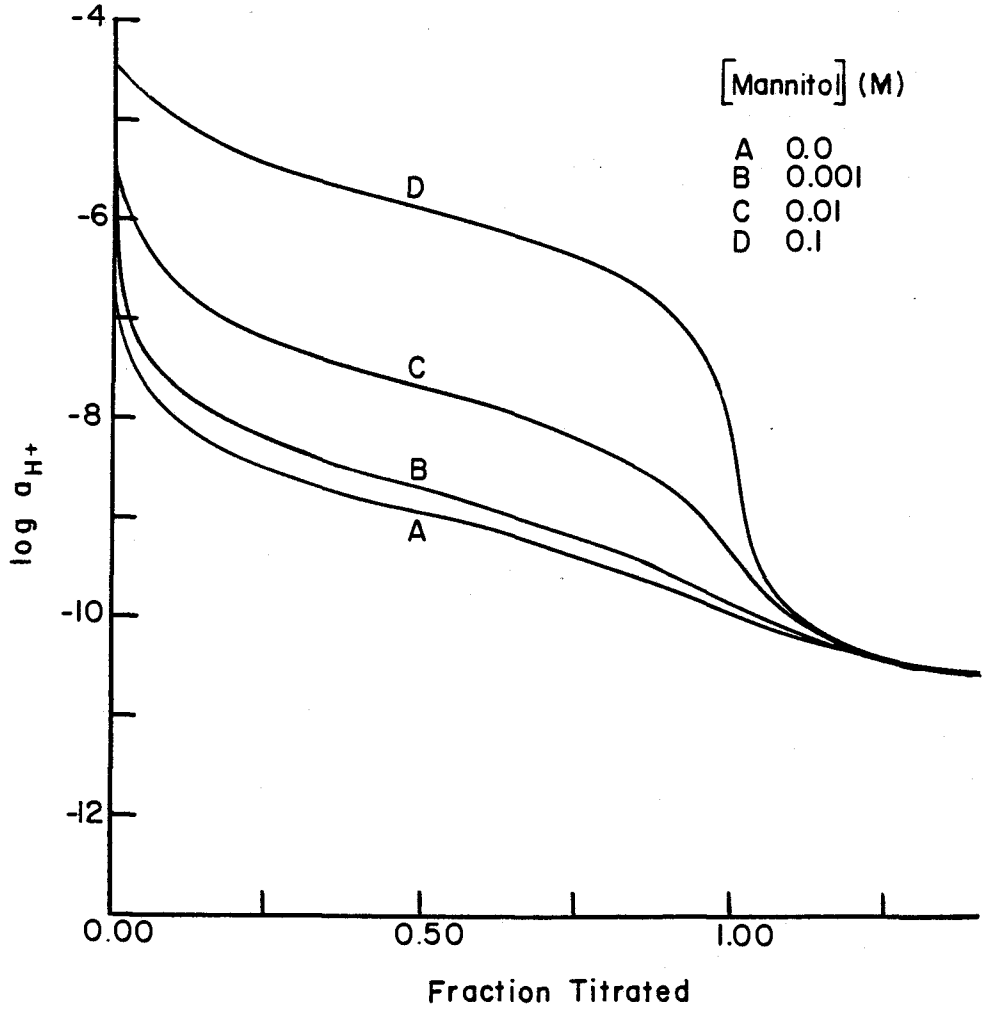

Figure 9. Theoretical Titration of $B(OH)_3$ in Mannitol. T = 25°C, I = 3.0. Fraction titrated represents moles of base added per mole of acid. Titrant was LiOH. The equilibrium system is defined in Table IV and Table II.

Experimental

Several boric acid solutions (with and without mannitol) have been titrated with LiOH.

Apparatus

An Ingold glass pH ion-selective electrode, model 5055-07, was employed as the indicating electrode (Figure 10). The glass membrane is 5 mm in diameter and designed for use at temperatures between 0° - 70°C in the pH range of 0 - 11. The special flat membrane surface allows for use in small sample volumes, because less solution is required for emersion of the membrane surface in a flat cell. Electrical resistance of the membrane is between 120 - 250 MΩ at 25°C. The interior electrolyte, which surrounds the Ag/AgCl electrode, is a pH 7 buffer solution with a defined potassium chloride concentration. An internal shield extends the length of the electrode body providing electrical shielding.

A GamRad double junction reference electrode model, PHE 54473, was also employed (Figure 10). The upper chamber is filled with a 4 M KCl saturated AgCl gel, and the lower chamber is filled with a 4 M KNO_3 gel. Both chambers were rinsed and refilled per recommended handling instructions. The electrode has an Ag/AgCl internal

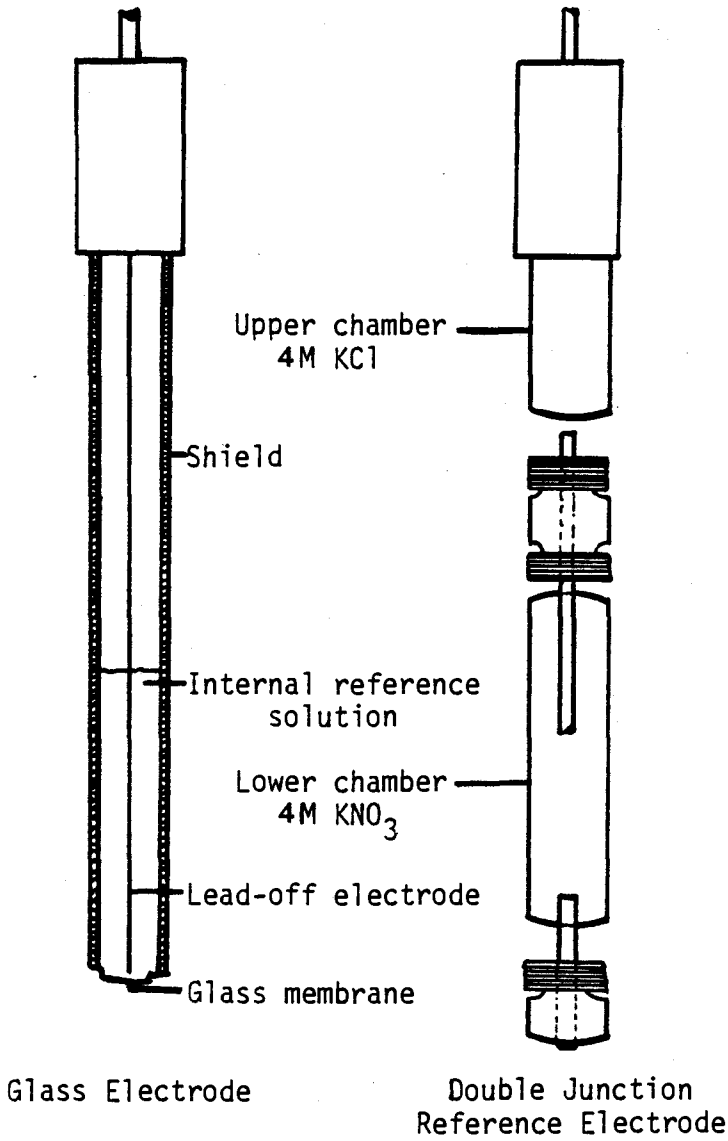

Figure 10. Glass and Reference Electrodes.

reference element and the junctions are porous ceramic cemented into a nylon base.

An Orion 701A digital pH/mV meter was used to measure the potential between the electrode pair. The meter has an input impedance of $10^{13}\Omega$.

The performance of the H^+ ion-selective electrode/double junction reference electrode pair was tested before it was used for boron concentration determinations. The results of these tests are given in Appendix B. Good consistency was found between calibrations with activity standards and with concentration standards. Activity standards have been used to calibrate the electrode pair in this study.

An automatic titration system, developed by C.M. Seyfert (12), was used for all experimental titrations. In the titration system the response of the electrode pair is continually monitored to ensure that the change in the potential with time, m, is less than a specified threshold (m = 0.001 mV/s), before the next addition of titrant. For a given set of time and potential data (t_iE_i), the potential is expressed as a linear function of time

$$E_i = mt_i + p \qquad (17)$$

The values of m and p are calculated to yield the best fit to the experimental data by minimizing the sum of squares,

Y_i, with respect to the parameters m and p

$$Y_i = mt_i + p - E_i \qquad (18)$$

The automatic titration system was built with a Metrohm 655 Dosimat to deliver titrant solution under the control of a Rockwell AIM-65 microprocessor. The millivolt response is read and stored by the microcomputer and made available for print out and data manipulation following the completion of the titration. From previously determined $E^{\circ'}_{cell}$ and s values the pH at each equilibrium point is calculated and included in the final print out.

Reagents

The chemicals used in this study were all reagent grade and diluted with deionized water to the desired concentration. (The deionized water was prepared by passing house deionized water through a Millipore^R, catalog #2030 000 70, system consisting of an activated charcoal bed and two mixed ion exchange beds). Solutions were stored in polyethylene bottles to minimize contamination from the borosilicate glass.

Procedure

The sample volume was pipetted into a water jacketted

beaker, thermostated to 25°C unless otherwise specified. The solution was stirred at a constant rate and nitrogen gas passed over the surface of the solution during electrochemical measurement. The solution was titrated with LiOH to an excess of 1.5 moles base per mole boric acid. At the conclusion of each analysis the sample solution was removed by suction and the cell rinsed several times with deionized water.

Results and Discussion

Titrations of 0.0010 M, 0.010 M, 0.10 M, and 0.53 M $B(OH)_3$ were performed in the absence of mannitol. Figures 11-14 provide a comparison between the experimental and computed titration curves. The log of the H^+ activity is plotted versus the fraction titrated. The experimental and theoretical titration curves are contiguous at log a_{H^+} values less than 11. A slight deviation is observed at log a_{H^+} values greater than or equal to 11. This deviation is caused by the glass electrode responding to other ions (i.e. Li^+) in solution, alkaline error. The deviation is less than 0.2 log a_{H^+} units in magnitude, which is consistent with expected values. The correspondence of the experimental and computed titration curves supports the equilibrium model of the boric acid/borate system. The inflection point of

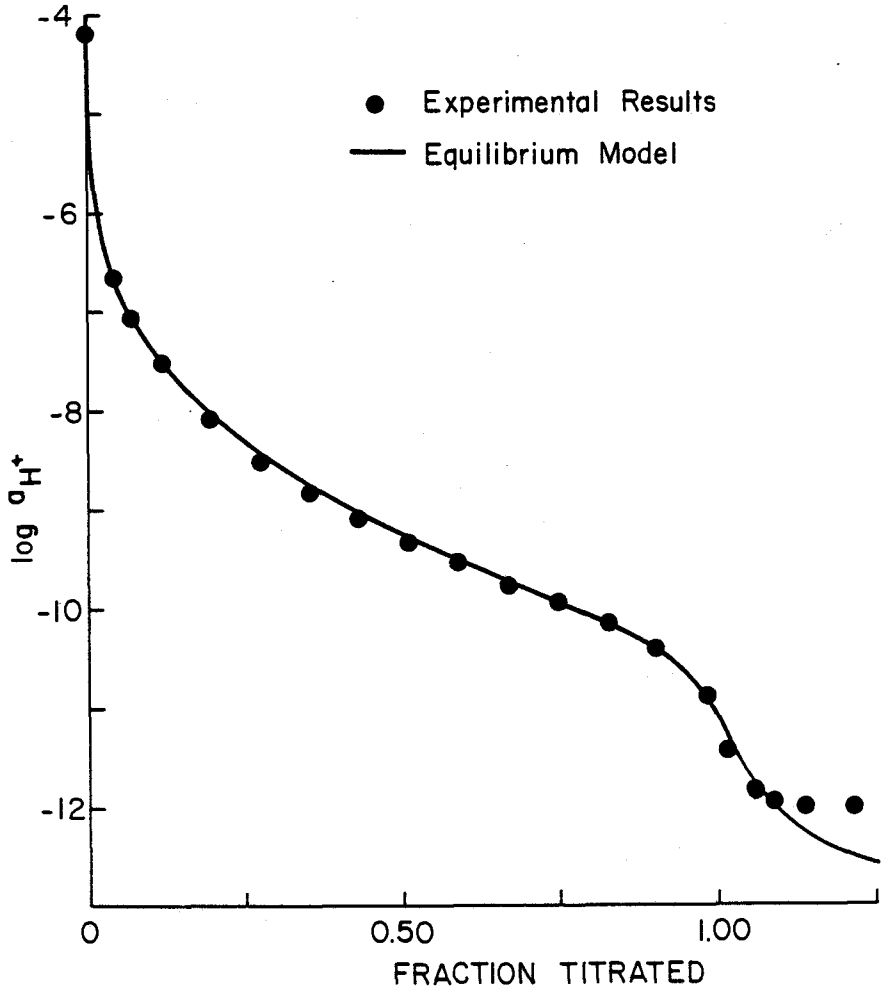

Figure 11. Titration of 0.53 M $B(OH)_3$ with 1.00 M LiOH. T = 25°C. Fraction titrated represents moles of base added per mole of acid.

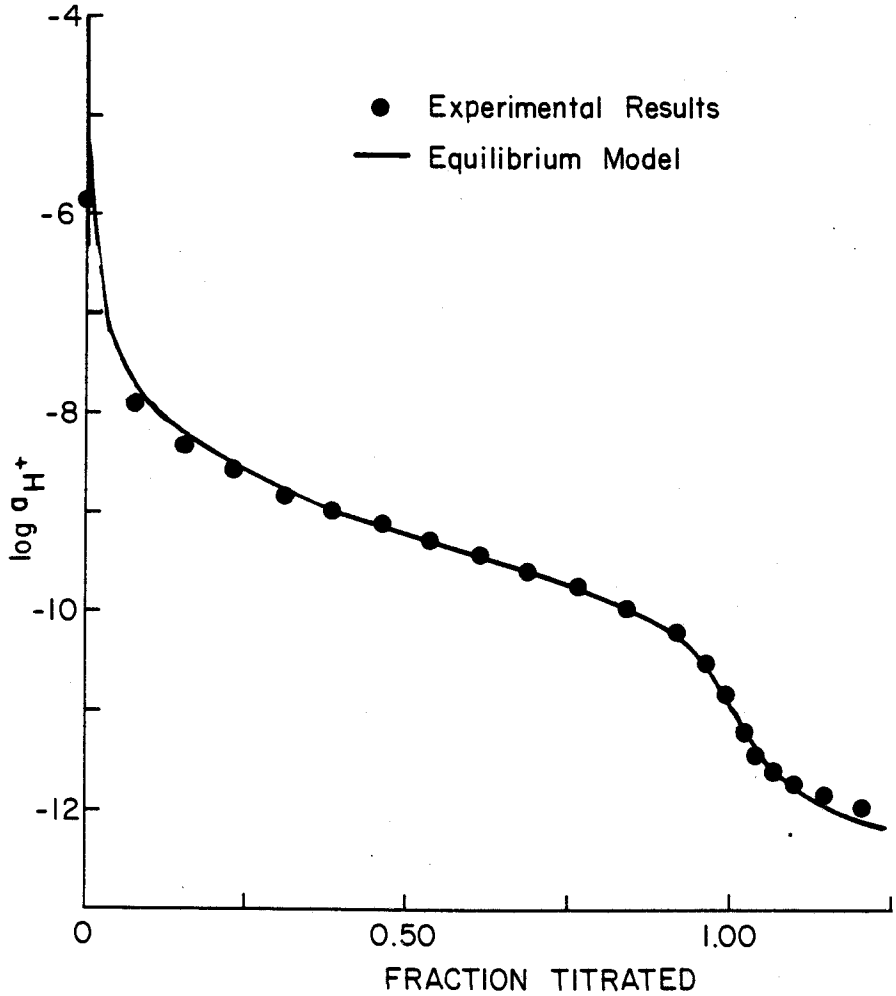

Figure 12. Titration of 0.10 M $B(OH)_3$ with 1.00 M LiOH. T = 25°C. Fraction titrated represents moles of base added per mole of acid.

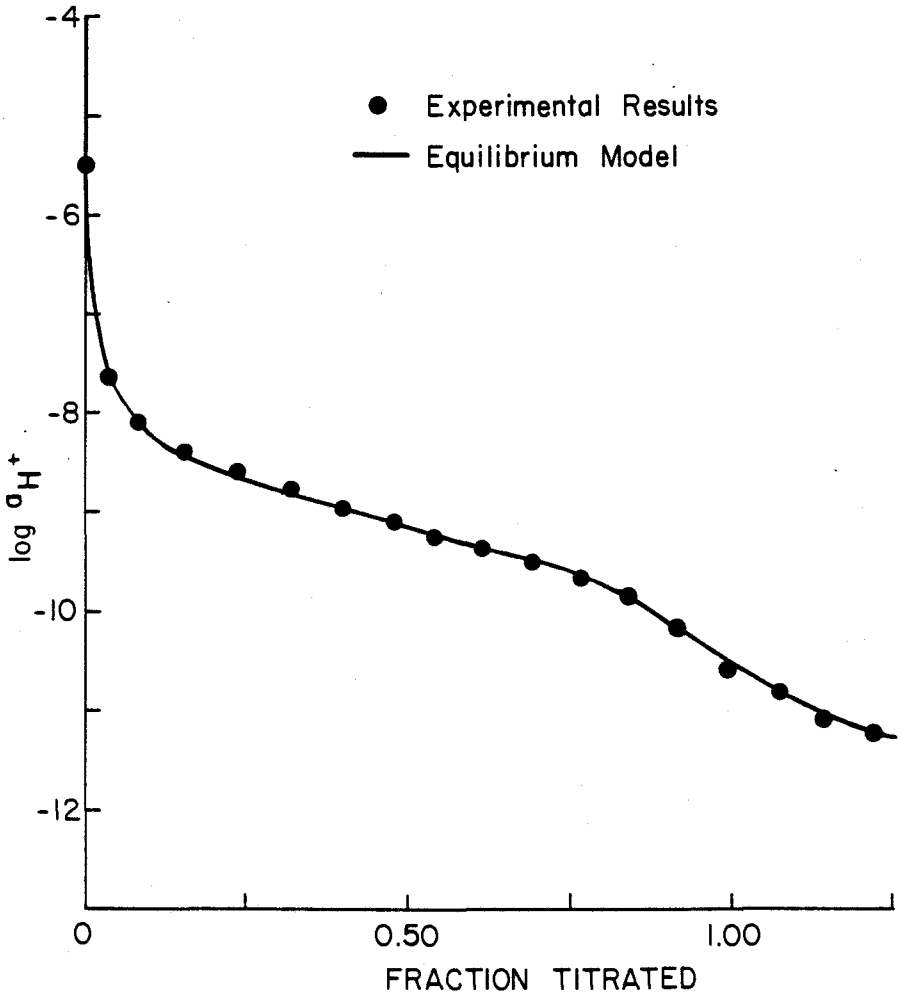

Figure 13. Titration of 0.010 M $B(OH)_3$ with 0.100 M LiOH. T = 25°C. Fraction titrated represents moles of base added per mole of acid.

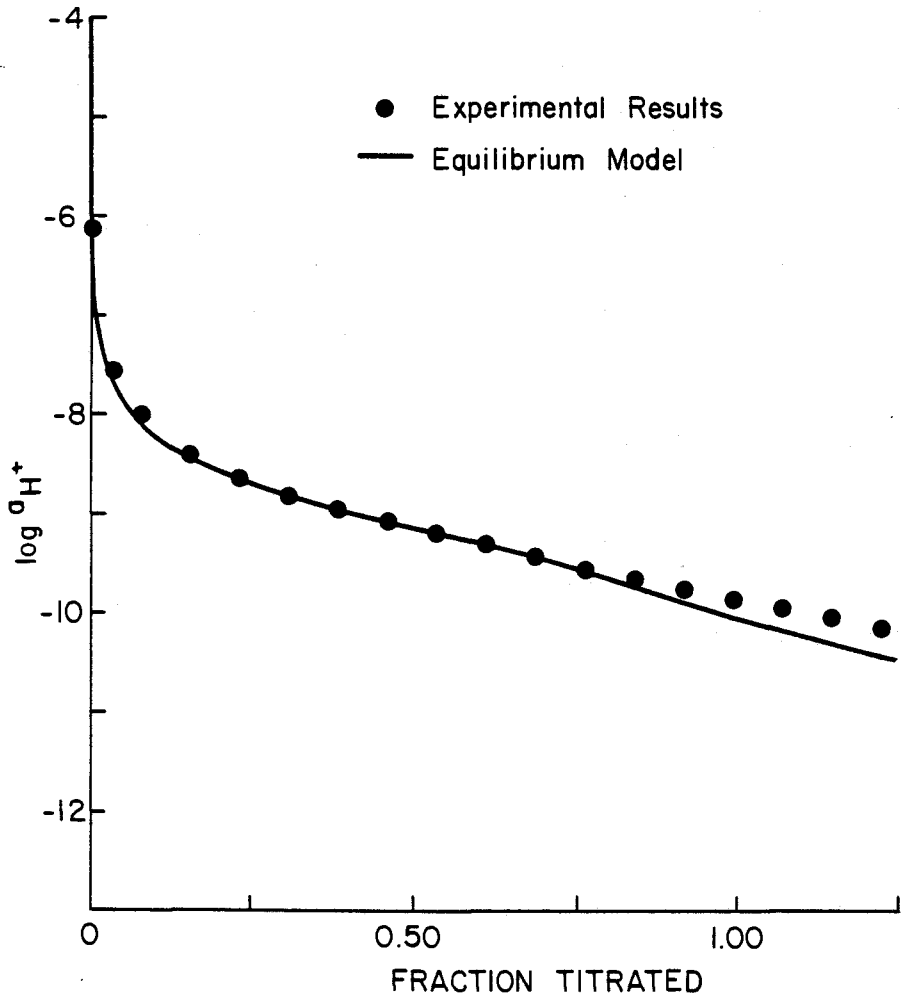

Figure 14. Titration of 0.0010 M $B(OH)_3$ with 0.100 M LiOH. T = 25°C. Fraction titrated represents moles of base added per mole of acid.

the potentiometric titration curve is observed to occur at the equivalence point of the titration (fraction titrated equal to 1.0). It is important to note that the inflection point of the potentiometric titration curve is difficult to detect at the lower concentrations.

In a subsequent set of experiments the effect of mannitol was investigated. From the equilibrium calculations which included mannitol, the potential of the electrode at the equivalence point was observed to be dependent upon both the concentration of mannitol and boric acid, Figure 9. Of further concern is the amount of mannitol to be added per titration, the method of titration endpoint detection, and the volume of sample required per analysis. Titrations of the boric acid/mannitol solutions were performed using the laboratory titration apparatus which had been programmed to function as a typical commercial analyzer (13). Sample volumes are initially determined by the operator based on the expected boric acid concentration. Table V provides a list of the analysis procedure, the breakdown of sample concentration to sample volume, and the excess of mannitol present. If, after completion of the titration, the boric acid concentration falls outside of the predetermined sample range, a second analysis is performed.

Titrations were performed on samples from within each

Table V. $B(OH)_3$ Sample Breakdown and List of Analysis Procedures.

Range $[B(OH)_3]$ (mg/L)	Range $[B(OH)_3]$ (M)	Sample Volume (mL)	Excess Mannitol
TB $\leq$ 200	$\leq$ 0.02	10	100[a]
200 < TB $\leq$ 2000	$\leq$ 0.20	2.5	10[a]
TB > 2000	>0.20	0.5	5[b]

[a] moles mannitol/moles maximum boric acid
[b] moles mannitol/moles minimum boric acid

Analysis Procedures

1. Sample volume pipetted into the water jacketted beaker.
2. 10 mL deionized water is added to cover tip of pH electrode.
3. If the solution is basic, 0.1 M HCl is added to bring solution to pH = 4.
4. 2.5 mL of 0.5 M mannitol is added.
5. Solution is titrated with 0.100 M LiOH to pH = 8.5.
6. The microcomputer computes $[B(OH)_3]$.
7. Solution is removed by suction and the beaker rinsed several times with deionized water.

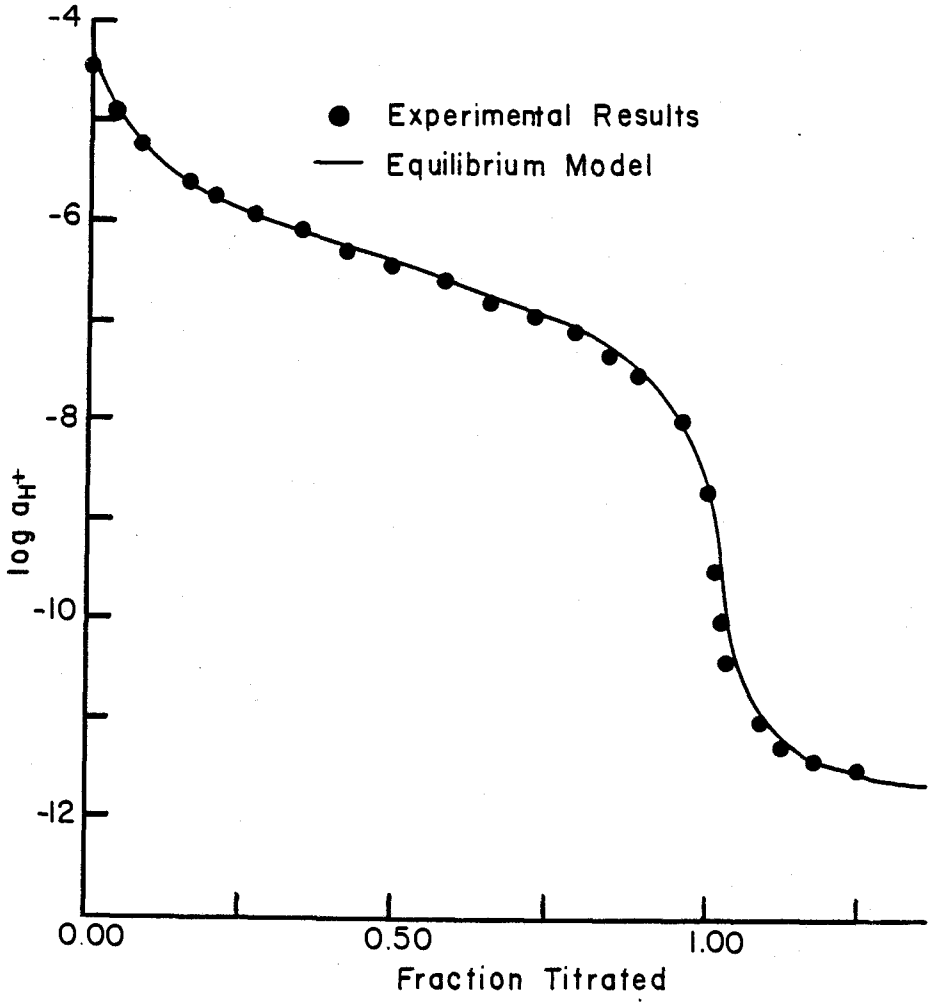

Figure 15. Titration of 0.50 M $B(OH)_3$ in Mannitol. Titrant = 0.100 M LiOH, Volume of sample = 0.50 mL, Volume of 0.5 M mannitol = 2.5 mL, Volume of H_2O = 10.0 mL, T = 25°C. Fraction titrated represents moles of base added per mole of acid.

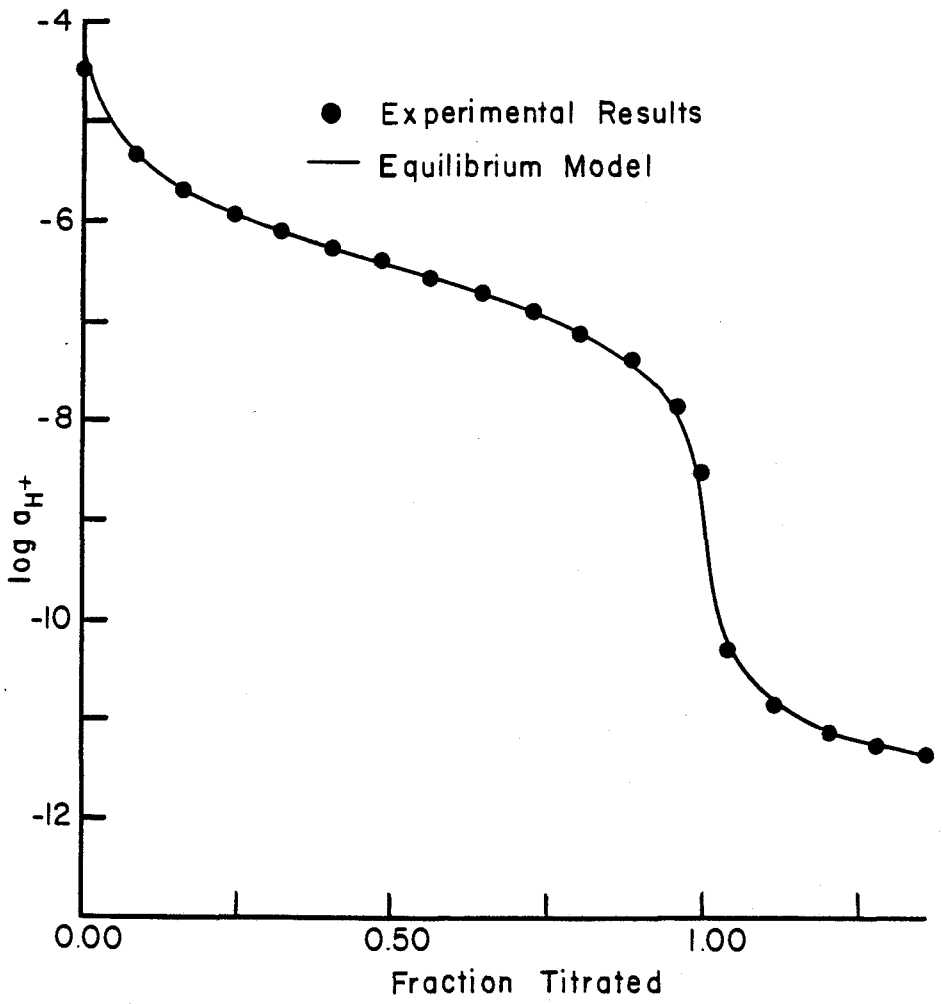

Figure 16. Titration of 0.050 M $B(OH)_3$ in Mannitol. Titrant = 0.100 M LiOH, Volume of sample = 2.5 mL, Volume of 0.5 M mannitol = 2.5 mL, Volume of H_2O = 10.0 mL, T = 25°C. Fraction titrated represents moles of base added per mole of acid.

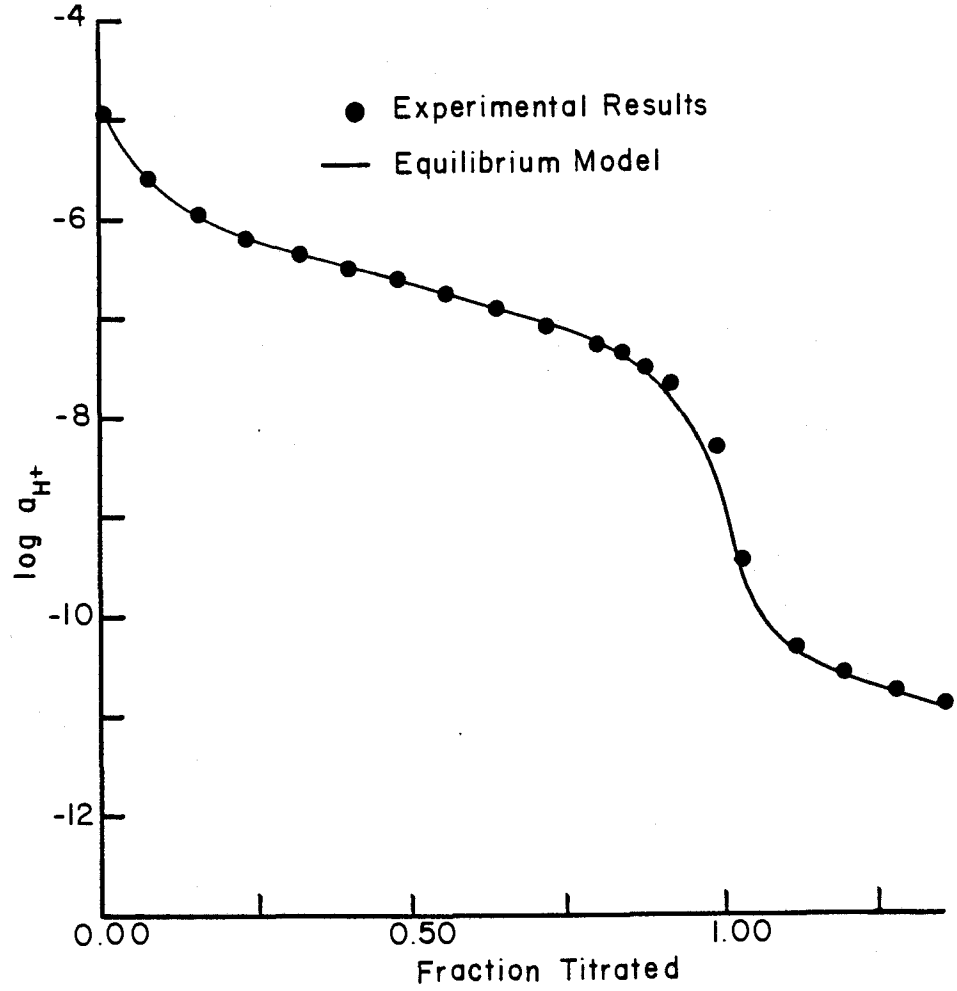

Figure 17. Titration of 0.0050 M $B(OH)_3$ in Mannitol. Titrant = 0.100 M LiOH, Volume of sample = 10.0 mL, Volume of 0.5 M mannitol = 2.5 mL, Volume of H_2O = 10.0 mL, T = 25°C. Fraction titrated represents moles of base added per mole of acid.

concentration range. The experimental and computed titration curves are illustrated in Figures 15-17. The agreement between the curves is good. The good agreement between the experimental and computed titration curves is consistent with the stoichiometry and equilibria of the boric acid/borate/mannitol system. The inflection point of the potentiometric titration curve occurs at the endpoint of the titration. Commercial titration apparatuses titrate to a fixed endpoint of log a_{H^+} = -8.5. Within this concentration range the inflection point of the titration curve corresponds to log a_{H^+} = -8.5 $\pm$ 0.02. Table VI lists the fraction titrated determined at the fixed log a_{H^+} = -8.5, and the percent relative error. The titration to a fixed endpoint of log a_{H^+} = -8.5 was found to be adequate for samples in the concentration range.

Conclusion

The concentrations and volumes of mannitol, titrant and sample used were found to be suitable for determining the concentration of boric acid in the range specified. The addition of mannitol to sharpen the endpoint is necessary below 0.10 M boric acid concentration. Mannitol should be in excess relative to boric acid by approximately a factor of ten below 0.10 M and a factor of 100 below 0.01 M boric acid.

Table VI. Fraction Titrated by Fixed Endpoint Detection.

$[B(OH)_3]$ (M)	Endpoint Fraction Titrated	% Relative Error (%)[a]
0.0050	1.023	2.3
0.050	1.005	0.5
0.50	0.996	-0.4

[a] % Relative Error =

$$\frac{\text{fraction titrated} \log a_{H^+} - 8.5 - 1.00}{1.00} \times 100$$

where 1.00 is the fraction titrated at the equivalence point of the titration.

The titration to a fixed endpoint of log a_{H^+} = -8.5 was found to be adequate for samples in the range, provided the electrodes are frequently standardized.

Evaluation of the pH electrode Appendix B, indicated that the most likely interference will be a change in the value of $E^{o'}$, Equation 7. The interference will not alter the equivalence point, but will alter the position of the endpoint relative to the log a_{H^+} of -8.5. It is therefore recommended that the detection of the endpoint by a derivative technique be employed.

SPECTROPHOTOMETRIC ANALYSIS

Introduction

A number of reagents have been employed for the spectrophotometric determination of boron. Of them, the most widely used reagents are curcumin (14, 15) and carminic acid (16,17). The curcumin method involves evaporation of an acidified boron/curcumin solution to dryness, followed by dissolution of the residue into ethyl alcohol. The carminic acid method requires use of concentrated sulfuric acid and a lengthly equilibration step. Both methods are unsuited for rapid analysis or automated procedures.

Azomethine H, 4-hydroxy-5-[[(2-hydroxyphenyl) methylene]amino]-2,7-napthalene disulphonic acid, has been recommended by Korenman (18) as a reagent for detecting boron qualitatively. In recent years several researchers have demonstrated the use of azomethine H for quantitative determination of boron concentration in steel (19), raw water (5) and plant tissue (20) samples. The procedure for its use is suitable for automation. Other advantages for use of this reagent over use of other spectrophotometric reagents include rapid analysis time, simplicity of procedure, and small sample volumes. Because of these advantages, azomethine H was selected for

use in the spectrophometric determination of boron concentrations in this study.

The initial spectrophotometry studies focused on the determination of the stability constants and molar absorptivities for each species, and the rate constants for each chemical reaction. Determination of these values enabled calculation of the absorbance signal for any set of boric acid concentration, azomethine H concentration, and time conditions. In these studies the pH was maintained at 5.0 ± 0.2 with a buffer consisting of 0.147 M acetic acid and 0.097 M ammonium acetate. The pH range was selected because of previous studies by Capelle (19). The buffer also maintains a constant ionic strength environment, $I \simeq 0.1$ M. Within this pH range, at boric acid concentrations below 0.1 M, the only significant boron species present (determined in the previous section of this thesis) is the monomeric boric acid species. A temperature of 25°C was selected to provide consistency between the potentiometry and spectrophotometry studies.

The final spectrophotometry studies focused on the design and testing of a flow system for the determination of boron concentration via three analysis modes: stopped flow, continuous flow, and flow injection. In stopped flow analysis, the reagent and boron containing sample are mixed and pumped into the spectrophotometer cell, flow is stopped, and the formation of the complex is monitored as

time passes. Long reaction times are possible, allowing for detection of lower boron concentrations. In continuous flow analysis, the reagent and samples are mixed and pass continuously through the spectrophotometer cell, allowing for detection of more samples per hour. In flow injection analysis, a plug of the sample is injected into a flowing stream of the reagent. The sample reacts with components of the carrier stream as it passes through a mixing coil to the spectrophotometer cell. The advantage of this mode is the small sample volumes required.

Theory

In the following sections the theories applied in the interpretation of the experimental data are discussed.

Spectrophotometry

Spectrophotometric methods are based upon the measurement of decrease in radiant power of a beam of light as it passes through an absorbing medium of known dimension. When light of a small wavelength range passes through a sample containing an absorbing species, the radiant power of the beam is progressively decreased as more of the energy is absorbed by molecules in solution. The decrease in radiant power depends upon the

concentration of the absorber and the length of the path traversed by the beam. The transmittance, T, of a solution is defined as the ratio of the intensity of light transmitted through the sample solution to the intensity of light transmitted through a blank solution which does not absorb light. The experimental absorbance is defined as $-\log T$, and has been given the symbol abs. The Beer-Lambert law relates the absorbance to the concentration C of the absorbing species and the optical path length b as follows:

$$abs = \varepsilon bC \tag{19}$$

In this equation, ε is the molar absorptivity, which is dependent on wavelength. In spectrophotometric determinations a calibration curve of abs versus C is prepared from measurements of absorbance standards. This curve is then used to determine C in a sample from the measured absorbance for the sample.

The total absorbance of a solution at a given wavelength is equal to the sum of the absorbances of the individual species present. Thus, for a multicomponent system

$$abs_{total} = \sum_{i}^{n} abs_i = \sum_{i}^{n} \varepsilon_i bC_i \tag{20}$$

where the subscript i refers to all absorbing substances. To obtain accurate results with spectrophotometry it is

desirable for the absorbance measured to be due predominately to the analyte. Absorption due to other species should be compensated by a blank measurement. The absorbance signal should generally be in the range of 0.01 to 2.0 absorbance units (A.U.) for highest accuracy. Below 0.01 A.U. or above 2.0 A.U. the precision decreases.

Although many substances absorb strongly in the visible and near UV wavelength regions, many others do not. Boric acid is one of those substances which do not absorb. To determine the concentration of the nonabsorbing boron, $B(OH)_3$ is reacted with a reagent to form an absorbing reaction product. It is important that the reagent be selective for the species to be determined, in order to prevent interference from other species in solution. The reagent azomethine H has been selected for use in this study because of the rapid analysis time and the simplicity of its procedure. Azomethine H is readily available as the condensation product of H-acid, 8-amino-1-naphthol-3,6-disulphonic acid, and salicaldehyde. (Since only the H acid derivative was used in this study, azomethine H will be referred to as azomethine). In aqueous solution azomethine, Figure 18, is orange, whereas H-acid and salicaldehyde are practically colorless. Boron is complexed by the oxygen of the hydroxyl groups of the azomethine molecule.

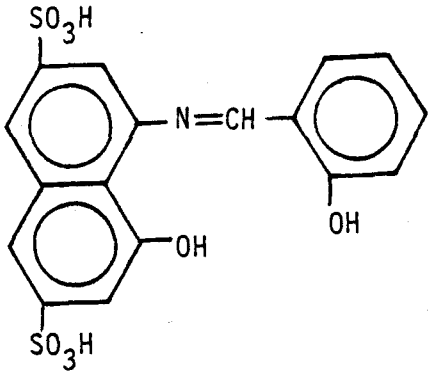

Figure 18. Structure of Azomethine H.

Chemical Equilibrium

As will be shown, an equilibrated solution of azomethine, A, and boron, B, contains: free azomethine and boron, an azomethine dimer, and 1:1 and 2:1 azomethine boron complexes. The reactions for the formation of these complexes can be expressed as

$$2A \rightleftarrows A_2 \quad (21)$$

$$A + B \rightleftarrows AB \quad (22)$$

$$2A + B \rightleftarrows A_2B \quad (23)$$

where AB and A_2B are the 1:1 and 2:1 complexes, and A_2 is the azomethine dimer. Whether some component of the buffer was involved in the formation of the dimer was not investigated.

Capelle (19) determined that the development of the azomethine/boron complexes during the initial two hours is fairly rapid, but 10 to 14 hours are necessary for the system to equilibrate ($T = 20^{o} \pm 5^{o}C$, pH = 5.2). In this section the theory and equations which characterize the azomethine/boron system in equilibrium are presented, time $>$ 12 hours. Chemical kinetics which characterize the system before equilibrium is reached are discussed in the next section.

The absorption spectra for an equilibrted solution of azomethine and boron and for the azomethine reagent are

shown in Figure 19. The azomethine/boron complexes exhibit a broad band centered at 412.5 nm. The azomethine monomer and dimer exhibits a broad peak centered at 341 nm. Capelle (19) observed that the maximum equilibrium absorbance signal from the complexes was obtained with solutions buffered to pH 5.2, but that the absorbance signal remained constant within the pH range 4.8 to 5.6.

The measured absorbance signal can be expressed as

$$\frac{abs}{b} = \varepsilon_A[A] + \varepsilon_{A_2}[A_2] + \varepsilon_{AB}[AB] + \varepsilon_{A_2B}[A_2B] + \varepsilon_B[B] \quad (24)$$

from Equation 20. All absorbance values have been normalized to a 1 cm path length. The absorbance due to boric acid is insignificant within the wavelength range studied. Material balance equations for the total azomethine and boron concentrations, TA and TB may be written.

$$TA = [A] + 2[A_2] + [AB] + 2[A_2B] \quad (25)$$

$$TB = [B] + [AB] + [A_2B] \quad (26)$$

The relationship between the concentration of the complexes and reactants can be expressed as

$$K_A = \frac{[A_2]}{[A]^2} \quad (27)$$

$$K_1 = \frac{[AB]}{[A][B]} \quad (28)$$

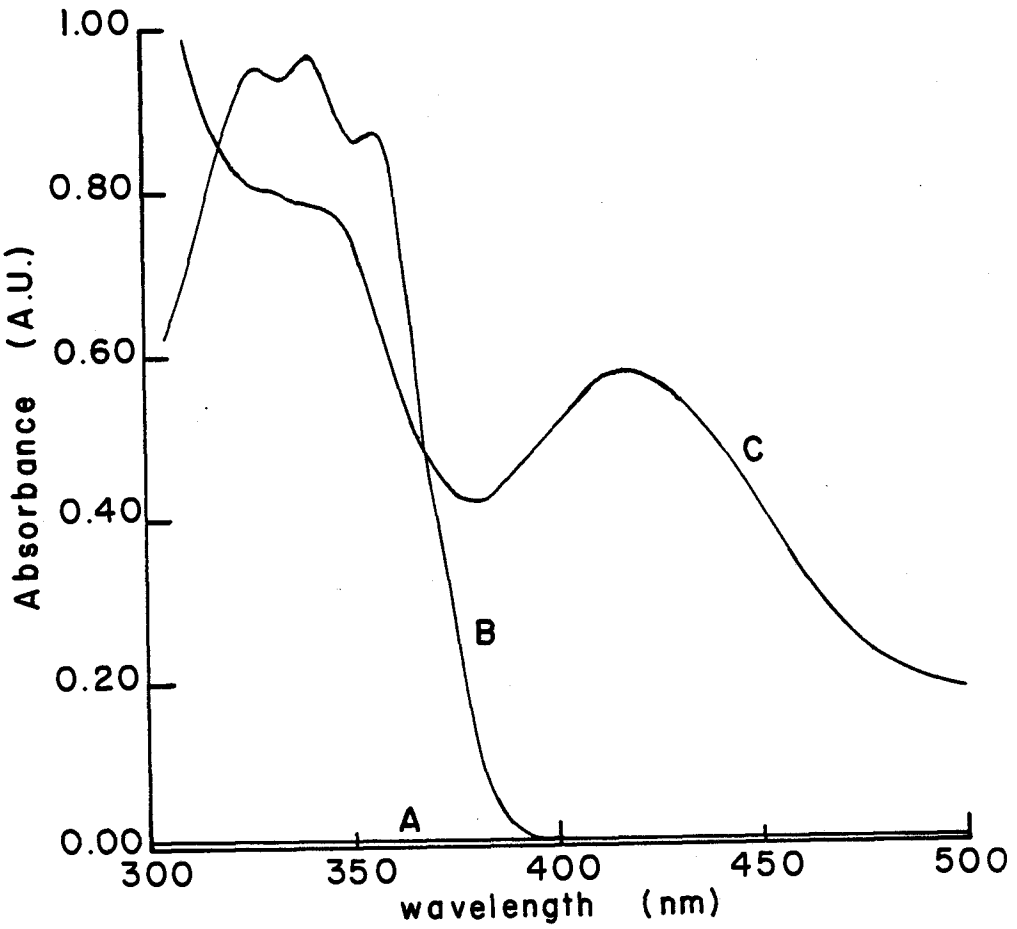

Figure 19. Absorbance Spectra.
Buffer: 0.147 M acetic acid/0.097 M ammonium acetate, pH = 5. Azomethine H: 1.0×10^{-4} M. $B(OH)_3$ = 0.1 M.
Curve A: Buffer vs Buffer.
Curve B: Azomethine H/Buffer vs Buffer.
Curve C: $B(OH)_3$/Azomethine H/Buffer vs Buffer.

$$\beta_2 = \frac{[A_2B]}{[A]^2[B]} \qquad (29)$$

where K_A is the stability constant for the azomethine dimer, K_1 is the step wise stability constant for the AB complex, and β_2 is the cumulative stability constant for the A_2B complex. Thus, to completely characterize the absorbance of the system the values for the molar absorptivities and stability constants must be determined.

Spectrophotometry is a widely used technique for the study and determination of stability constants. However, complications arise when fitting to absorbance measurements because not only are the stability constants to be determined but also the molar absorptivities for each species. The computer program FITEQL (21) is used in determining stability constants and molar absorptivities for the boron/azomethine species. The program is general in scope, having the capability to evaluate constants for any species which can be expressed as the product of the components. A set of components is defined such that every species can be written as the product of a reaction involving only the components. The representation of the species in terms of the components is unique. Specific parameters (e.g. stability constants and molar absorptivities) in the chemical equilibrium problem are adjusted to yield the optimal fit of the model to the

experimental data. The optimization procedure involves the iterative application of a linear approximation of the chemical equilibrium equations and a linear least squares fit. Whereas MICROQL (10) (described in the potentiometry section) is used to determine total or free component concentrations from given stability constants, FITEQL (21) is used to determine stability constants from total and free component concentrations.

Chemical Kinetics

The rate of a reaction is expressed as the change in concentration of a reactant or product with time. An equation that gives the reaction rate as a function of concentration is referred to as a rate law. The rate law for any chemical reaction must be determined experimentally. A rate law which can be used to describe the formation of the AB and A_2B complexes has been determined to be

$$\frac{d[AB]}{dt} = k_{f1}[A][B] - k_{b1}[AB] \qquad (30)$$

$$\frac{d[A_2B]}{dt} = k_{f2}[A]^2[B] - k_{b2}[A_2B] \qquad (31)$$

where k_f, and k_b, are the forward and backward rate constants. The rate law can be expressed in terms of only the complex concentrations and the total azomethine

and boron concentrations by combining Equations 25 and 26 with Equations 30 or 31.

$$\frac{d[AB]}{dt} = k_{f1}(TA-2[A_2B]-[AB])(TB-[A_2B]-[AB])-k_{b1}[AB] \quad (32)$$

$$\frac{d[A_2B]}{dt} = k_{f2}(TA-2[A_2B]-[AB])^2(TB-[A_2B]-[AB])-k_{b2}[A_2B] \quad (33)$$

The concentration of the A_2 species (Equation 25) is found to be negligible. The reaction order with respect to the concentration of one particular species, Ci, is defined as

$$\text{order with respect to species i} = \left(\frac{\partial \log \text{ rate}}{\partial \log C_i}\right)_{C_j} \quad (34)$$

where the reaction rate is evaluated under conditions such that the concentrations of the other species, C_j, are constant. The definition of Equation 34 and the graph of log rate versus log concentration are used in practice as a means of formulating an alegebraic relation between rection rate and species concentration. A rate law involving reaction orders greater than 1 cannot always be solved directly. In this case the solution to the rate equation can be approximated by numerical integration, whereby the concentrations of the species are repetitively determined for small changes in time. This numerical integration has been performed according to the trapezoidal rule.

Insight into the problems of kinetic analysis can be gained when certain simplifying assumptions are made with regards to Equation 30 and 31.

Case I. The reaction does not approach equilibrium during the period of time under consideration and the magnitude of the back reaction is negligible compared to that of the forward reactions:

$$\frac{d[AB]}{dt} = k_{f1}\,(TA-2[A_2B]-[AB])(TB-[A_2B]-[AB]) \qquad (35)$$

$$\frac{d[A_2B]}{dt} = k_{f2}\,(TA-2[A_2B]-[AB])^2(TB-[A_2B]-[AB]) \qquad (36)$$

Case II. The assumption in Case I holds. Also the concentration of either complex formed is negligible compared to the total concentration of boron or azomethine thus [B] ~ TB and [A] ~ TA are effectively constant:

$$\frac{d[AB]}{dt} = k_{f1}\,TA\,TB \qquad (37)$$

$$\frac{d[A_2B]}{dt} = k_{f2}\,TA^2TB \qquad (38)$$

These cases can be applied to a reaction whether it is the only reaction or one of many occurring in solution. The assumptions which apply, however, must be specified for each case.

Experimental

The experimental section has been divided into two

parts. In the first section the apparatuses, reagents and procedures used in determining the equilibrium and kinetic constants are described. In the second section the design and operation of a flow system for the determination of boron concentration are described.

Apparatus

A Cary 118C UV-vis spectrophotometer with 1 and 10 cm glass cells and an ISCO V4 variable detector with 0.5 cm glass flow cell were used for all spectrophotometric measurements. All absorbance values have been normalized to a 1 cm path length.

Reagents

The chemicals used in the study were all reagent grade. Deionized water was used for dilution to the desired concentration. Solutions were stored in polyethylene bottles to minimize possible contamination from borosilicate glass. Aqueous solutions of the azomethine reagent are stable for 12 hours. After this period, the solution shows signs of decomposition, probably due to oxidation and/or hydrolysis. Ascorbic acid (2.2 grams per gram of azomethine) is added as a stabilizer. The ascorbic acid does not absorb within the wavelength range of interest. Aqueous solutions of

the reagent and ascorbic acid are stable for 24 hours. The buffer consisted of 0.147 M acetic acid and 0.097 M ammonium acetate.

Procedure

Solutions were prepared by first mixing the boric acid and buffer in a volumetric flask, followed by addition of the azomethine reagent, and dilution with deionized water to volume. Solutions were kept in a constant temperature bath except during absorbance measurements. The concentrations of azomethine and boric acid for four sets of experiments are given in Table VII. The change in absorbance versus time was recorded continuously for 10 minutes. Additional absorbance measurements were made at two hour intervals for 25 hours. If the absorbance of a solution exceeded 2 A.U., the solution was diluted in a 1:4 ratio with the buffer solution. Dilution was performed in the absorbance cell. Disassociation of the complexes upon dilution was not detected within the time of measurement.

Results and Discussion

Equilibrium

Before an attempt is made to discuss the interaction of azomethine with boron, it is useful to consider the

Table VII. Experimental Concentations.

Experiment	TA (M)	TB (M)
I	$1.00 \times 10^{-5} - 2.5 \times 10^{-3}$	0.00
II	5.00×10^{-4}, 1.00×10^{-3}, 1.00×10^{-3}	5.00×10^{-4}, 1.00×10^{-3}, 2.00×10^{-3}
III	$1.00, 2.0, 5.0 \times 10^{-5}$ $1.00, 2.0, 5.0 \times 10^{-4}$ $1.00, 2.0, 5.0 \times 10^{-3}$	2.00×10^{-3}
IV	1.00×10^{-4}	$1.00, 5.00 \times 10^{-4}$ $1.00, 5.00 \times 10^{-3}$ $1.00, 5.00 \times 10^{-2}$ $1.00, \quad \times 10^{-1}$

aqueous chemistry of azomethine alone. In Experiment I the absorbance signal of the azomethine solution remained constant during the time of measurement. A linear relationship between absorbance and the total azomethine concentration was observed with solutions less concentrated than 2.0×10^{-4} M. Figure 20 illustrates this relationship at a wavelength, λ, of 341 nm, the absorption maximum of the azomethine reagent. With sample concentrations greater than 2.0×10^{-4} M a quadratic relationship was observed between absorbance versus total azomethine concentrations. Figure 21 illustrates this relationship at λ = 412.5 nm. Because the wavelength of maximum absorbance for the boron/azomethine complexes is known to be 412.5 nm, the data collected at this wavelength have been interpreted. The quadratic relationship provides evidence for the existence of more than a simple azomethine species. The data are interpreted in terms of two species: an azomethine monomer, A and an azomethine dimer, A_2.

The mass action equation for the formation of the dimer, the mass balance equation for azomethine, and Beer's law can be combined to form a relationship between the absorbance and ε_A, ε_{A_2} and K_A. From this relationship and the experimental data, values for the constants are determined.

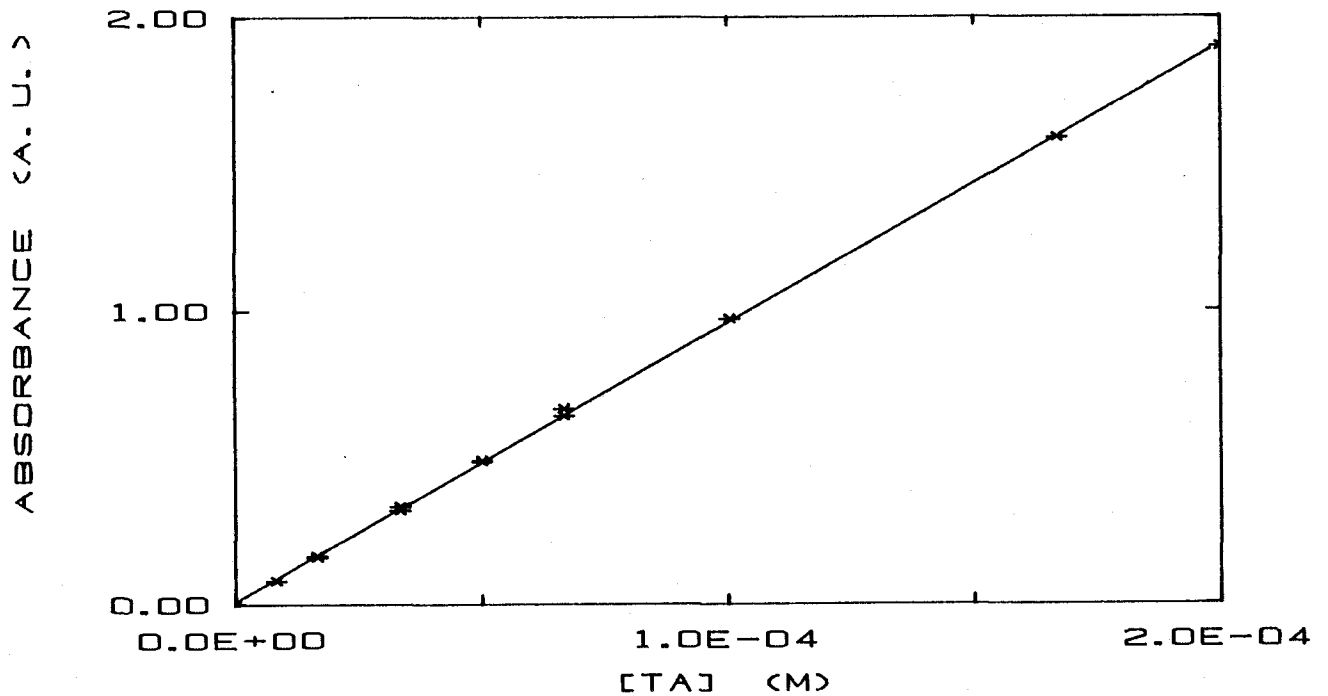

Figure 20. UV Absorbance of Azomethine H.
Wavelength = 341 nm, Acetate Buffer = 0.244 M, T = 25° C.
Data from Experiment I.

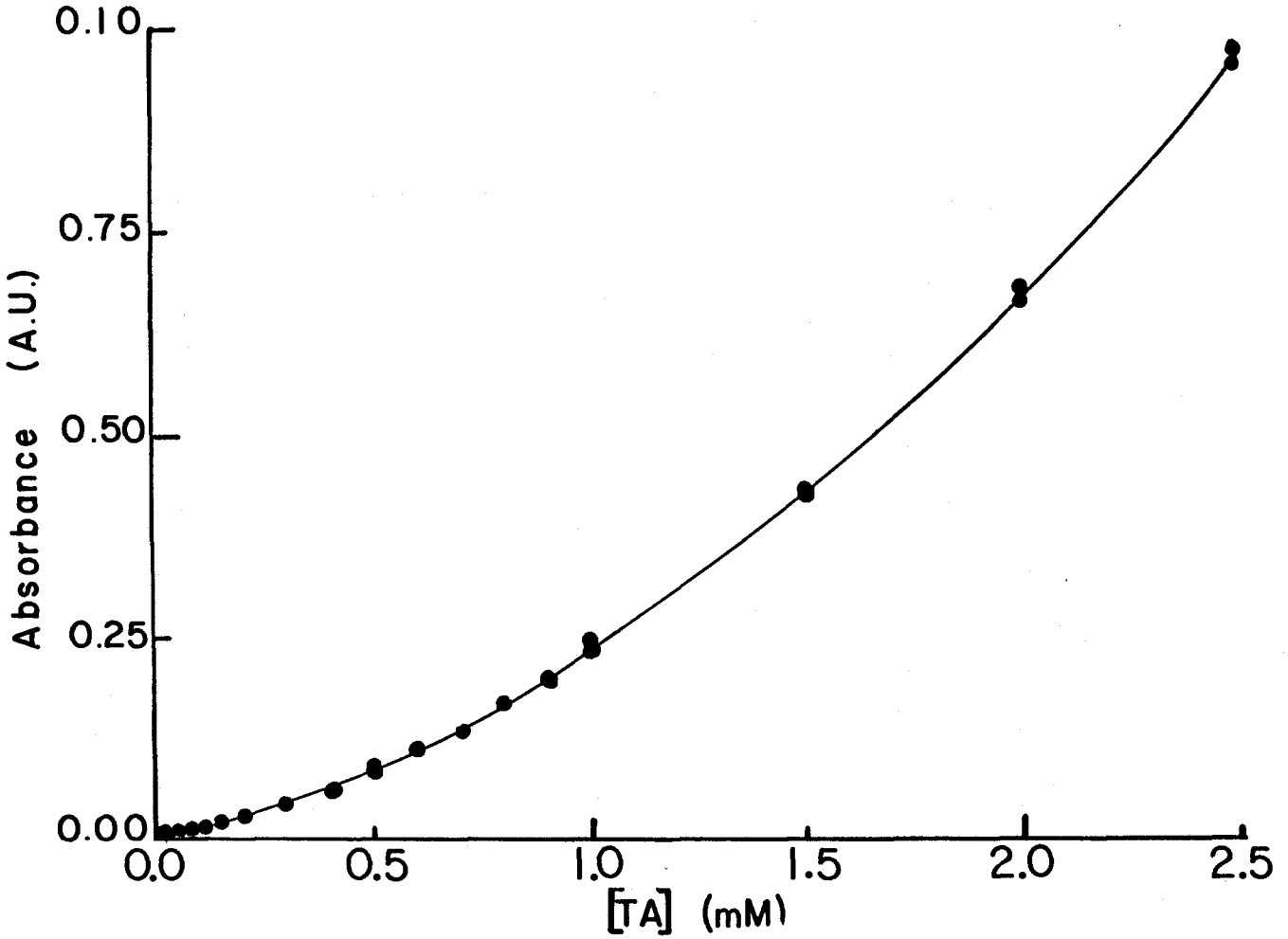

Figure 21. Visible Absorbance of Azomethine H.
Wavelength = 412.5 nm, Acetate Buffer = 0.244 M, T = 25°C.
Data from Experiment I.

The material balance equation for total azomethine, TA, in the absence of boron can be expressed as

$$TA = [A] + 2[A_2] \tag{39}$$

Equation 27 and 39 can be solved for [A] and $[A_2]$

$$[A] = \frac{-1 + (1 + 8\ K_A TA)^{1/2}}{4K_A} \tag{40}$$

$$[A_2] = \frac{1 + 4K_A TA - (1 + 8\ K_A TA)^{1/2}}{16K} \tag{41}$$

The appropriate roots from the quadratic equation have been chosen as not to violate the material balance equation. The absorbance is expressed as

$$\frac{abs}{b} = \varepsilon_A [A] + \varepsilon_{A_2} [A_2] \tag{42}$$

Substituting Equations 40 and 41 into Equation 42 yields

$$\frac{abs}{b} = \frac{\varepsilon_{A_2}\ 4K_A TA + (\varepsilon_{A_2} - 2\,\varepsilon_A)(1 - (1 + 8K_A TA)^{1/2})}{8K_A} \tag{43}$$

If the product $8K_A TA$ is small compared to 1, the square root term can be approximated by polynomial expansion

$$(1+8K_A TA)^{1/2} = 1 + 4K_A TA - 8(K_A TA)^2 + 32(K_A TA)^3 + \ldots \tag{44}$$

If K_A and TA are small (so that little of the dimer is formed) only the first two terms need to be included in the approximation.

$$(1 + 8K_ATA)^{1/2} \sim 1 + 4K_ATA \qquad (45)$$

and the absorbance is expressed as

$$\frac{abs}{b} \sim \varepsilon_A TA \qquad (46)$$

The experimental data were observed to fit Equation 46 when the total azomethine concentration was less than 2.0×10^{-4} M. As TA is increased, inclusion of the third term in the square root approximation becomes necessary

$$(1 + 8K_ATA)^{1/2} \sim 1 + 4K_ATA - 8(K_ATA)^2 \qquad (47)$$

and the absorbance is expressed as

$$\frac{abs}{b} \sim \varepsilon_A TA + (\varepsilon_{A_2} - 2\varepsilon_A)K_ATA^2 \qquad (48)$$

The experimental data were observed to fit Equation 48 when the total azomethine concentration was greater than 2×10^{-4} M. Inclusion of additional polynomial terms in the square root approximation was not required at concentrations less than 0.01 M TA.

Values for ε_A and the product $(\varepsilon_A - 2\varepsilon_{A_2})K_A$ have been determined from the first and second order

coefficients of a least-squares fit to the polynomial in Equation 48. If a second linear region had been observed at higher TA concentrations, where conversion of the monomer to the dimer was essentially complete, values of ε_{A_2} and K_A could have been resolved from the product $\varepsilon_{A_2} K_A$. This condition, however, was never observed. For convenience, K_A has been assigned the value of 1, which is consistent with the experimental observation that a negligible fraction of the azomethine is converted to the dimer over the concentration range studied. The values determined for ε_A, ε_{A_2}, and K_A are presented in Table VIII. The experimental absorbances along with the calculated absorbances have been graphed in Figure 22. Excellent agreement over the entire concentration is seen, supporting the validity of the model.

With an understanding of the azomethine equilibria it is possible to characterize the azomethine/boron equilibria. In Experiments II, III, and IV equilibrium was reached after 50 kiloseconds. A quadratic relationship was observed between absorbance and the total azomethine concentrations for a given constant total boron concentration. The relationship between the absorbance versus total azomethine suggests the presence of an A_2B species. There was also evidence for an AB species was in the equilibrium speciation. Equation 25-29 completely define the azomethine/boron system.

Table VIII. Azomethine H Equilibrium Constants.

Species	Symbol	Stability Constant	Molar Absorbitivity (A.U. cm^{-1} M^{-1})
Monomer	A	-	14
Dimer	A_2	$K_A = 1$	9.7×10^3

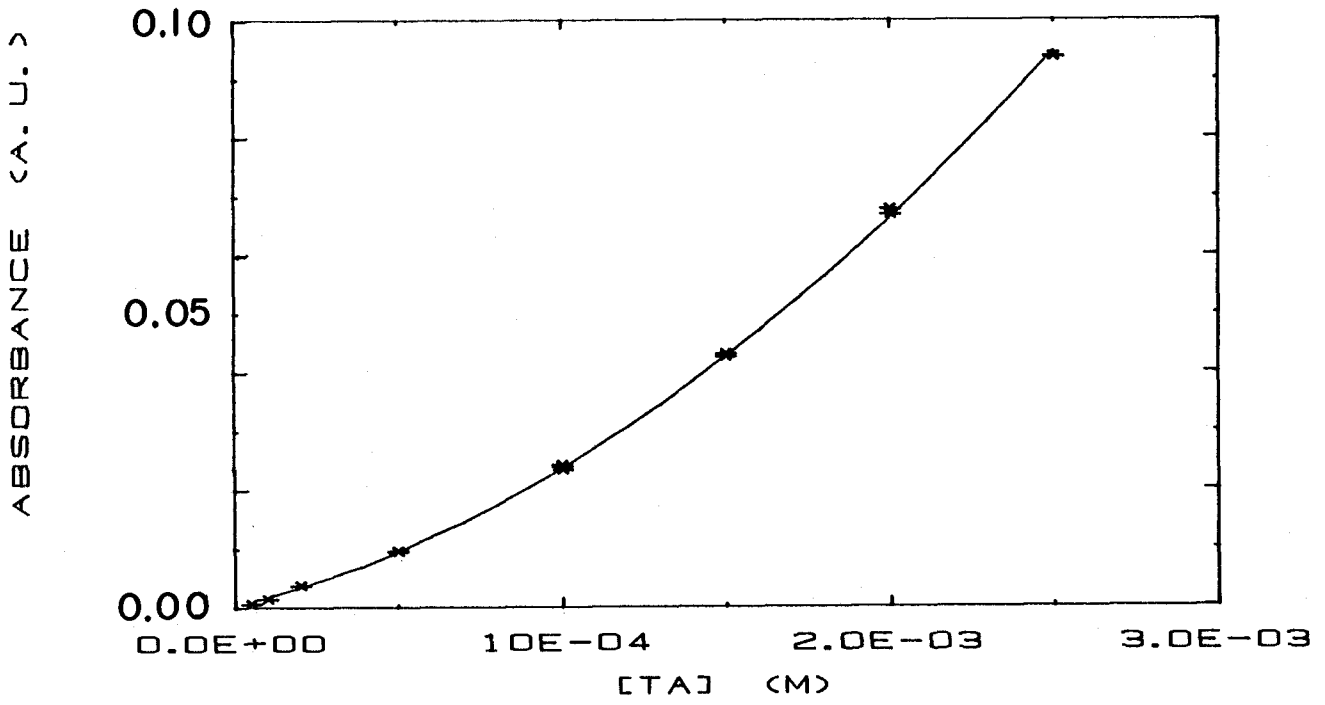

Figure 22. Absorbance of Azomethine H.
Wavelength = 412.5 nm, Acetate Buffer = 0.244 M, T = 25°C.
* Experimental Absorbances, Experiment I.
--- Calculated Absorbances, Equation 48 and Table VIII.

The equilibrium constant and molar absorptivity values for the azomethine monomer and dimer have been previously discussed. Values for the stability constants and molar absorptivity values for the boron/azomethine complexes have been determined using FITEQL (21). In the program the parameter adjustment procedure is based on minimizing the sum of squares, SOS, over all the experimental data points, m

$$SOS = \sum_{m} \left[\frac{Y^2_{(m)}}{s_Y{}^2_{(m)}} \right] \qquad (49)$$

where $Y_{(m)}$ is the difference between the calculated and the experimental absorbances. The calculated absorbance is determined from Equation 24, where the species concentrations have been determined using Equations 25 - 29 with the current values for the adjustable parameters. The propagation of experimental error, $s_{Y(m)}$ is calculated from

$$s_Y{}^2(m) = \left(\frac{\partial Y}{\partial TA} \right)^2 \Bigg|_m s_{TA}{}^2(m) + \left(\frac{\partial Y}{\partial TB} \right)^2 \Bigg|_m s_{TB}{}^2(m) \qquad (50)$$

$$+ \left(\frac{\partial Y}{\partial abs}\right)^2 \Bigg|_m s_{abs}^2 (m)$$

where s_{TA}, s_{TB}, and s_{abs} are the estimated errors in the experimental data. It is assumed that the errors in each term are independent (non-correlated) such that the sum of the cross terms is equal to zero. The derivatives that appear in the error propagation equation are calculated from the chemical equilibrium equations. The estimated errors in the experimental data have been calculated from the following formulae

$$s_{TA} = 1 \times 10^{-6} \text{ M} + 0.01 \text{ TA}$$

$$s_{TB} = 1 \times 10^{-6} \text{ M} + 0.01 \text{ TB}$$

$$s_{abs} = 4 \times 10^{-3} \text{ A.U.} + 0.01 \text{ abs}$$

where the first number in the formula is an estimation of the absolute error and the second is an estimation of the relative error in the experimental measurements.

Values for the stability constants and molar absorptivities for five equilibrium species have been calculated and are listed in Table IX. The experimental and calculated equilibrium absorbances have been graphed in Figure 23. The absorbances greater than 2.0 A.U. are effective absorbances, abs_{eff}, determined from measurements of diluted samples. A comparison of the

Table IX. Azomethine H/$B(OH)_3$ Equilibrium Constants.

Species	Symbol	Stability Constant	S.D.[a] of Stability Constant	Molar Absorptivity (A.U. $cm^{-1}M^{-1}$)	S.D.[a] of Molar Absorptivity (A.U. cm^{-1} M^{-1})
Azomethine H monomer	A	—	—	14	—
Azomethine H	A_2	$K_A = 1$	—	9.7×10^3	—
$B(OH)_3$	B	—	—	0.00	—
1:1 complex	AB	$K_1 = 7.9$	$\pm$ 13	6.7×10^3	$\pm 1.0 \times 10^4$
2:1 complex	A_2B	$\beta_2 = 1.2 \times 10^5$	$\pm 7.5 \times 10^3$	2.0×10^4	$\pm 9.8 \times 10^2$

[a] Number of data points = 18.
Data from Experiments II and III. Constants for A and A_2 determined previously using data from Experiment I.

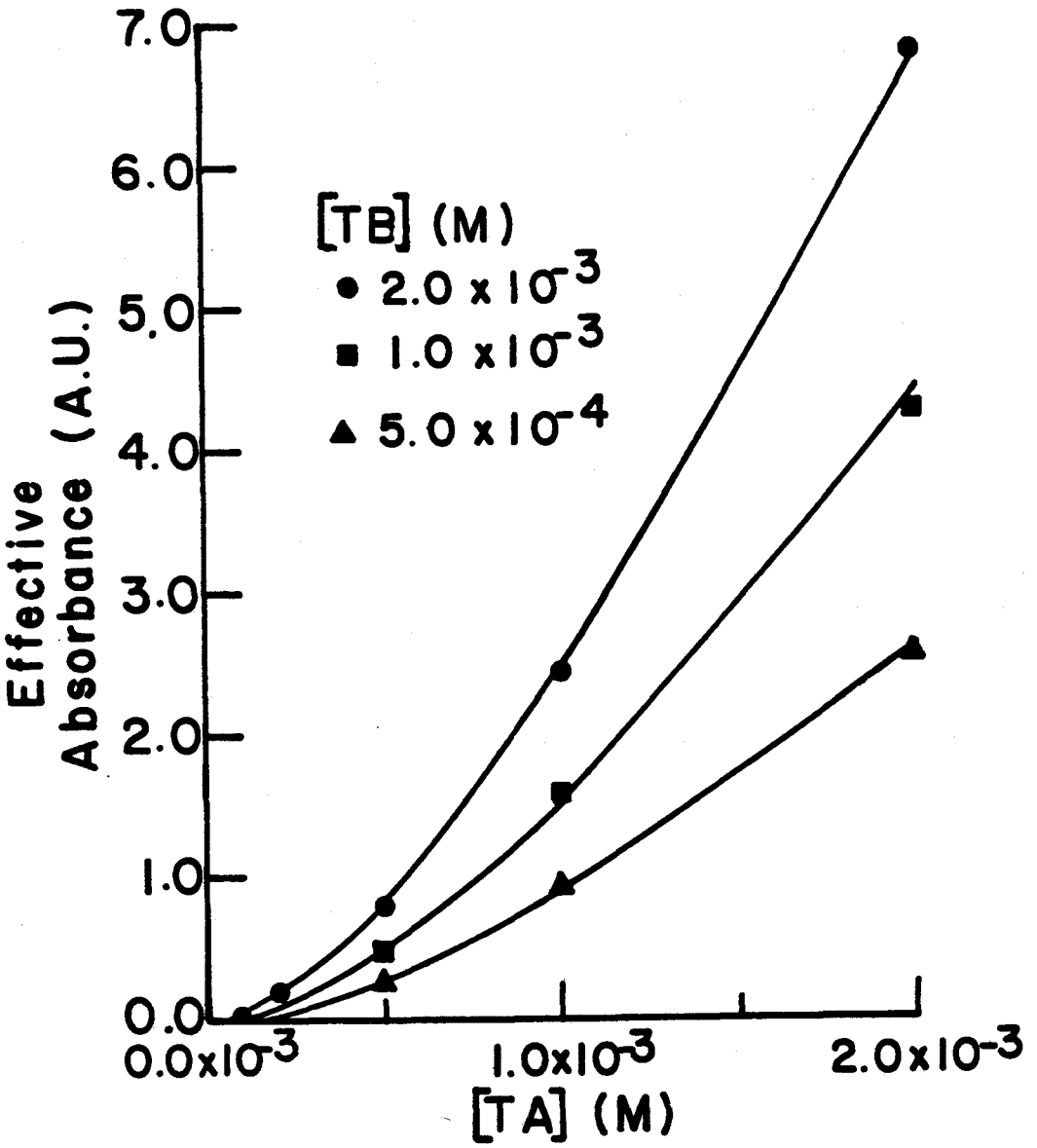

Figure 23. Equilibrium Absorbance.
Acetate buffer = 0.244 M, T = 25°C. Solid line represents calculated absorbance.
For $abs_{exp} > 2.0$ A.U., $abs_{eff} = abs_{exp} \times 5$.
Data from Experiment II.

experimental and calculated absorbances is presented in Table X. The relative error in the difference between the calculated and experimental absorbances is about 3%. When equilibrium constants and molar absorptivities are determined simultaneously from spectrophotometric data, there is a covariability in the values determined. Thus while the constants determined here represent the data very well, they are not necessarily the only combinations of ε and K which could represent the data. Some of the problems associated with this affect have been discussed by Johnansson (22). But, regardless of its lack of uniqueness, the equilibrium model is an excellent representation of the experimental data over the concentration range considered.

From Equations 25-29 a comparison of the absorbance contribution from each species is possible, Figure 24. The effective absorbance versus total azomethine has been plotted for total boron concentration 2×10^{-3} M. The A_2B species is the predominate absorbing species. The absorbance contributions from the azomethine monomer and dimer are comparable. The concentration of the monomer is large but its molar absorptivity is small, while the concentration of the dimer is small but its molar absorptivity is large. As the concentration of total azomethine is increased, formation of the A_2B species over

Table X. Comparison of Experimental and Calculated Equilibrium Absorbances.

TA (M)	TB (M)	abs^{exp} (A.U.)	abs^{cal} (A.U.)	$abs^{exp}-abs^{cal}$ (A.U.)	relative difference[a] (%)
2×10^{-3}	2×10^{-3}	6.822	6.765	0.057	0.84
2×10^{-3}	1×10^{-3}	4.266	4.427	-0.20	-4.7
2×10^{-3}	5×10^{-4}	2.552	2.634	-0.082	-3.2
1×10^{-3}	2×10^{-3}	2.444	2.498	-0.054	-2.1
1×10^{-3}	1×10^{-3}	1.590	1,565	0.025	1.6
1×10^{-3}	5×10^{-4}	0.937	0.909	0.028	3.0
5×10^{-4}	2×10^{-3}	0.810	0.830	-0.020	-2.4
5×10^{-4}	1×10^{-3}	0.491	0.489	0.002	0.41
5×10^{-4}	5×10^{-4}	0.280	0.272	0.008	2.9

[a] relative difference $= \dfrac{abs^{exp}-abs^{cal}}{abs^{exp}}$

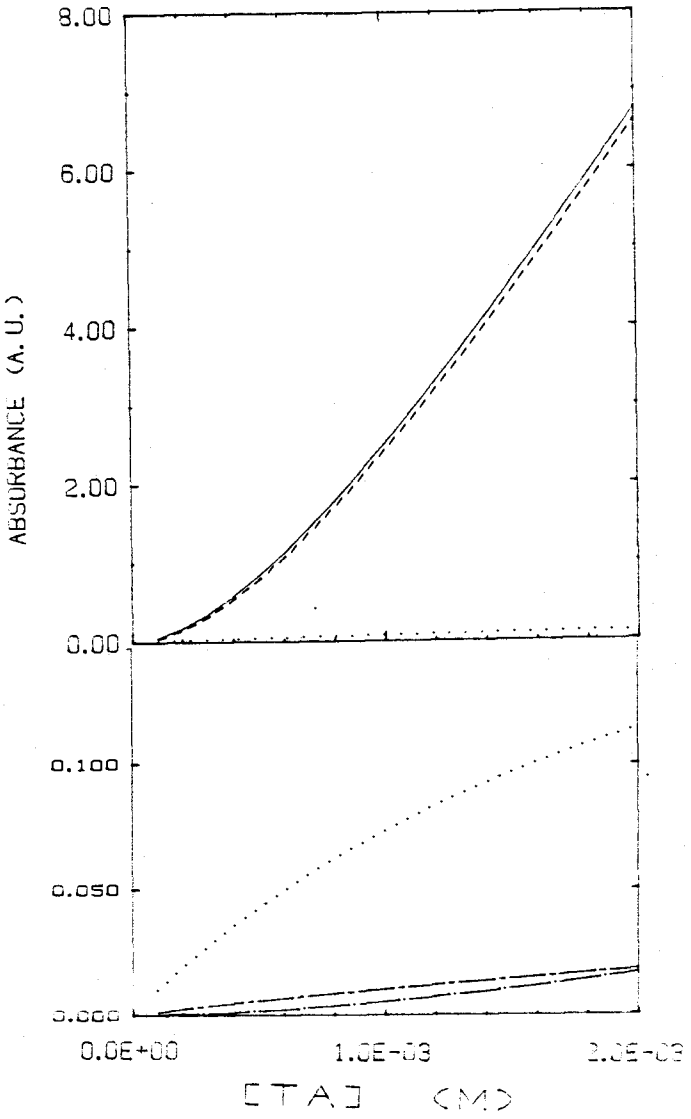

Figure 24. **Absorbance of Individual Species. TB = 2.0 x 10^{-3} M, Acetate Buffer = 0.244 M, T = 25°C.**
—— Total abs — – — A abs
---A_2B abs _·_ A_2 abs
..... AB abs

the AB species is favored. Because the A_2B species complexes two azomethine molecules, there is less and less of an increase in the free azomethine concentration per increase in the total azomethine concentration. This effect is observed in the bending over of the AB and A absorbance curves, and a bending up of the A_2B and A_2 absorbance curves.

Kinetics

The course of the reactions can be divided into two periods the initial period ($t < 1000$ s) in which the concentration of free azomethine and free boric acid remain approximately constant, and the long term ($1000 \text{ s} < t < 60$ ks) in which the concentration of the complexes becomes significant.

In Experiments II, III, and IV the absorbance during the initial 600 s was recorded as a function of time. From these recordings the initial rate, d(abs/b)/dt, has been calculated. During the initial 600 s the concentration of both complexes is negligible compared to the total boron and azomethine concentrations, and therefore Case II has been used to interpret the data. The plot of log rate versus log TA at constant TB defined a straight line with a slope of 2, and the plot of log rate versus log TB at constant TA defined a straight line

with a slope of 1. These plots suggest that the initial reaction is first order with respect to TB and second order with respect to TA.

A graph of the initial rate versus TA^2TB is shown in Figure 25. The solid line represents the function

$$\frac{d(abs/b)}{dt} = mTA^2TB + c \qquad (51)$$

which is a linear approximation describing the rate as a function of the product TA^2TB. The first term has been interpreted in terms of the formation of the A_2B complex. The value of the intercept c is small and corresponds to the contribution from the AB complex.

The initial rate law for the formation of the A_2B complex can be expressed as

$$\frac{d(abs_{A_2B}/b)}{dt} = \varepsilon_2 k_{f2}\ TA^2TB \qquad (52)$$

The value of the forward rate constant has been determined from the slope of the initial rate versus TA^2TB. The initial rate law for the formation of the AB complex can be expressed as

$$\frac{d(abs)_{AB}/b)}{dt} = \varepsilon_1\ k_{f1} TATB \qquad (53)$$

The value for the forward rate constant has been

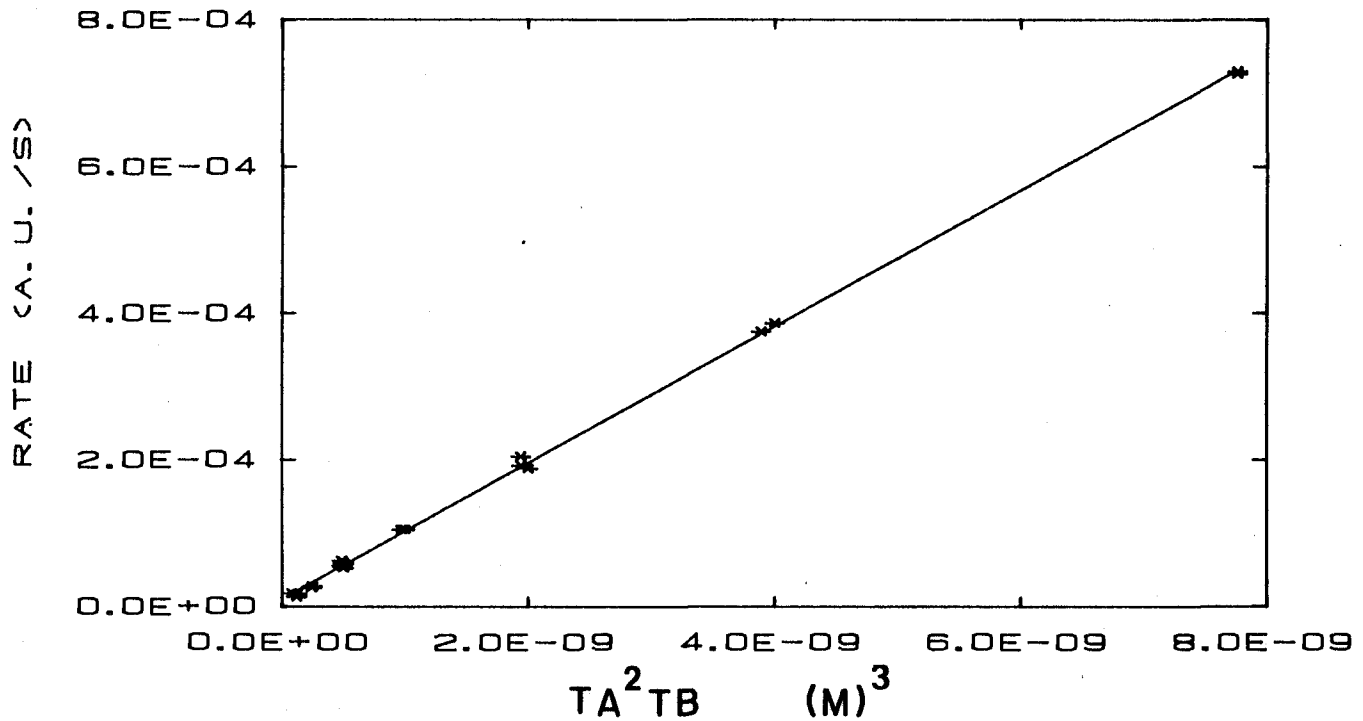

Figure 25. Initial Rate Analysis. Acetate Buffer = 0.244 M, T = 25°C, Rate = 93079 TA^2TB + 9.6 x 10^{-6}. Data from Experiments II, III, and IV.

determined by optimizing the fit of the calculated rates given by Equations 52 and 53 to the observed rate.

A graph of absorbance versus time for TA = 5×10^{-4} M, TB = 2×10^{-3} M during the initial 1000s is shown in Figure 26. These experimenal conditions favor the formation of the AB complex. The solid circles represent the experimental absorbance signal. The dashed line represents the absorbance contribution from the formation of the A_2B complex, and the dotted line represents the absorbance contribution from the formation of the AB complex. The solid line represents the total calculated absorbance as the sum of the absorbance from the A_2B and AB complexes. It is seen that even for experimental conditions favoring the formation of the AB species, the contribution of the AB species to the total absorbance is small and becomes less with time.

The above discussion assumes that the concentration of free azomethine and free boric acid remain approximately constant, and that the back reactions are insignificant (Case II). However, when considering the entire approach to equilibrium, the concentration of the complexes becomes significant in the material balance equations and the back reactions must be considered. To be consistent over the entire course of the reaction, from initial to equilibrium conditions, it is necessary to express the reaction rate as

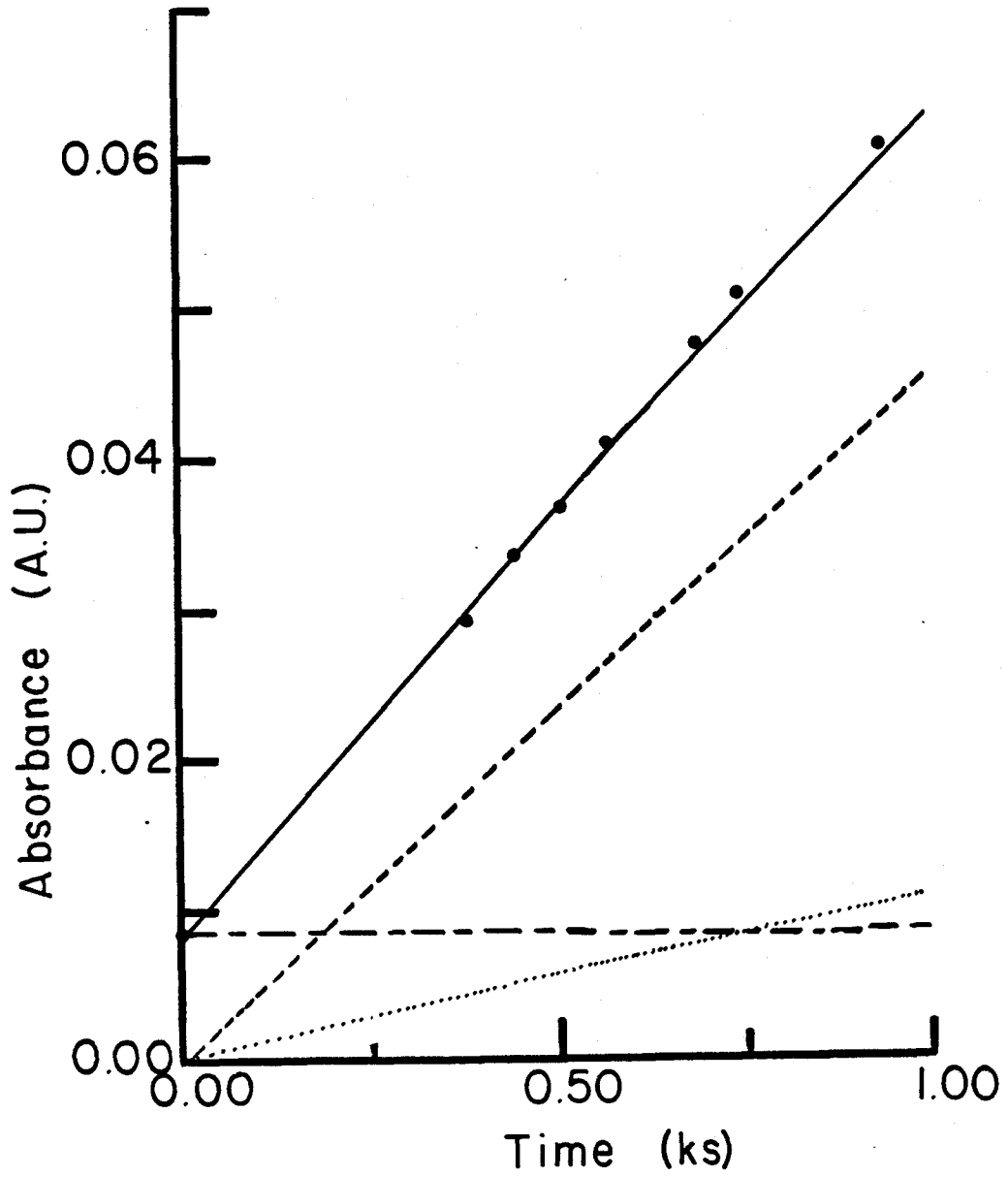

Figure 26. Initial Kinetics of Individual Reactions. TA = 5.0×10^{-4} M, TB = 2.0×10^{-3} M, Acetate Buffer = 0.244 M, T = 25°C.
• abs_{exp} --- A_2B abs ———A + A_2 abs
—— Total abs ..... AB abs

$$\frac{d(abs/b)}{dt} = \frac{\varepsilon_A d[A]}{dt} + \frac{\varepsilon_{A_2} d[A_2]}{dt} + \frac{\varepsilon_{AB} d[AB]}{dt} + \frac{\varepsilon_{A_2B} d[A_2B]}{dt} \quad (54)$$

where the rate equations for the AB and A_2B complexes are expressed in Equations 30 and 31. The relative values of the forward and backward rate constants are fixed by the relations $\beta_2 = k_{f2}/k_{b2}$ and $K_1 = k_{f1}/k_{b1}$. Values for the backward rate constants have been determined from the equilibrium stability constants. Values for both sets of rate constants are listed in Table XI.

The concentration of each complex during the approach to equilibrium has been approximated by simultaneous numerical integration of Equations 30 and 31 subject to Equations 25 and 26 at 10 second intervals (constants from Tables IX and XI). For each 10 s interval the rate integral is estimated by the area of a trapezoid. The sum of each of these areas results in an approximation of the total absorbance for a time t.

The experimental and computed absorbances have been plotted versus time. Figures 27-29 illustrate the absorbance development during the initial 1000s and Figures 30-32 illustrate the absorbance development during the entire approach to equilibrium. The experimental absorbances greater than 2.0 A.U. are effective absorbances, abs_{eff}, determined from measurements of solutions which have been diluted. In each figure TA is constant. The solid line represents the calculated

Table XI. Kinetic Rate Constants.

Species	Stability Constant	Forward Rate Constant	Backward Rate Constant
AB	7.9	$1.8 \times 10^{-3}\ s^{-1}M^{-1}$	$2.3 \times 10^{-4} s^{-1}$
A_2B	1.2×10^{5}	$4.7\ s^{-1}M^{-2}$	$4.0 \times 10^{-5} s^{-1}$

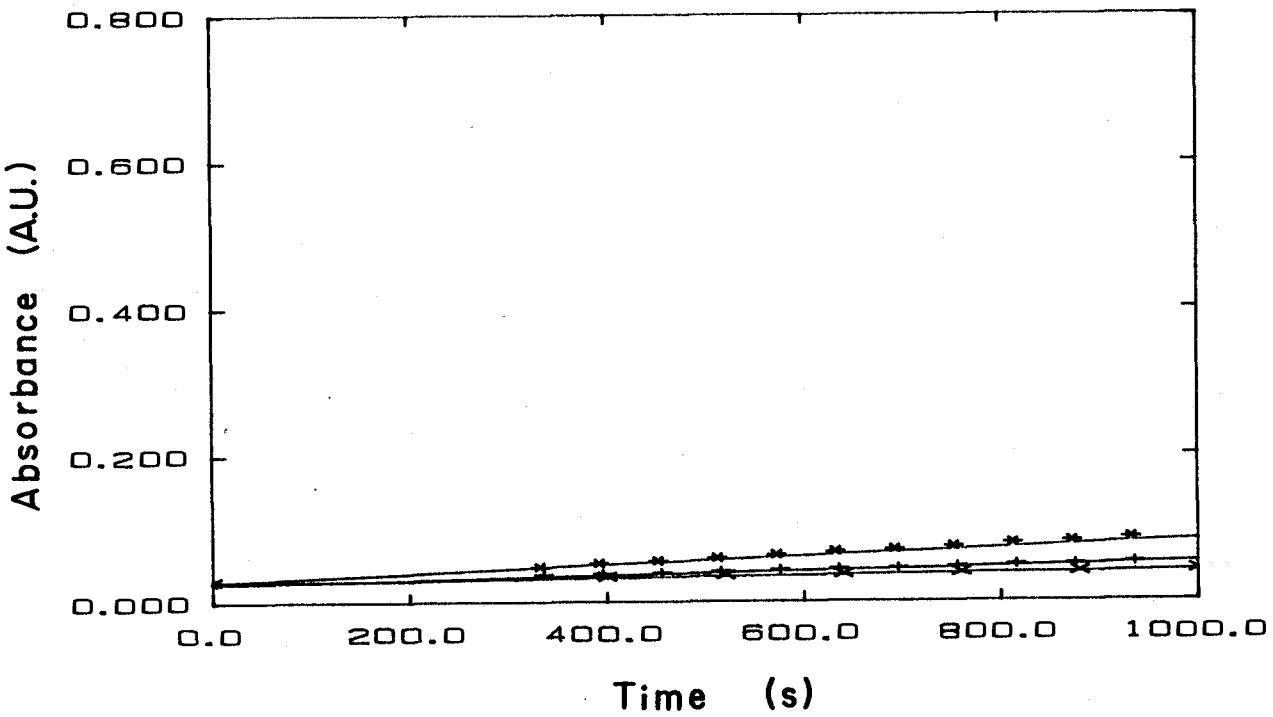

Figure 27. Initial Kinetics of Reaction: TA = 5.0×10^{-4} M.
Acetate Buffer = 0.244 M, T = 25°C.
Solid line represents calculated absorbance.
* TB = 2.0×10^{-3} M, + TB = 1.0×10^{-3} M, x TB = 4.0×10^{-4} M.

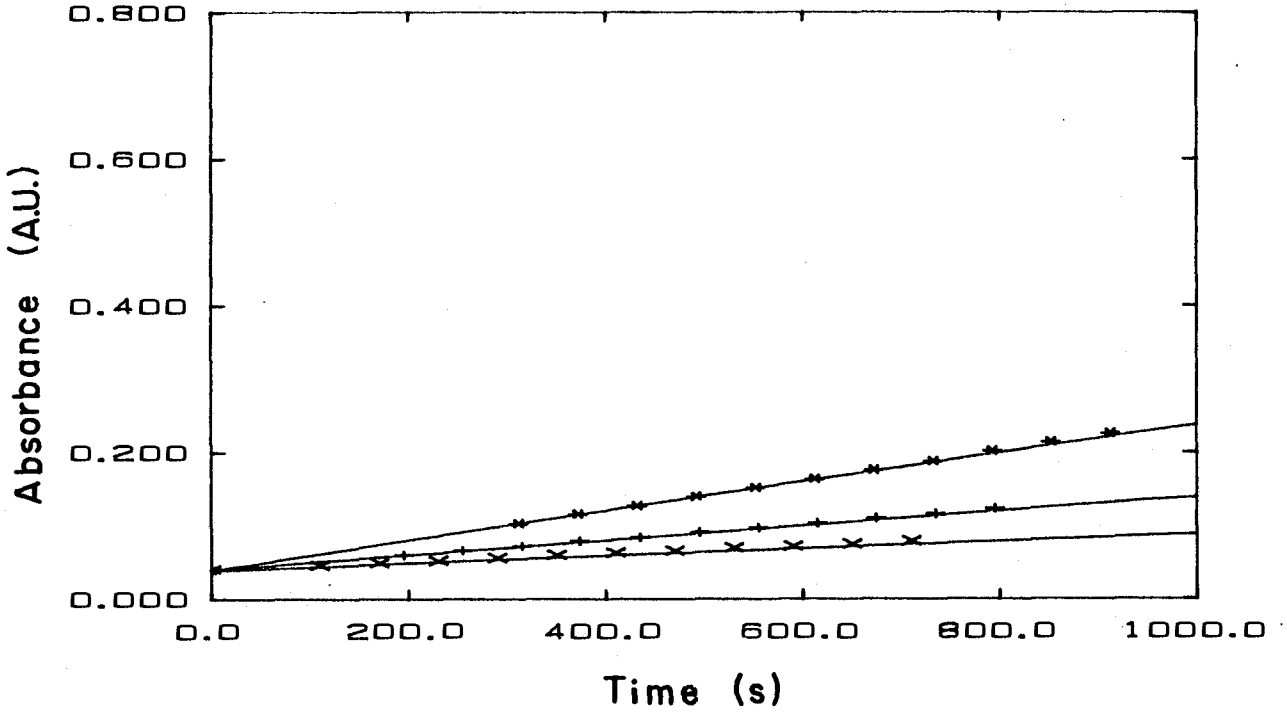

Figure 28. Initial Kinetics of Reaction: TA = 1.0×10^{-3} M.
Acetate Buffer = 0.244 M, T = 25°C.
Solid line represents calculated absorbance.
* TB = 2.0×10^{-3} M, + TB = 1.0×10^{-3} M, x TB = 5.0×10^{-4} M.

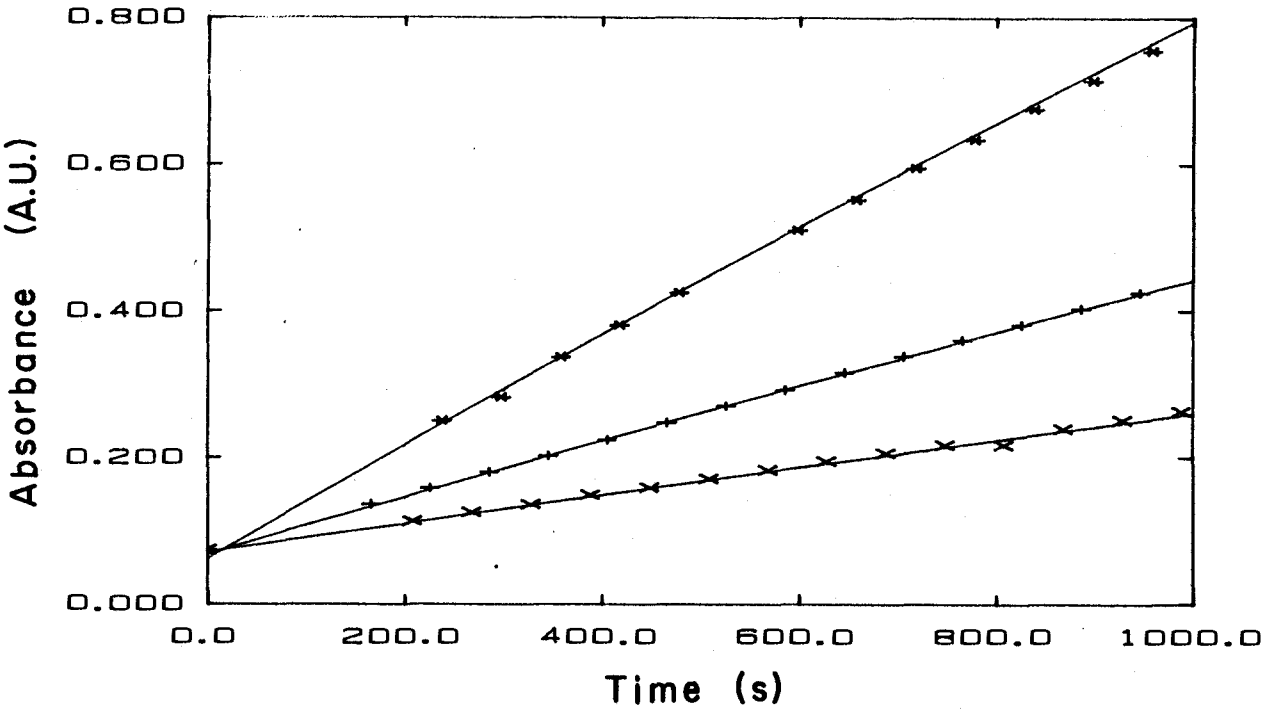

Figure 29. Initial Kinetics of Reactions: TA = 2.0×10^{-3} M.
Acetate Buffer = 0.244 M, T = 25°C.
Solid line represents calculated absorbance.
* TB = 2.0×10^{-3} M, + TB = 1.0×10^{-3} M, x TB = 5.0×10^{-4} M.

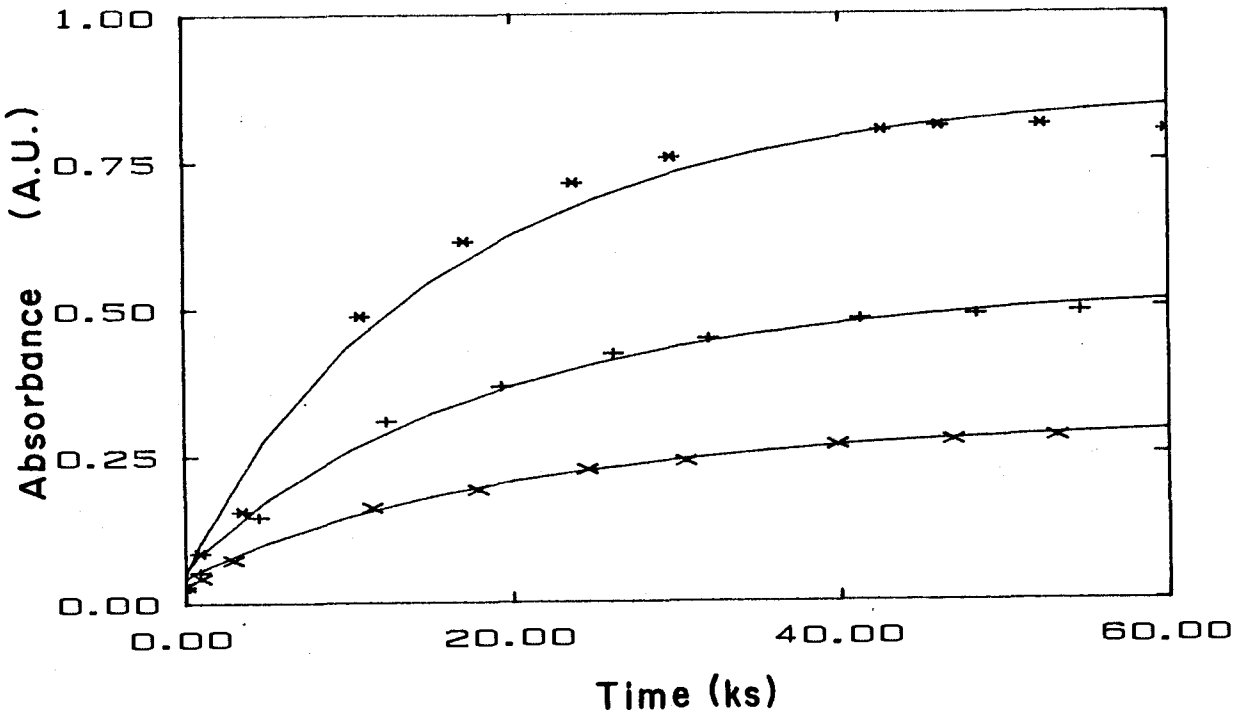

Figure 30. Kinetics of Reaction: TA = 5.0×10^{-4} M.
Acetate Buffer = 0.244 M, T = 25°C.
Solid line represents calculated absorbance.
* TB = 2.0×10^{-3} M, + TB = 1.0×10^{-3} M, x TB = 5.0×10^{-4} M.

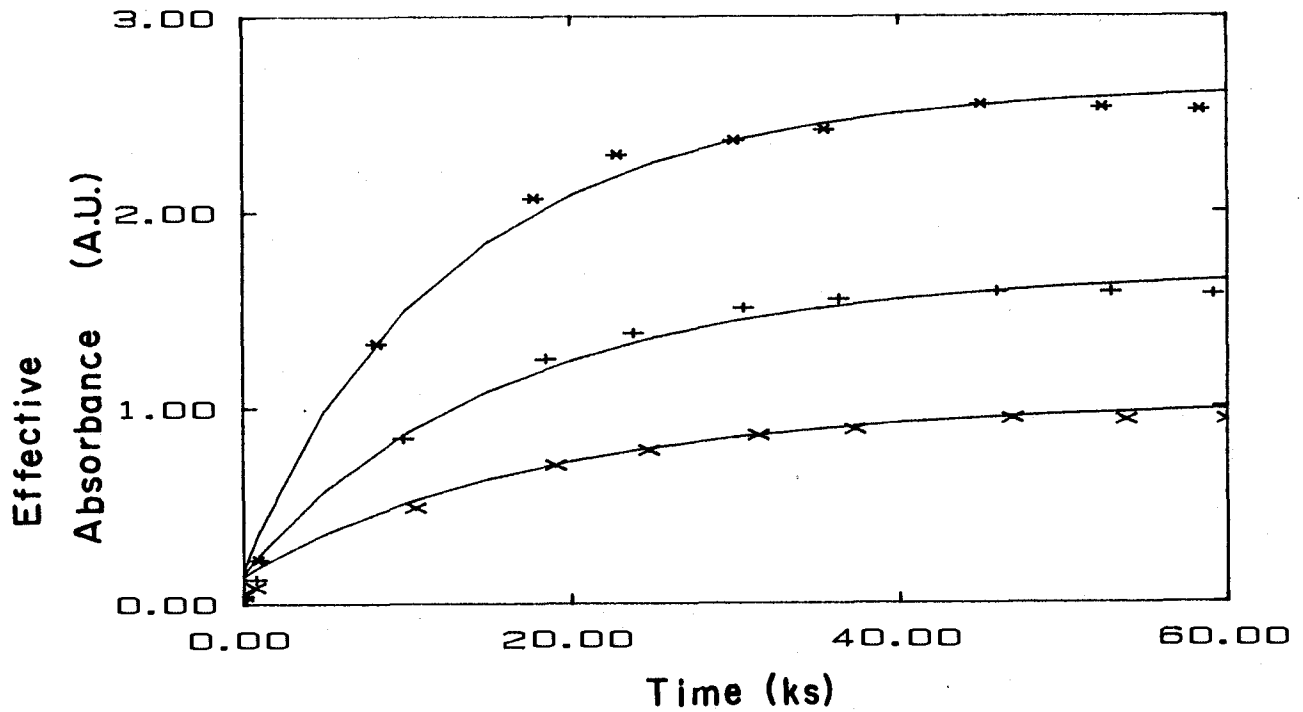

Figure 31. Kinetics of Reaction: TA = 1.0×10^{-3} M.
Acetate buffer = 0.244 M, T = 25°C.
Solid line represents calculated absorbance.
* TB = 2.0×10^{-3} M, + TB = 1.0×10^{-3} M, x TB = 5.0×10^{-4} M.
For $abs_{exp} > 2.0$ A.U., $abs_{eff} = abs_{exp} \times 5$.

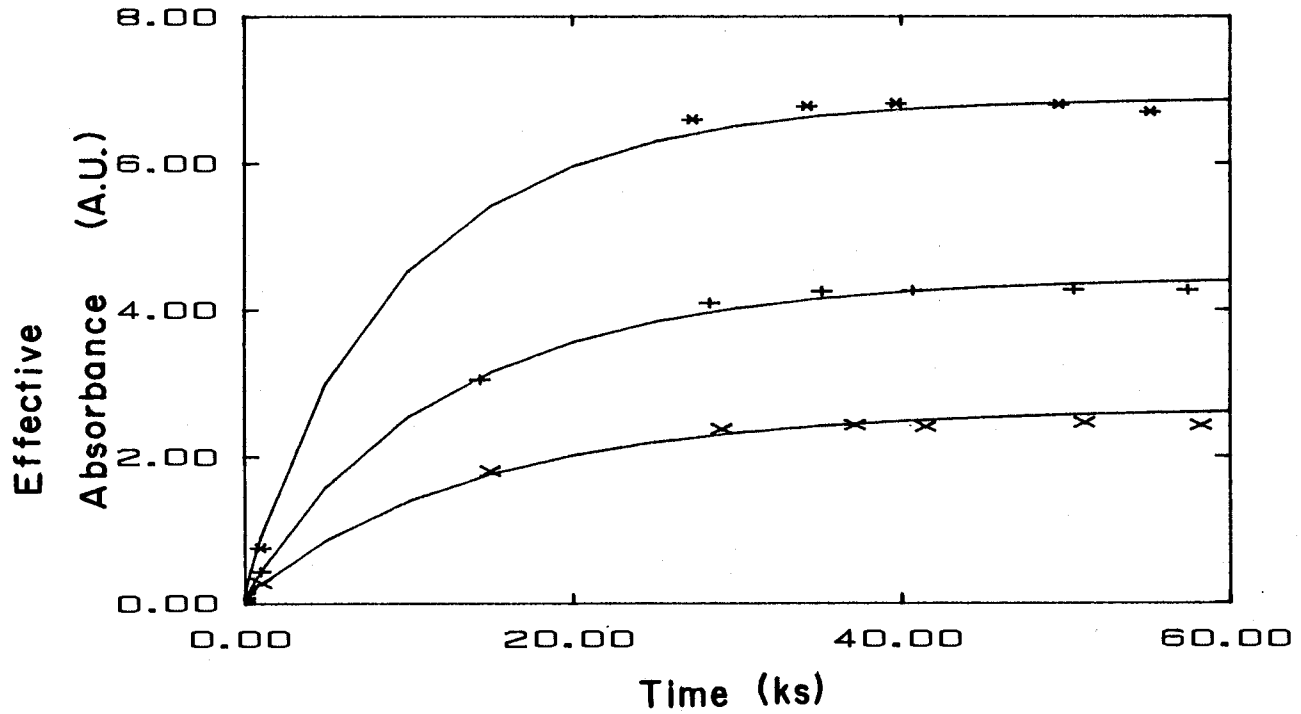

Figure 32. Kinetics of Reaction: TA = 2.0×10^{-3} M.
Acetate Buffer = 0.244 M, T = 25°C.
Solid line represents calculated absorbance.
* TB = 2.0×10^{-3} M, + TB = 1.0×10^{-3} M, x TB = 5.0×10^{-4} M.
For abs_{exp} > 2.0 A.U.μ $abs_{eff} = abs_{exp} \times 5$.

absorbance at time t by the integration described in the preceding paragraph. The *, +, and x represent the experimental absorbances for TB = 2×10^{-3}M, 1×10^{-3} M, and 5×10^{-4} M, respectively.

The absorbance development is linear with respect to time during the initial 1000s. Figures 27-29 have been graphed on the same absorbance axis scales to illustrate that the increase in the rate is greater per increase in TA as compared to the same increase in TB. Higher concentrations of TA will enable determination of lower boron concentrations for a fixed measurement time because a greater absorbance signal is obtained.

Figures 30-32 have been graphed on different absorbance axis scales to illustrate that the absorbance development curves follow the same general shape. The equilibrium absorbances have been previously discussed and are graphed in Figure 23. The length of time to equilibrate is similar for all solutions within this concentration range.

It is of interest to show the contribution of each complex to the total absorbance. A graph of the computed concentrations of each species during the approach to equilibrium is provided in Figure 33, TA = 5×10^{-4} M and TB = 2×10^{-3} M. These experimental conditions are favorable for the formation of the AB complex. The absorbance contribution for each species is provided in Figure 34. The shape of the total absorbance versus time

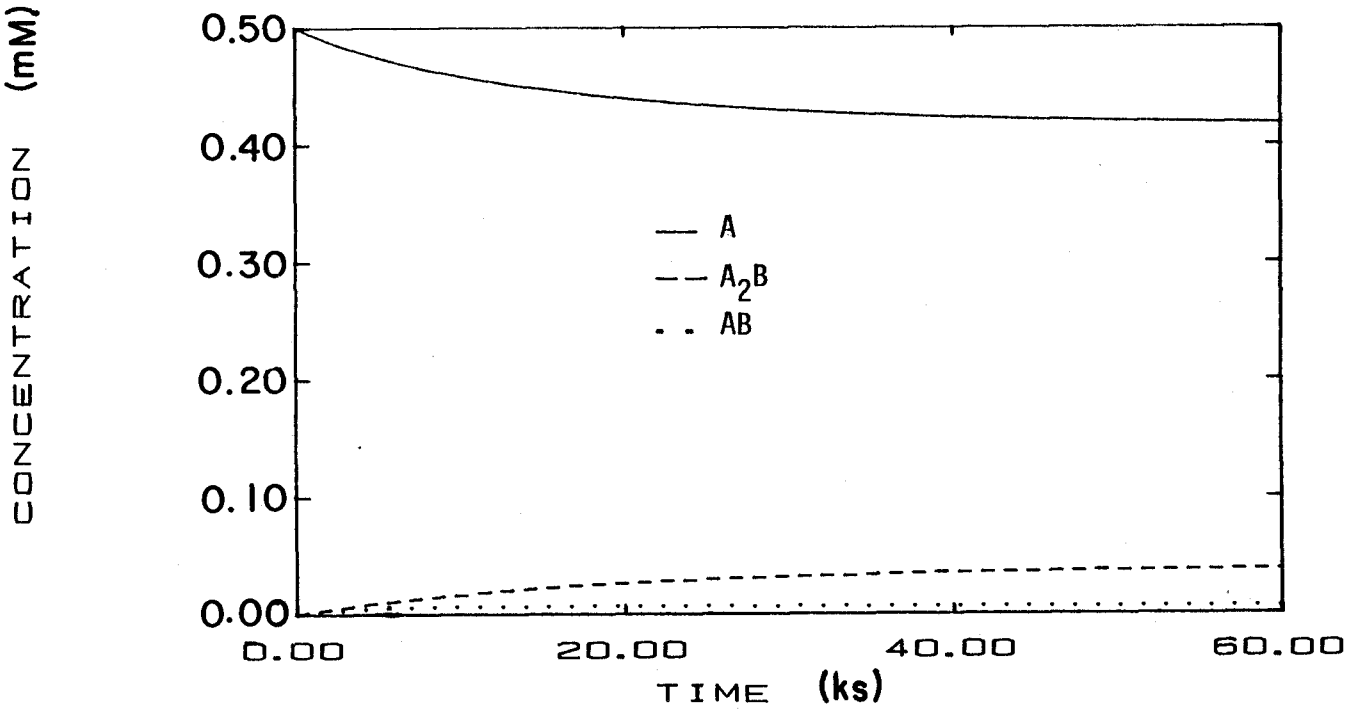

Figure 33. Kinetics of Individual Reactions. Concentration vs. Time. TA = 5.0×10^{-4} M, TB = 2.0×10^{-3} M, Acetate Buffer = 0.244 M, T = 25°C.

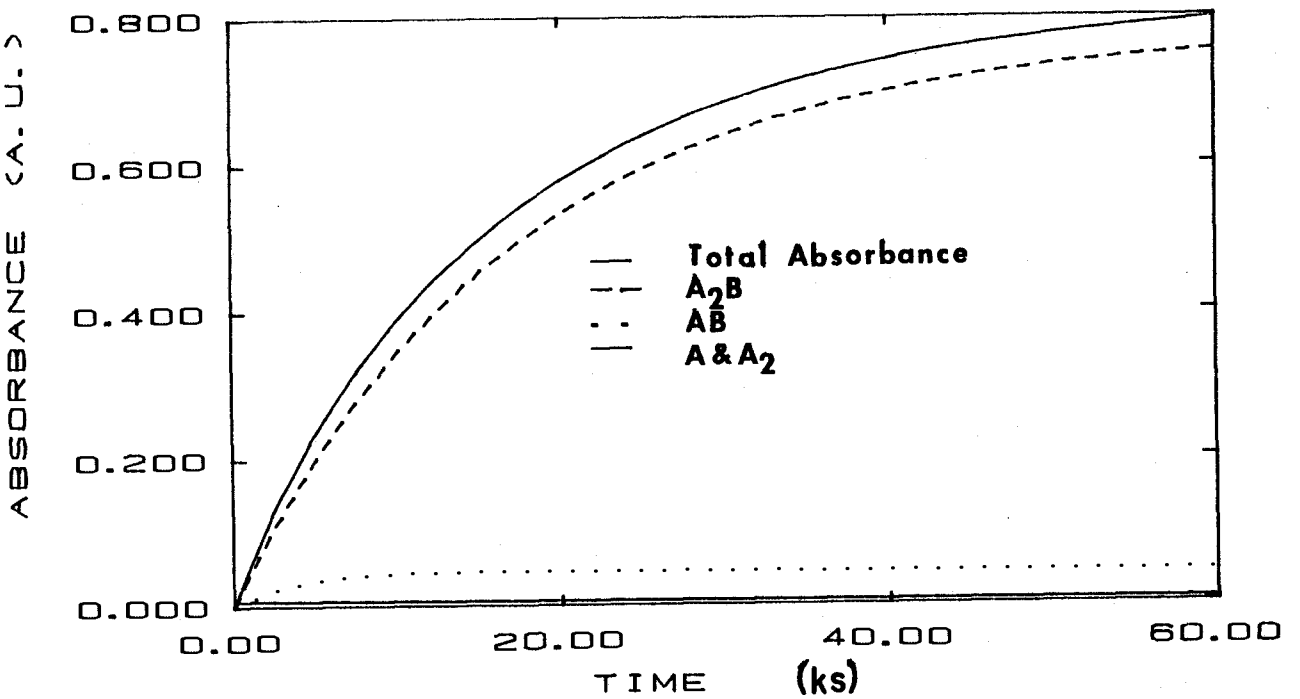

Figure 34. Kinetics of Individual Reactions. Absorbance vs Time. TA = 5.0×10^{-4} M, TB = 2.0×10^{-3} M, Acetate Buffer = 0.244 M, T = 25°C.

curve is due primarily to the absorbance of the A_2B complex. The AB species has been shown to be important during the initial 1 ks (Figure 26).

The rate equations and corresponding rate constants have been empirically determined. Thus while the equations and constants presented here represent the data very well, they are not necessarily the only interpretation which could represent the data. But, regardless of its lack of uniqueness, the kinetic model is an excellent representation of the experimental data over the concentration range considered.

Predictions of the total absorbance and species concentration during the system's approach to equilibrium are possible. These predictions are useful in determining optimal experimental parameters for the analysis of boron within a specified concentration range. This application is demonstrated in the flow system optimization section of this thesis.

Application

A flow system has been designed for the determination of boron concentration via three different kinetic analysis modes: stopped flow, continuous flow, and flow injection. In stopped flow analysis, the reagents and analyte are mixed and pumped into the flow through detector, flow is stopped and the formation of the

complex is monitored as time passes. Long reaction times are possible, allowing for more complete development of the colored complex and detection of lower concentrations. Because the absorbance of the blank does not vary significantly with time, although the reagent is being constantly consumed, only a single blank measurement is necessary.

In continuous flow analysis, the reagents and analyte are mixed and flow continuously through a delay loop to the detector. The short reaction times in continuous flow analyses increase sample throughput, but decrease sensitivity. However, with high concentrations of boric acid the sensitivity is sufficient.

Flow injection analysis is based on injection of a liquid sample into a moving carrier stream of reagent. The injected sample forms a zone that disperses on its way to the detector. In this zone the sample reacts with components of the carrier stream forming a colored species to be sensed in the flow through detector. A typical recording has the form of a sharp peak, the height of which is related to the concentration of the analyte. The advantage of this mode is the extremely small sample volumes (100 μL) required. The disadvantage is the low sensitivity due to the small sample size and short

reaction time. However, the low sensitivity is not a problem with high concentrations of boric acid.

With kinetic methods the rate of formation of the colored complexes is of importance rather than the equilibrium absorbance signal. Kinetic methods have been defined and classified by Pardue (23). The techniques presented here are fixed time methods, where the absorbance signal is recorded at a fixed measurement time.

There are several advantages in using kinetic methods for analytical purposes as opposed to equilibrium methods. The kinetic method is faster since measurements are made before equilibrium is reached. The dynamic range of a kinetic method can be extended by adjusting the time of measurement. Kinetic methods have certain limitations since they involve the detection of a quantity related to the rate of reaction. These limitations include the need for strict control of reaction conditions (e.g. pH, temperature, time).

Flow System Design

A diagram of the flow system is provided in Figure 35. For continuous and stopped flow analysis, the 2-way valve is in position A. The 3-channel pump allows different concentrations of the azomethine reagent and acetate buffer to be prepared. The standards or samples

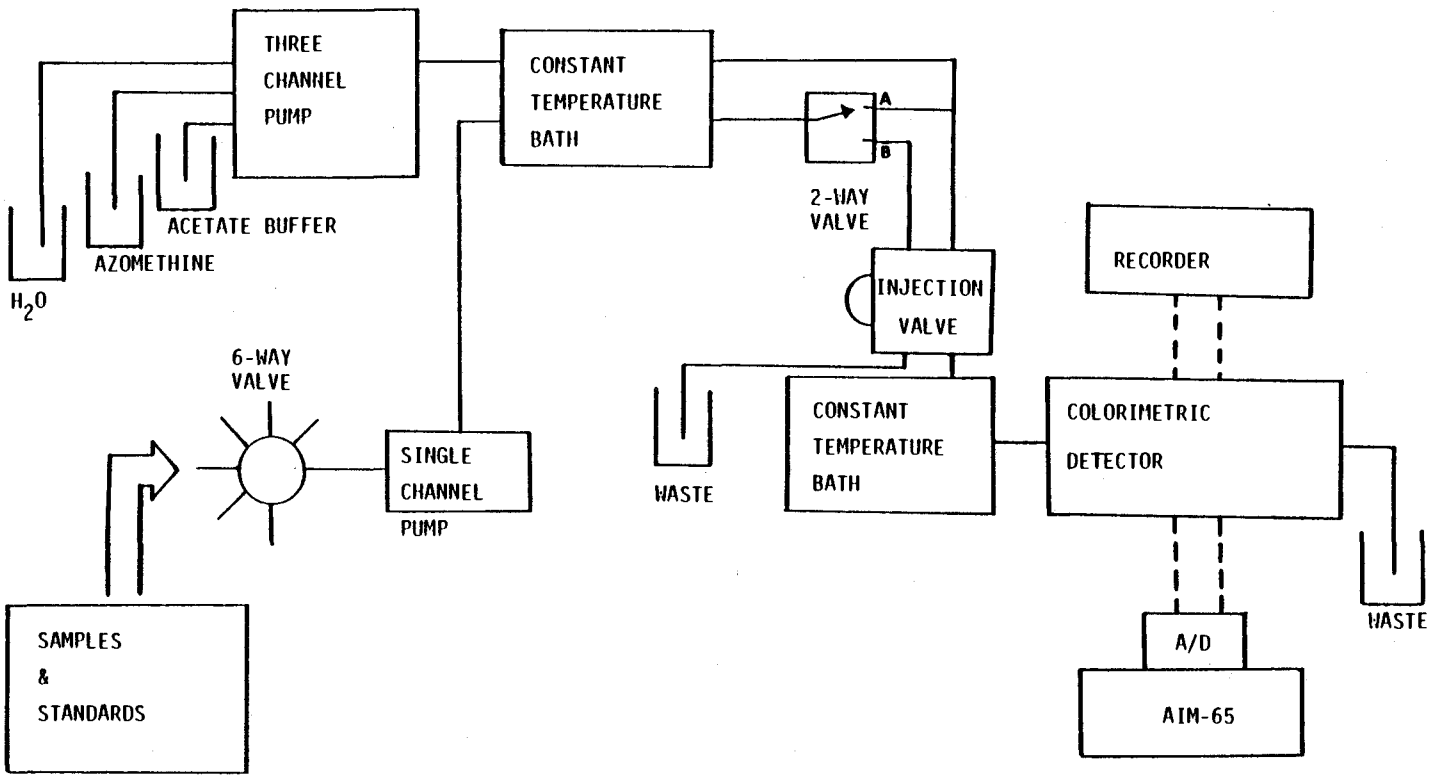

Figure 35. Flow System for Spectrophotometric Analysis. Pumps, valves, and data acquisition controlled by microprocessor.

are selected with the 6-way valve and pumped to a tee by the single channel pump. At the tee the reagent/buffer solution and sample solution merge, and flow through a mixing coil submerged in a constant temperature bath, and on to the absorbance flow cell. After measurement the solution flows into a waste container. Continuous measurements are made while the solution is passing through the flow cell. In stopped flow analysis the flow is stopped while the solution is present in the flow cell and the progress of the reaction is monitored for the portion of time of interest. The flow is stopped by halting both pumps.

For flow injection measurements the 2-way valve is in position B. The reagent/buffer solution is prepared as described previously. The selected sample is pumped to the injection loop by the single channel pump with the excess sample solution flowing into a waste container. The sample is introduced as a plug into the reagent/buffer main stream. The combined flow goes through the mixing coil, absorbance flow cell, and into the waste container. The flow injection measurements are made when the plug travels through the flow cell and absorbance peak heights are measured.

Components for the system which were adaptable to microcomputer control were selected for use. The injection loops and valves were equipped with pneumatic

activators to allow computer controlled switching. The major components of the system are each described in greater detail in the following paragraphs. Table XII contains a list of the components and their sources.

Components

The 3-channel pump is a microprocessor controlled solvent delivery system, designed for pumping up to three solvents in various compositions at precisely controlled flow rates and pressures. External remote control of the pump unit is made with a +5 volt pulse to either the run or stop hook ups. The control unit monitors the flow rate feedback loop to minimize flow variations. Flow rates from 0.1 to 9.9 mL/min are possible with 3% accuracy. The pump usually operates at 2.0 mL/min combined flow. The buffer comprises 50% of the flow volume with the remaining 50% a dilution of a 0.015 M azomethine solution.

The automatic sample injector is a 6 port rotary injector. The advantage of this injector is that a wide range of injection loop volumes may be installed. In the load position solvent bypasses the injection loop which is being filled with sample. Solvent flows through the sample loop in the inject position. With complete loop loading volumetric precisions of 0.05% are possible. The absorbance flow cell used in the system was designed for

Table XII. Flow System Components.

Component	Source	Comments
3-channel pump	Spectrophysics	Model 8700
Automatic Sample Injector	Rheodyne	Model 7126, pneumatic actuator Model 7163, solenoid valve positive sensing switch
Constant Temperature Bath	HAAKE	3 gallon, circulating pump maintains T $\pm$ 0.1^{o}C
2-way valve	Rheodyne	Model 5301, slider valve Model 5300, pneumatic actuator
6-way valve	Rheodyne	Model 5011
Single-channel pump	Fluid Metering, Inc.	Model RHSY1CKC
Flow Cell	ISCO	5 mm path length cat. #68-0080-045
Colorimeter	ISCO	Model V4 variable wavelength detector
Recorder	Linear Instruments	Model 585, duel channel
A/D	Analog Devices	#574 for 8 bit analog to digital interface
AIM-65	Forthought Products	

absorbance detection in high pressure liquid chromatography. The flow cell cross section is seen in Figure 36. The 0.5 cm light path contains 3.5 µL of illuminated volume. The flow path follows a z-shape which provides a longer path length than a straight through flow configuration. The flow is away from the light source of the V^4 variable wavelength absorbance detector.

The V^4 is a variable wavelength photometric detector. The optical system includes a diffraction grating monochromator. A tungsten lamp is the light source in the 350-750 nm range, and a deuterium lamp is the light source in the 190-350 nm range. Wavelength accuracy is $\pm$ 1 nm with $\pm$ 0.5 nm repeatability. The spectral bandpass is 5 nm. The recorder output is connected to an external strip chart recorder and an analog to digital converter, A/D.

Teflon tubing was used for all flow paths. The mixing coil is comprised of 15 loops, each 13 cm in diameter.

Computer control was emphasized in the design and construction of the flow system so that operation of the system could be controlled by software. A Rockwell AIM-65 microcomputer has been programmed to control the entire system.

For convenience, the main program was written to accomplish these tasks in BASIC, while assembly language

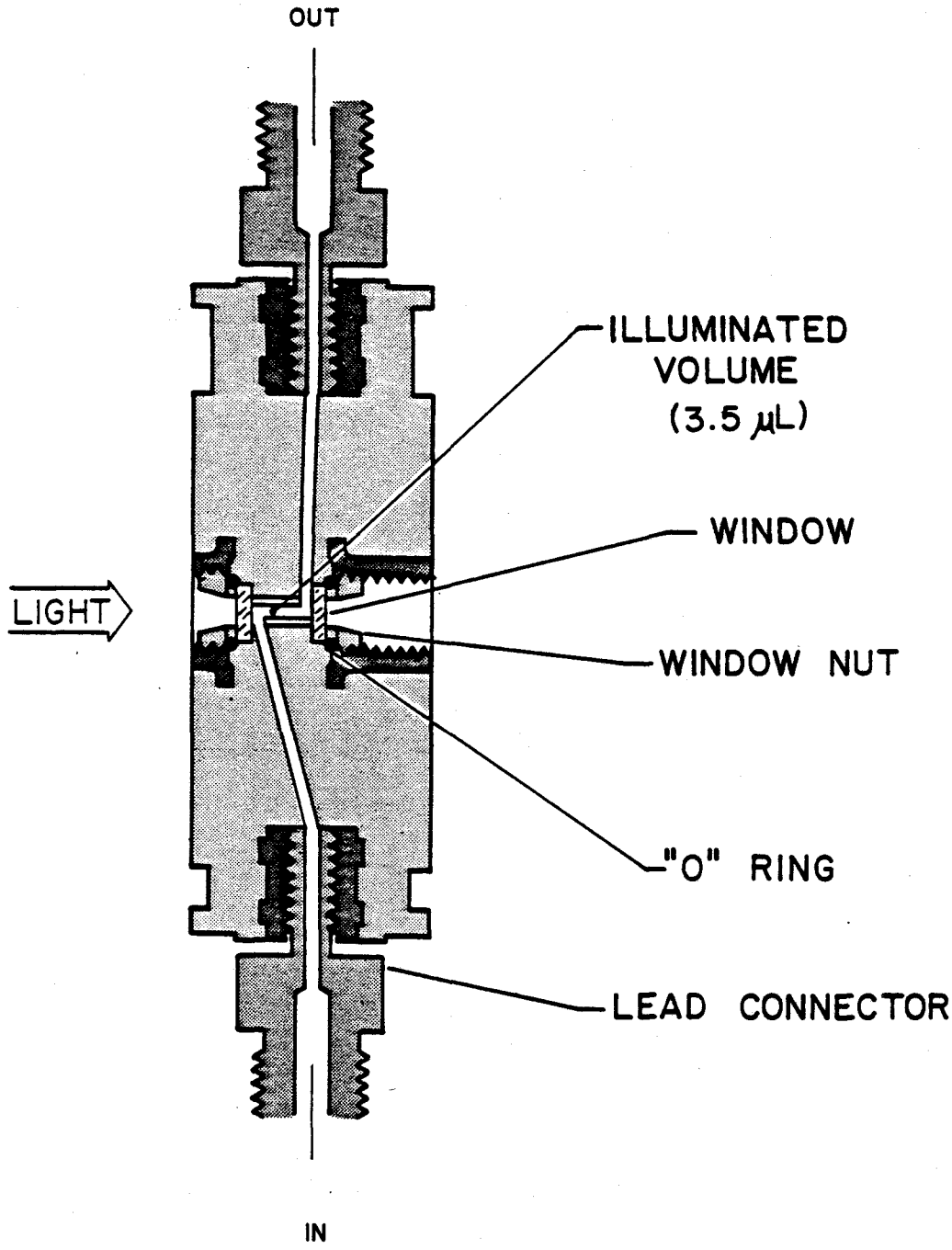

Figure 36. Absorbance Flow Cell. Path length = 0.50 cm.

subroutines are utilized for data collection and control of the system components. A single program is used for all three modes. Absorbance data is stored in data files which are read by a second program for calibration and concentration calculations. A complete listing of both programs is provided in Appendix C.

Optimization of Flow System Parameters

The parameters of this system have been optimized with regards to the range of boron concentrations expected in nuclear reactor coolant water and the signal limitation of the colorimeter (0.01 - 1.00 A.U.) per absorbance range scale setting.

The parameters considered are

- flow rates
- timing
- total azomethine H concentration
- stopped flow development time
- injected sample volume

Adjustments of the flow rate of each pump were made to obtain the desired mixing ratio of the sample:buffer:reagent. A compromise between rapid rates for rinse out of the flow cell and complete filling of the sample lines and slow rates for maximum delay periods was necessary. A 1:1:1 ratio of sample:buffer:reagent was desired. The flow rate of the 3-channel pump was set at 2 mL/min and the single channel pump was set at 1 mL/min.

At these flow rates 350 seconds were required to rinse out the single channel pump and the flow cell, and to fill the sample line. The delay time from sample/reagent mixing to absorbance detection was 30 seconds.

The optimum value of total azomethine H concentration can be calculated from the estimated concentration of boron, the analysis time, and the integrated form of the initial rate equation, Equation 51

$$\frac{abs}{b} = (mTA^2TB + c)t \qquad (55)$$

In this equation m is the slope of the initial rate versus TA^2TB, and c the absorbance intercept. The maximum concentration of $B(OH)_3$ is approximately 0.9 M (solubility of $B(OH)_3$ at 25°C) (11), which will be ~ 0.3 M in the flow cell after on-line dilution. If this sample is to be analyzed via continuous flow analysis (t ~ 30s) and have an absorbance signal of 1 A.U., the azomethine H concentration in the flow cell must be ~ 1.5 mM. The 3-channel pump reservoir has been filled with an 0.015 M azomethine and diluted on-line to obtain a 1.58 mM reagent solution.

The stopped flow development time was also determined from Equation 55 for an absorbance of 0.01 with a 5×10^{-4} M boric acid solution. A delay time of 500 seconds would provide enough time for color development and make the

total analysis time less than 20 minutes per sample.

The sample loop volume for flow injection analysis was selected as to obtain the tallest peak possible yet still have complete mixing of the sample plug with the reagent flow. A 100 µL loop was best able to meet both criteria.

The following list summarizes the parameters for the flow system

Flow rate	3-channel pump	= 2 mL/min
	single channel pump	= 1 mL/min
Azomethine H concentration in flow cell		= 0.0015 mM
Delay in online rinsing		= 350 s
Delay for continuous sample/ reagent mixing		= 30 s
Stopped flow development time		= 500 s
Sample loop volume		= 100 µL

The following experiments for analysis mode testing and comparison studies verify the values determined for each parameter.

Flow System Testing

Procedure

At the start of any analysis the reagent reservoirs are filled with the appropriate solutions. The standard and sample solutions are placed in the sample reservoirs. Three or four standards are analyzed and a calibration curve of abs versus C is prepared. This curve is then used to determine the concentration of boron in a sample from the measured absorbance for the sample. Each day, before the flow system is shut down, the system is flushed with deionized water. The experimental concentrations and analysis specific conditions are provided in Table XIII.

Results

Linear calibration curves for the stopped flow, continuous flow, and flow injection analysis are shown in Figures 37, 38, and 39 respectively. Evaluations of the calibration curves and analysis for unknowns are presented in Tables XIV, XV, and XVI respectively. The calibration curve is determined by linear least squares regression, all uncertainty associated with the y variable, and all points weighted equally. The calibration equation is expressed as

$$abs = a + b[B(OH)_3] \qquad (56)$$

Table XIII. Flow System Experimental Conditions.

Analysis Mode	TB Range (M)	Specific Conditions
Stopped Flow	5×10^{-4} to 1×10^{-2}	reaction time = 530 s
Continuous Flow	1×10^{-2} to 5×10^{-1}	reaction time = 30 s
Flow Injection	1×10^{-2} to 6×10^{-1}	reaction time = 30 s sample volume = 108 µL

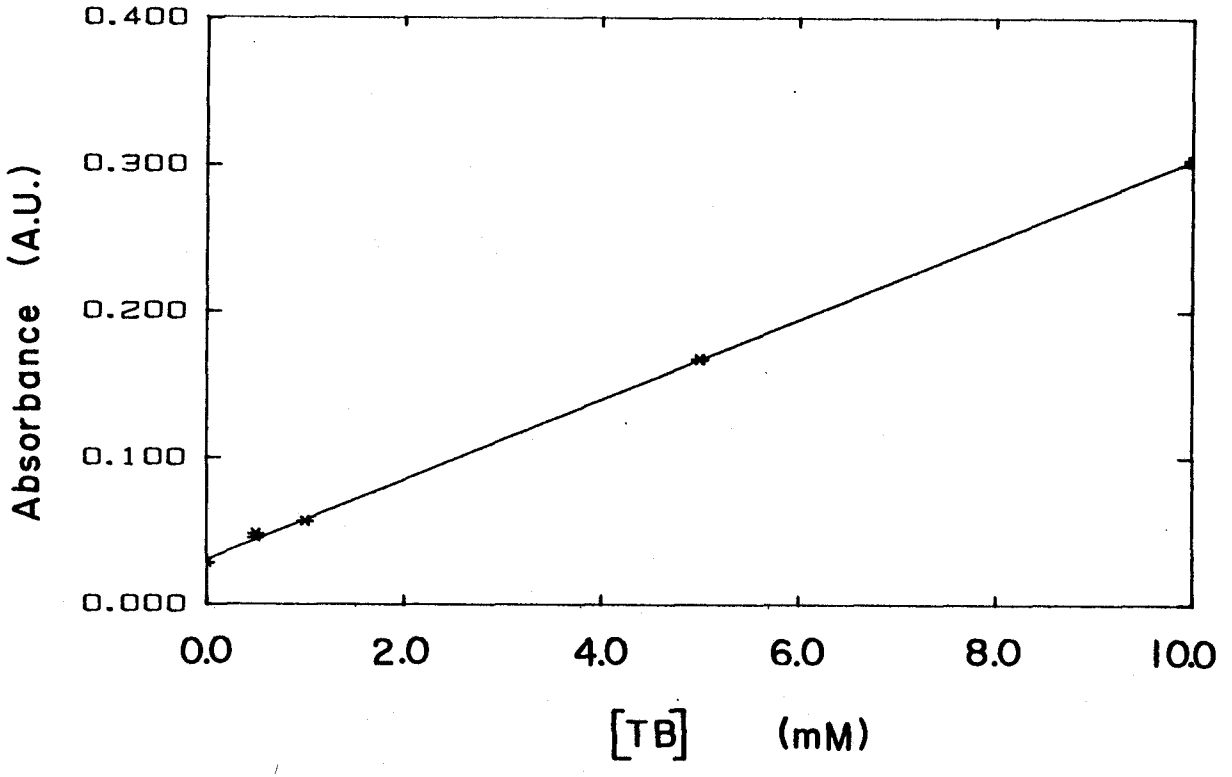

Figure 37. Stopped Flow Analysis.
TA = 0.0047 M, 1 mL/min.,
Acetate Buffer = 0.73 M, 1 mL/min.,
Sample 1 mL/min.
T = 25°C,
Development Time = 530 s.

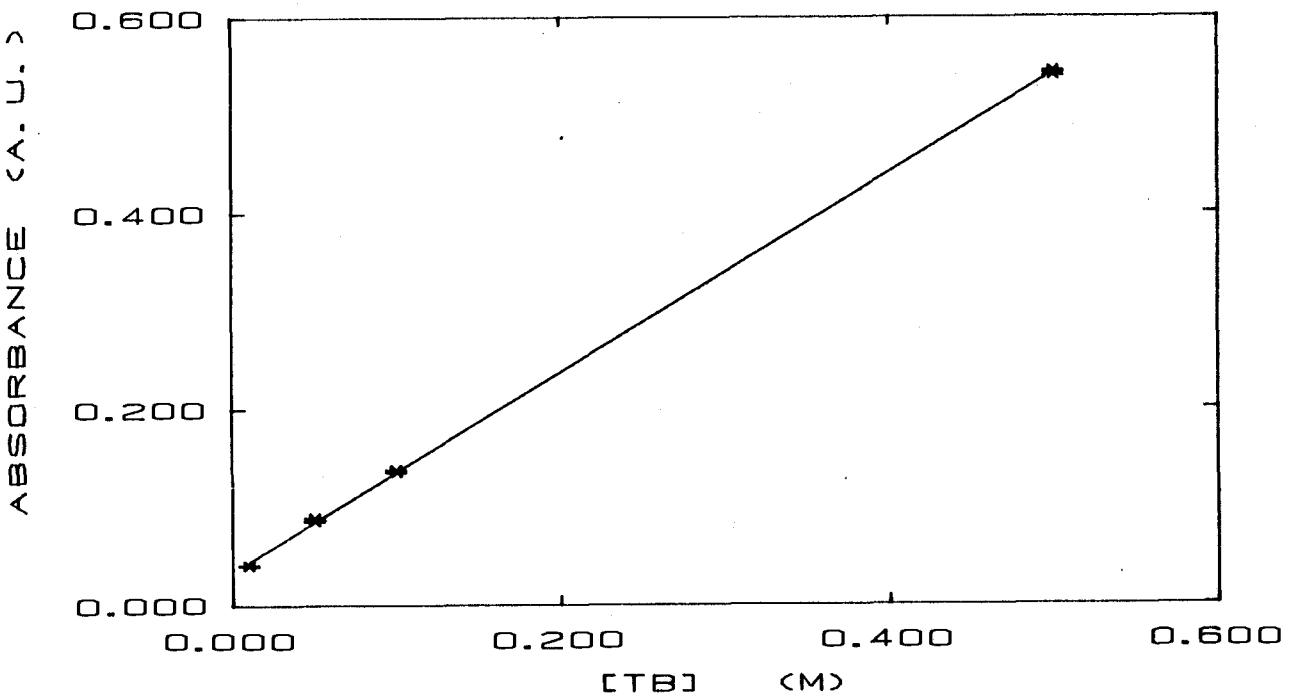

Figure 38. Continuous Flow Analysis.
TA = 0.0047 M, 1 mL/min., Acetate Buffer = 0.73 M, 1 mL/min.,
Sample 1 mL/min.,
T = 25°C, Development Time = 30 s.

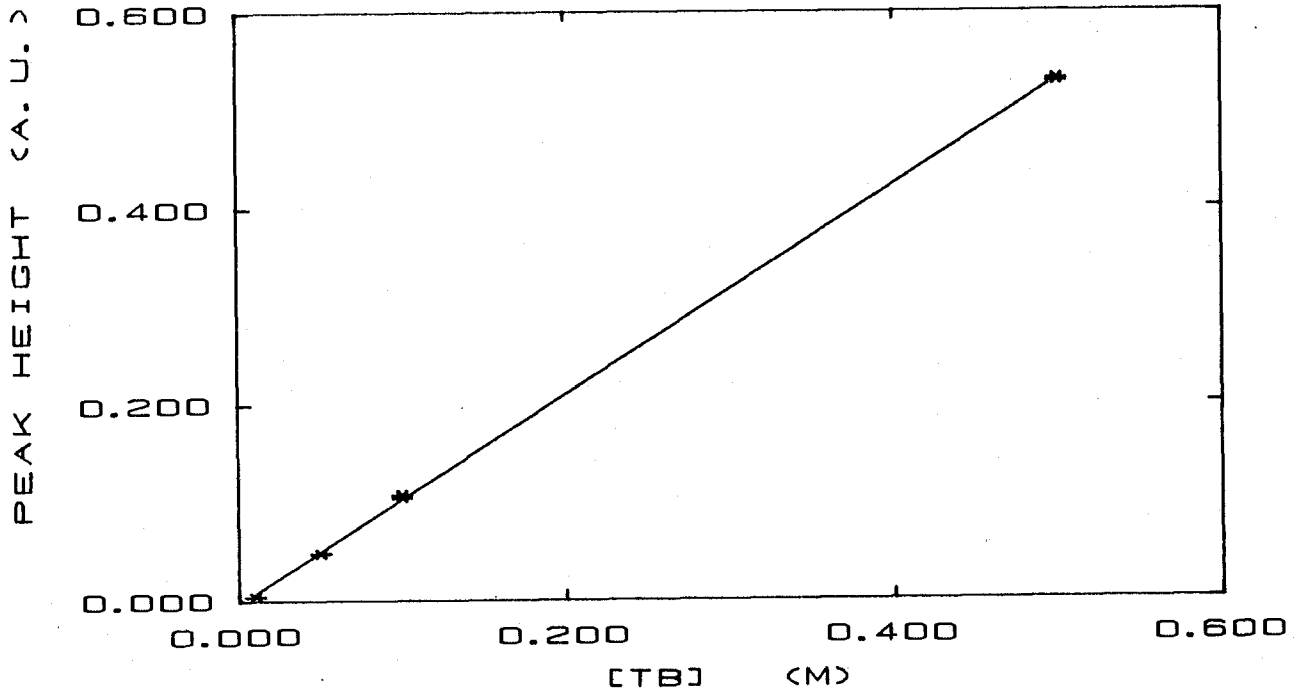

Figure 39. Flow Injection Analysis.
TA = 0.0047 M, 1 mL/min., Acetate Buffer = 0.73 M, 1 mL/min.,
Sample Volume = 100 µL,
T = 25°C, Development Time = 30 s.

Table XIV. Determination of $[B(OH)_3]$ by Stopped Flow Analysis.

$[B(OH)_3]^{exp}$ (M)	abs^{exp} (A.U.)	abs^{cal} (A.U.)	$abs^{cal}-abs^{exp}$ (A.U.)
Data			
.0100	.3041	.3034	-6.5E-04
.0100	.3027	.3034	7.5E-04
5.00E-3	.1668	.1669	1.4E-04
5.00E-3	.1668	.1669	1.4E-04
5.00E-3	.1675	.1669	-5.6E-04
1.00E-3	.0567	.0577	1.0E-03
1.00E-3	.0567	.0577	1.0E-03
1.00E-3	.0567	.0577	1.0E-03
5.00E-4	.0481	.0441	-4.0E-03
5.00E-4	.0481	.0441	-1.2E-03
0	.0281	.0304	2.3E-03

Slope	27.30	(A.U./M)
Intercept	.0304	(A.U.)

$[B(OH)_3]^{exp}$ (M)	abs^{exp} (A.U.)	$[B(OH)_3]^{cal}$ (M)	S.D. $[B(OH)_3]^{cal}$ (M)
Data for Unknown			
2.50×10^{-3}	0.0996 0.0982	2.51×10^{-3}	5.0×10^{-5}
2.50×10^{-3} [a]	0.0996 0.0996	2.53×10^{-3}	5.0×10^{-5}

[a] Unknown sample was a solution of $B(OH)_3$ in standard test matrix.

Table XV. Determination of $[B(OH)_3]$ by Continuous Flow Analysis.

$[B(OH)_3]^{exp}$ (M)	abs^{exp} (A.U.)	abs^{cal} (A.U.)	$abs^{cal}-abs^{exp}$ (A.U.)
Data			
0	.0248	.0320	7.21E-03
0	.0274	.0320	4.63E-03
0	.0280	.0320	4.07E-03
0	.0284	.0320	3.65E-03
.0500	.0858	.0832	-2.60E-03
.0500	.0855	.0832	-2.32E-03
.0500	.0857	.0832	-2.54E-03
.100	.1374	.1344	-3.09E-03
.100	.1356	.1344	-1.25E-03
.100	.1373	.1344	-2.00E-03
.500	.5426	.5436	1.08E-03
.500	.5394	.5436	4.21E-03
.500	.5450	.5436	-1.38E-03
.0500	.0894	.0832	-6.20E-03
.0500	.0868	.0832	-3.62E-03
.100	.1385	.1344	-4.11E-03
.0100	.0400	.0423	2.24E-03
.0100	.0404	.0423	1.82E-03
.0100	.0411	.0423	1.12E-03
Slope	1.023	(A.U./M)	
Intercept	.0320	(A.U.)	

$[B(OH)_3]^{exp}$ (M)	abs^{exp} (A.U.)	$[B(OH)_3]^{cal}$ (M)	S.D. $[B(OH)_3]^{cal}$ (M)
0.600[a]	0.6498 0.6614	0.609	3.7×10^{-3}
0.0250[a]	0.0590 0.0588	0.0262	2.8×10^{-3}
0.0250	0.0592 0.0584	0.0262	2.8×10^{-3}

[a] Unknown samples were solutions of $B(OH)_3$ in standard test matrix.

Table XVI. Determination of $[B(OH)_3]$ by Flow Injection Analysis.

$[B(OH)_3]^{exp}$ (M)	abs^{exp} (A.U.)	abs^{cal} (A.U.)	$abs^{cal} - abs^{exp}$ (A.U.)
Data			
.0500	.0483	.0501	1.78E-03
.0500	.0485	.0501	1.54E-03
.100	.108	.1034	-4.71E-03
.100	.108	.1034	-4.63E-03
.100	.104	.1034	-1.49E.03
.500	.5294	.5302	7.82E-04
.500	.5283	.5302	1.92E-03
.500	.5312	.5302	-9.84E-04
.0100	.0044	.0074	2.94E-03
.0100	.00045	.0074	2.95E-03

Slope	1.067	(A.U./M)
Intercept	.0033	(A.U.)

$[B(OH)_3]^{exp}$ (M)	abs^{exp} (A.U.)	$[B(OH)_3]^{cal}$ (M)	S.D. $[B(OH)_3]^{cal}$ (M)
Data For Unknown			
0.600[a]	0.6340 0.6370	0.599	2.8×10^{-3}
0.250[a]	0.2652	0.252	3.0×10^{-3}
0.250	0.2621 0.2646	0.250	2.2×10^{-3}

[a] Unknown samples were solutions of $B(OH)_3$ in standard test matrix.

Unknown concentrations are determined as

$$[B(OH)]_3^{cal} = (abs^{exp}-a)/b \qquad (57)$$

where abs^{exp} is the experimental absorbance and $[B(OH)_3]^{cal}$ the calculated boric acid concentration. The standard deviation in the unknown concentration is determined as

$$S.D.[B(OH)_3]^{cal} = \left[\left(\frac{d[B(OH)_3]^{cal}}{d\ abs^{exp}} \right)^2 S.D._{abs^{exp}}^2 + \left(\frac{d[B(OH)_3]^{cal}}{da} \right)^2 S.D._a^2 + \left(\frac{d[B(OH)_3]^{cal}}{db} \right)^2 S.D._b^2 \right]^{1/2} \qquad (58)$$

The confidence limits, C.L. can be determined from

$$C.L. = \pm S.D._{[B(OH)_3]^{cal}} \times t_{\alpha\phi} \qquad (59)$$

with α the level of uncertainty and $\phi = n-2$, where n is the number of points in the calibration curve.

The methods of analysis can be compared as to: range of detectable $B(OH)_3$ concentration, accuracy of unknown determination, run time, and total analysis time. The

lower limit of the concentration range can be defined in two ways.

The theoretical limit of detection is defined as the concentration which yields an absorbance equal to the absorbance of the blank plus two times the standard deviation of the absorbance of the blank.

$$abs_{tdl} = abs_{blank} + 2(S.D._{abs}) \qquad (60)$$

A more practical limit of detection for the azomethine/boron sysem is defined similarly, but in terms of the background absorbance (abs_{bck}), because the blank absorbs less than the background.

$$abs_{pdl} = abs_{bck} + 2(S.D._{abs}) \qquad (61)$$

Converted to concentration with the calibration curve (Equation 56), these detection limits are

$$C_{tdl} = \frac{2(S.D._{abs})}{b} \qquad (62)$$

$$C_{pdl} = \frac{abs_{bck} - abs_{blank} + 2(S.D._{abs})}{b} \qquad (63)$$

The upper limit of the concentration range is defined as the concentration of boric acid having an absorbance which exceeds the readout of the colorimeter (1~ A.U.). Comparison of the methods was performed using the flow

system with the parameters listed in the optimization section. Table XVII presents a comparison of the 3 analysis modes. For boric acid concentrations greater than 1 mM the flow injection method provides for the quickest analysis time and the highest accuracy. The stopped flow analysis provides for analysis of lower boric acid concentrations but with a longer analysis time. Determination of the "unknown" sample concentration was not hindered in solutions of the test matrix. Extrapolation of the calibration curve was possible on both the higher and lower concentration ends. The theoretical absorbances compare favorably with the experimental absorbances for all three analysis modes.

Conclusion

The equilibrium and kinetic calculations were proven to be effective for describing the experimental data. Overall accuracy of the equilibrium calculations is about 3%. The kinetic calculations are especially useful during the initial 1000 s for determining experimental parameters for kinetic method analysis.

The flow system described has been shown to be effective for rapid, simple, and accurate determination for boron at the concentrations expected by the nuclear industry. The spectrophotometric kinetic analysis shows

Table XVII. Comparison of Flow System Analysis Modes.

Parameter Measured	Stopped Flow	Continuous Flow	Flow Injection
Reaction time (s)	530	30	30
Analysis time per run (s) new sample	1200	500	450
Analysis time per run (s) same sample	1200	500	180
Slope of Calibration Curve (A.U./M)	27.3	1.02	1.07
Average reagent background absorbance (A.U.)	0.0427	0.0425	0.0456
S.D. of reagent background absorbance (A.U.)	9.5×10^{-4}	8.6×10^{-4}	5.7×10^{-4}
Theoretical concentration limit (M)	7.0×10^{-5}	1.7×10^{-3}	1.1×10^{-3}
Practical concentration limit (M)	5.6×10^{-4}	0.012	5.0×10^{-3}

Table XVII. continued.

Parameter Measured	Stopped Flow	Continuous Flow	Flow Injection
Relative standard deviation (%) (for several unknown concentrations)	2% (2.50×10^{-3} M)	0.6% (0.600 M) 5% (0.0250 M)	0.5% (0.600 M) 1% (0.250 M)

freedom from test matrix interferences. The system provides an easy trade off between rapid analysis and lower concentration range.

CONCLUSION

Chemical equilibrium models have been developed to characterize the boric acid/mannitol system and the boric acid/azomethine H system. For each system, a set of components, species, and equations have been defined which completely represent the equilibria, and can be used to predict the species concentrations in solution under the given experimental conditions.

Stability constants for the polyborate species and the boric acid/mannitol complexes available from the literature were found to describe the experimental results adequately. However, since many sets of species of various degrees of protonated forms have been involved in explaining the experimental data, it is not clear which species actually exist in aqueous solution. Future studies to determine which species actually exist are indicated, along with studies to characterize the kinetics of the reactions yielding the boron mannitol complexes and the reactions yielding the polyborate species.

Values for the stability constants and molar absorptivities of the boric acid/azomethine H species have been determined by a least square fit of chemical equilibrium equations to experimental data. The stability constants and molar absorptivities were adjusted to yield

the optimal fit of the equilibrium equations to the experimental data. While there is some covariability in the values which have been determined, the agreement between the experimental and computed equilibrium absorbances confirm that the values can be used to describe the experimental absorbance signal.

The rate of formation of the colored AB and A_2B complexes has also been characterized. No attempt was made to interpret the reaction mechanisms in determining the empirical rate law. The kinetic model which describes the course of the reaction is consistent with experimental data from initial to equilibrium conditions. The agreement between the experimental and computed rates confirms that the rate constants and rate laws can be used to predict the absorbance signal given the total boric acid and azomethine concentrations, and the time. An application of these equations was demonstrated in the optimization of the flow system.

Future studies of the boric acid/azomethine H system include correlation of the stability constants, stoichiometry, and rate constants via another monitoring technique (e.g. fluorescence). Studies could also include the pH dependence of the equilibria and the reaction rates.

Nuclear Chemistry Application

The intention of this research was to test the chemical methods and associated equipment under experimental conditions representative of those in nuclear power plants. Both the potentiometic titation method and the spectrophotometric method have been found suitable for determination of boron concentration in nuclear reactor coolant water.

With the potentiometric method the amount of base necessary to neutralize the boric acid is determined. Since nuclear reactor coolant water is virtually a pure $B(OH)_3$ solution, an acid and base titration is generally sufficient for the determination of boron. The endpoint of the titration can be detected with a glass ion-selective electrode/reference electrode pair. Since $B(OH)_3$ is a weak acid the endpoint is difficult to detect for dilute solutions. Mannitol is added to the sample to form a more acidic $B(OH)_3$/mannitol complex for which the endpoint is more easily detected. The addition of mannitol to sharpen the endpoint was found to be necessary below about 0.1 M $B(OH)_3$. Mannitol should be in excess relative to $B(OH)_3$ by approximately a factor of ten below 0.1 M $B(OH)_3$ and a factor of hundred below 0.01 M $B(OH)_3$.

The use of azomethine H as the color reagent yielded good results in the spectrophotometric analysis. The A_2B

species was determined to be the predominate abosrbing species. Solutions in the range 0.5 mM - 20 mM could be analyzed with stopped flow analysis, and 5 mM - 0.9 M with continuous flow analysis, and 5 mM - 0.9 M with flow injection analysis. The range of detectable $B(OH)_3$ concentrations for flow injection analysis corresponds to the concentration range of boron expected in reactor coolant under post accident conditions.

BIBLIOGRAPHY

1. Kankare, J. J., "Determination of Stability Constants of Mononuclear Complexes by Potentiostatic Titration. Mannitol-Boric Acid System", Analytical Chemistry, 45, 2050-2056, (1973).

2. Knoeck, J. and Taylor, J. K., "Aqueous Boric Acid-Borate-Mannitol Equilibria", Analytical Chemistry, 41, 1730-1734, (1969).

3. Connor, J. M. and Bulgrin, V. C., "Equilibria Between Borate Ion and Some Polyols in Aqueous Solution", Journal of Inorganic and Nuclear Chemistry, 29, 1653-1961, (1967).

4. Smith, R. M. and Martell, A. E., Critical Stability Constants vol. 3 and 4, Plenum Press, New York, 1976.

5. Edwards, R. A., "Automatic Determination of Boron (0.10-10.0 mg/L) in Raw and Waste Waters", Analyst, 105, 139-146, (1980).

6. Bates, R. G., Determination of pH. Theory and Practice, John Wiley and Sons, New York, 1973.

7. Durst, R. A., Ed., Ion Selective Electrodes, N.B.S. Special Publication 314, U.S. Government Printing Office, Washington, 1969.

8. Eisenmann, G., Glass Electrodes for Hydrogen and Other Cations. Principles and Practice, Marcel Dekker, Inc., New York, 1967.

9. Bard, A. S. and Faulkner, L. R., Electrochemical Methods. Fundamentals and Applications, John Wiley and Sons, New York, 1980.

10. Westall, J.C., MICROQL A Chemical Equilibrium Program in BASIC. Swiss Federal Institute of Technology EAWAG CH-8600 Duebendorf, Switzerland, 1979.

11. Pourbaix, M., Atlas of Electrochemical Equilibria in Aqueous Solutions, National Association of Corrisien
xas, 1966.

M., Oregon State University, unpublished

1, 2, 4

13. Perreault, R. A. and Michalek, S. A., " Application of the Digichem 3000 Programmable Chemical Analyzer to On-line Process Control", Analysis Instrumentation, 20, 53-64, (1982).

14. EPA-600/4-79-020, "Methods for Chemical Analysis of Water and Wastes", U.S.E.P.A., Cincinnati, Ohio, (1979).

15. Choi, W. and Chen, K.Y., Analysis of Boron in Water Using an Improved Curcumin Method , Water Technology/ Quality, 153-157, March 1979.

16. Samsoni, Z. and Szeleczky, A., "Examination of Factors Influencing the Sensitivity and Accuracy of Boron Determination by Carminic Acid", Mikrochimica Acta, 1, 445-453, (1980).

17. Standard Methods for the Examination of Water and Wastewater, 14th ed., Washington, D.C., (1976).

18. Korenman, I. M., Zh. Analit Khimii, 2, 153, (1947).

19. Capelle, R., "Microdosage Colorimétrique du Bore en Milieu Aqueax, au Moyen de Réactifs á Groupment Azoïque ou Imine Dérivés des Acides H er K", Analytica Chimica Acta, 24, 555-572, (1961).

20. Basson, W. D., Bohmer, R. G., and Stanton, D. A., "An Automated Procedure for the Determination of Boron in Plant Tissue", Analyst, 94, 1135-1141 (1069).

21. Westall, J. C. FITEQL A Computer Program for Determination of Chemical Equilibrium Constants From Experimental Data, Department of Chemistry, Oregon State University, May 1982.

22. Johansson, L., "On the Use and Misuse of the Spectrophotometric Method for the Study of Inner- and Outer-sphere Complexes in Solution", Acta Chemica Scandinavica, 25, 3569-3576, (1971).

23. Pardue, H. L. "A Comprehensive Classification of Kinetic Methods of Analysis Used in Clinical Chemistry", Clinical Chemistry, 23, 2189-2201, (1977).

24. "Analysis for Dissolved Hydrogen, Dissolved Oxygen, Boron, Chloride, pH, and Conductivity under Normal and Post-accident Conditions", prepared for Commonwealth Edison Company by P. J. Battagic, W. Lechnick, J. R. Riddle, R. C. Rice, Cyrus Rice Division, NUS Corporation, October, 1980.

APPENDICES

APPENDIX A

Nuclear Power Plant Review

Reactor Description

Nuclear fission produces the energy generated by nuclear power plants. Figure A-1 provides a cut-away diagram of a nuclear reactor of the pressurized water type. The fuel of the nuclear reactor is uranium-235. Typically, uranium is enriched to about three percent uranium-235 and used in the form of UO_2 pellets. The pellets are encased in zirconium or stainless-steel tubes to compose the fuel rods. Rods composed of cadmium or boron are used to control the fission process by absorbing neutrons. These control rods regulate the number of neutrons present to sustain the reaction chain but prevent the core from overheating. The reactor is started by using a neutron source which initiates the chain reaction. Examples of the ways that the uranium-235 nucleus splits are:

$$
{}^{1}_{0}n + {}^{235}_{92}U \rightarrow
\begin{cases}
{}^{144}_{55}Cs + {}^{90}_{37}Rb + 2\,{}^{1}_{0}n \\
{}^{146}_{57}La + {}^{57}_{35}Br + 3\,{}^{1}_{0}n \\
{}^{142}_{56}Ba + {}^{91}_{36}Kr + 3\,{}^{1}_{0}n
\end{cases}
\qquad \text{(A-1)}
$$

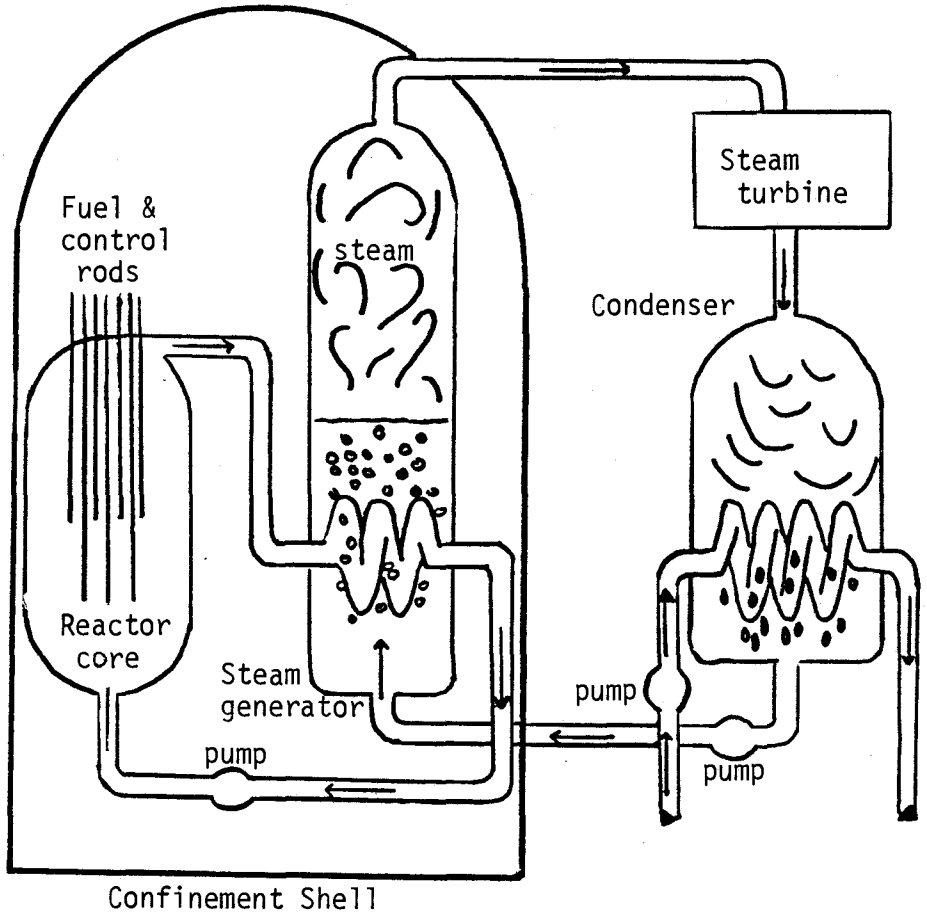

Figure A-1. Diagram of a Nuclear Reactor of the Pressurized Water Type.

On the average 2.4 neutrons are produced by every fission of uranium-235. Reactions that multiply in this fashion are called branching chain reactions.

The primary cooling liquid (water) circulates through the reactor core, transporting the heat generated by the fission process to a steam generator in the secondary coolant system. The primary coolant usually contains boron that absorbs neutrons and provides additional tempering of the fission process. The primary coolant heats the secondary coolant from which steam is generated to drive a turbine that is in turn connected to an electrical generator. The primary coolant is in a closed system and subsequent coolants never pass through the reactor core. A concrete shell surrounds the entire reactor system, shielding personnel from radiation.

As of October 1980, all licensed nuclear power plant were required to have the capability to obtain and analyze reactor coolant samples for the determination of radionuclides, boron, chloride, hydrogen ion, and dissolved hydrogen and oxygen gases. Of first chemical priority is boron (24). Boron is present as boric acid, $B(OH)_3$, or the borate anion, $B(OH)_4^-$, and functions as a moderator for the fission process as follows:

$$^{10}B + {}^{1}n \rightarrow {}^{7}Li + {}^{4}He \qquad (A-2)$$

Boron-10 reacts with a neutron and decays to lithium-7 and an alpha particle. Boron-10, which accounts for twenty percent of the naturally occurring boron, has a high cross section for neutron absorption. The concentration of boron in the primary coolant system also functions to ensure shutdown of the reactor should it become necessary.

Accident Scenario

A possible accident begins with the rupture of a check valve in the primary coolant line. Highly radioactive water (up to 350,000 gallons) flows out the break into the containment building. The water collects in the sump. Subsequent low levels of coolant in the reactor could cause overheating of the core, in which case, some of the fuel rods would burst or partially melt. Steam containing radioactive iodine would escape from the break and into the containment structure. Jets, located within the concrete building, spray a 30% NaOH solution, reducing the iodine to the iodide ion and adding to the solution in the sump. To prevent further overheating of the core, the water in the sump is partially purified and circulated within the primary coolant flow system. Circulation is continued to maintain water over the core and achieve long term heat removal.

Chemical Concerns

The water in the sump is a complex matrix. Typical concentrations, as determined by the Nuclear Regulatory Commission, NRC, of the matrix components are provided in Table A-I. Under normal conditions the boron concentration is determined by analyzing a grab or on-line sample. The concern of this research is that the chemical methods and associated equipment be tested under experimental conditions representative ot those in nuclear power plants. Table A-II provides a list of concerns of the nuclear power plants which are briefly described in the following paragraphs. This list provided the guidelines by which the investigated analytical methods were evaluated.

The accuracy, range, and time requirements specified by the NRC for nuclear power plants under post-accident conditions are presented in Table A-III. The accuracy of the calibration depends on the integrity of the standards. If standards are renewed regularly, proper calibration should present no problem.

A chemical interferent is any species within the matrix which affects the analysis and leads to erroneous results. Chemical interferences create a serious problem in some methods. The last two constituents of the test matrix (Table A-I) have been omitted from the laboratory

Table A-I. Test Matrix for Postaccident Conditions (24).

Substance		C[mg/kg]
1. Fission Products		
	I^-	40
	Cs^+	250
	Ba^{2+}	10
	La^{3+}	5
	Ce^{4+}	5
2. $B(OH)_3$ (PWR) Moderator		
	B (III)	2000
3. NaOH (PWR) Containment Spray		
	NaOH	3000
4. LiOH (PWR) pH-Control		
	Li^+	2
5. Cl^- Impurity		
	Cl^-	10
6. Corrosion Products		
7. Oil From Sump		
	10 w 40 1000 mg/kg	1000

Table A-II. Criteria for Evaluation of Chemical Analysis.

1.	Analytical Capabilities
	Accuracy, precision, range
	Analysis time
	Calibration
	Chemical interferences
	Physical interferences
	Radiation interferences
2.	Practical Application
	Automation
	Ease of use
	Maintenance requirements
	Reliability
	Cost
3.	Capabilities vs. Requirements
	Post-accident analyses
	Routine analyses
	Radiation exposure to personnel

Table A-III. Monitoring Requirements for Post-Accident Conditions (24).

Range	50 - 1000 mg/L BWR	(5 mM - 100 mM)
	50 - 6000 mg/L PWR	(5 mM - 600 mM)
Accuracy	± 5% TB ≥ 1000 mg/L	(± 5% TB ≥ 100 mM)
	± 50 mg/L TB < 1000 mg/L	(± 5 mM TB < 100 mM)
Time	Within 3 hours	

test solution. The corrosion products, which come from leaching of the concrete or corroding of the metal fittings, are minimized by an epoxy paint which covers all exposed surfaces in the containment building. The concentration of the corrosion products is considered insignificant. Oil from within the sump may become entrained in the coolant or may float to the top of the sump and not be circulated through the coolant system.

Sample pressure and temperature, as well as the ambient pressure and temperature are the main physical interferences. Most analytical instrumentation for coolant water monitoring is designed to work with samples temperatures in the range 20-50°C and pressures in the range 15-75 p.s.i.g. The equipment for reducing coolant water temperature and pressure to this range is available. However, the effect of variations in temperature and pressure of the sample is still a matter of concern for almost all analytical methods.

Probably the most serious problem for all methods is the interference from radiation. Radiation is not regularly considered among possible interferences in the development of analytical methods, and there is little background knowledge on the effect of radiation on analytical methods. Furthermore, most sensors are sensitive to radiation to some degree.

The need to perform analyses under post-accident conditions and to minimize the exposure of personnel to radiation favor methods of analysis which can be automated. In post-accident conditions, automation allows the operator to be physically removed from the radiation and reduces the possibility of human error induced by stress. Furthermore, current development of analytical instrumentation is in the direction of increased automation. Within another decade automated methods will predominate in many laboratories. The ease of use, maintenance requirement, and reliability of the analysis is generally more favorable with an automated method. Therefore, for the nuclear power industry, for which automation carries particular advantages, the degree of automation should be an important criterion for evaluation of analytical methods.

Instrumentation which can be used for analysis under normal conditions as well as under post-accident conditions offers the advantage that operators will be familiar with instrumentation in case of accident, calibration standards will be checked frequently, and equipment maintenance must be carried out regularly. In effect, use of an instrument for routine monitoring insures that the instrument is in operational condition.

This review has briefly outlined the requirements of nuclear power plants for the analysis of boron. Both the potentiometric titration method and the spectrophotometric method fulfill the criteria in Table A-II and are recommended for the determination of boron in nuclear reactor coolant water.

APPENDIX B

Testing of pH Electrode Pair

Calibration of Electrode Pair

The electrode pair can be calibrated in solutions of known hydrogen ion activity or in solutions of known hydrogen ion concentration. The activity standards are often taken as the National Bureau of Standards, NBS, standard buffers. The concentration standards are often solutions of diluted strong acids or bases in a medium of constant ionic composition. The advantage of using standards of known hydrogen ion concentration is that they can be prepared from solutions of salts and strong acids which can be stored virtually indefinitely. The buffer solutions used for hydrogen ion activity standards are susceptible to bacterial contamination and should be prepared fresh every few months. The advantage of the buffer solution is that buffers can be chosen whose log a_{H^+} values bracket the log a_{H^+} values of the sample solution, rendering a long extrapolation of the calibration curve unnecessary. To illustrate the difference the electrode pair was calibrated with both activity standard and concentration standard solutions, Table B-I. The results are presented in Figure B-1. A calibration curve with $E^{\circ'}_{cell} = 462$ mV and $s = 58.4$ mV was

Table B-I. Standards for Calibration of Glass Electrode.

H^+ activity standards (NBS Buffers)	
log a_{H^+}	Composition (6)
-4.008	0.0500 m potassium hydrogen phthalate
-6.865	0.0250 m KH_2PO_4, 0.0250 m Na_2HPO_4
-9.180	0.100 m borax [$Na_2B_4O_7.10H_2O$]

H^+ concentration standards
x M HCl
(0.1-x) M KCl

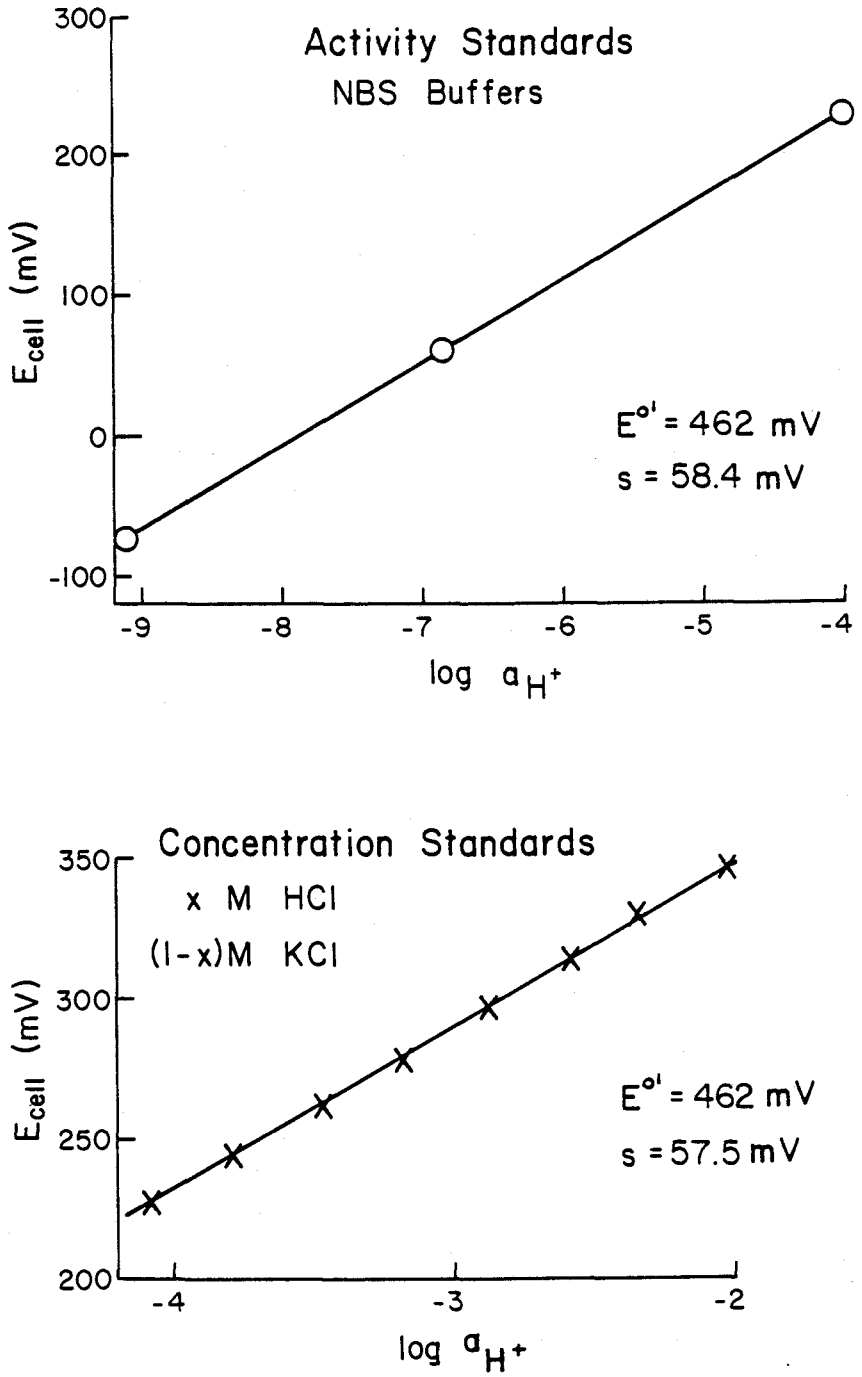

Figure B-1. Calibration of pH electrode pair with activity and concentration standards.

obtained with the activity standards, and $E^{o'}_{cell}$ = 462 mV and s = 57.5 mV with the concentration standards. Concentrations were converted to activities with Equations 10, 11 and 12, with I = 0.1 M, and γ_{H^+} = 0.825. The agreement between $E^{o'}_{cell}$ and s by both calibration methods indicates that either method could be used. The activity standard values have been used in this case for study in the log a_{H^+} range 4 - 11.

Dilute Solutions

To test the performance of the electrode pair in extremely dilute or poorly buffered solutions, it was calibrated in one set of HCl standards made up in distilled water and another set of standards made up in 0.1 M KCl, Figure B-2. The electrode pair performed equally well in both media, indicating that reliable measurements could be made in dilute boric acid solutions.

Long Term Drift

To determine the frequency of calibration and long term drift characteristics of the electrode pair, the response of the electrode pair and the reference electrode against another double junction reference electrode were monitored over a three month period with the same test solution (0.02 M HNO_3 + 0.10 M KNO_3). Between

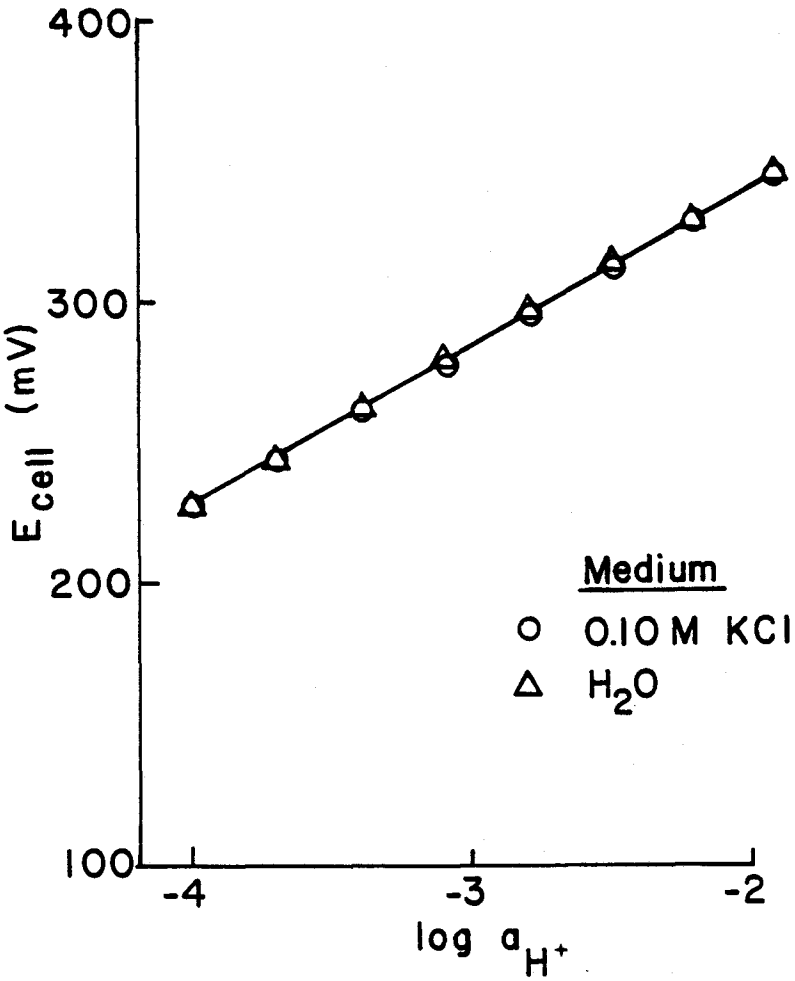

Figure B-2. Calibration Plot for pH Electrode Pair Showing Effect of Supporting Electrolyte (Ionic Strength).

measurements, the electrodes were stored in a 0.01 M HNO_3 + 0.10 M KNO_3 solution. The data in Figure B-3 indicates a monotonic drift over the entire period with an accumulated drift of less than 20 mV (0.35 pH units) for the glass electrode and less than 5 mV (0.1 pH units) for the reference electrode pair. For satisfactory performance weekly calibration is indicated, but for optimum performance and to insure detection of any malfunctioning bi-weekly or daily calibration is recommended.

Effect of Temperature

Probably the most significant factor affecting the constancy of $E^{o'}_{cell}$ and s is temperature. In principle the electrode pair must be calibrated at the temperature at which it is to be used. Experiments were carried out to test this effect. Data for calibration of the electrode with 3 NBS buffers (pH = 4, 7, and 10) at 5 different temperatures in the range 20° - 50°C are shown in Figure B-4. The dependence of $E^{o'}_{cell}$, s, and the log a_{H^+} of the buffers on temperature is summarized in Table B-II.

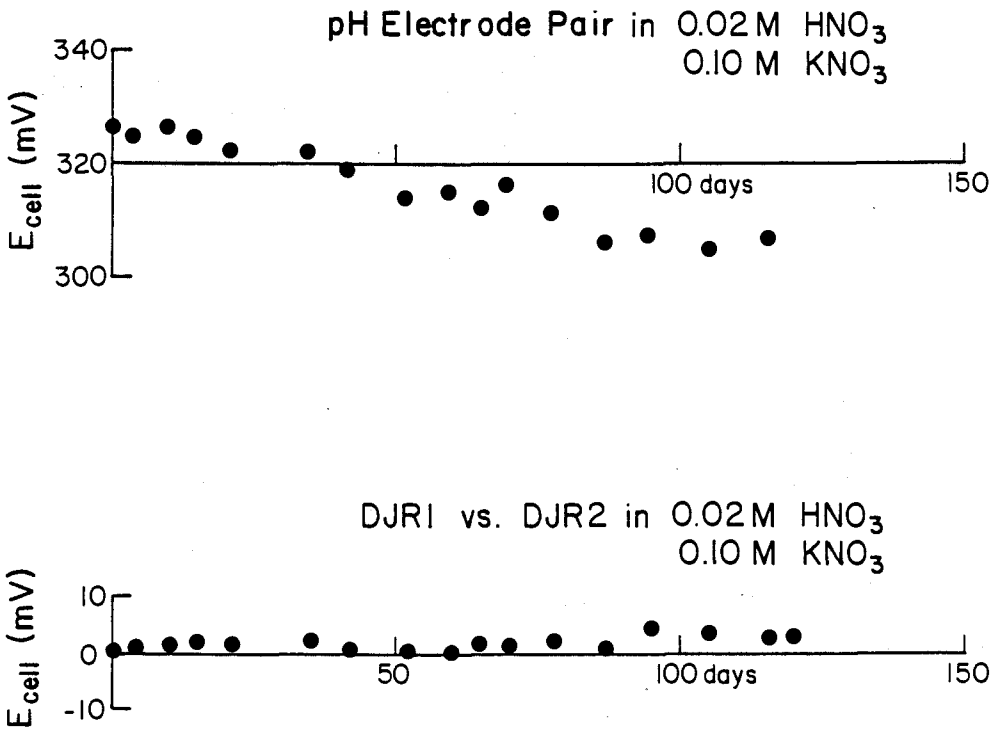

Figure B-3. Long-term Drift of pH Electrode Pair and Double Junction Reference Electrodes.

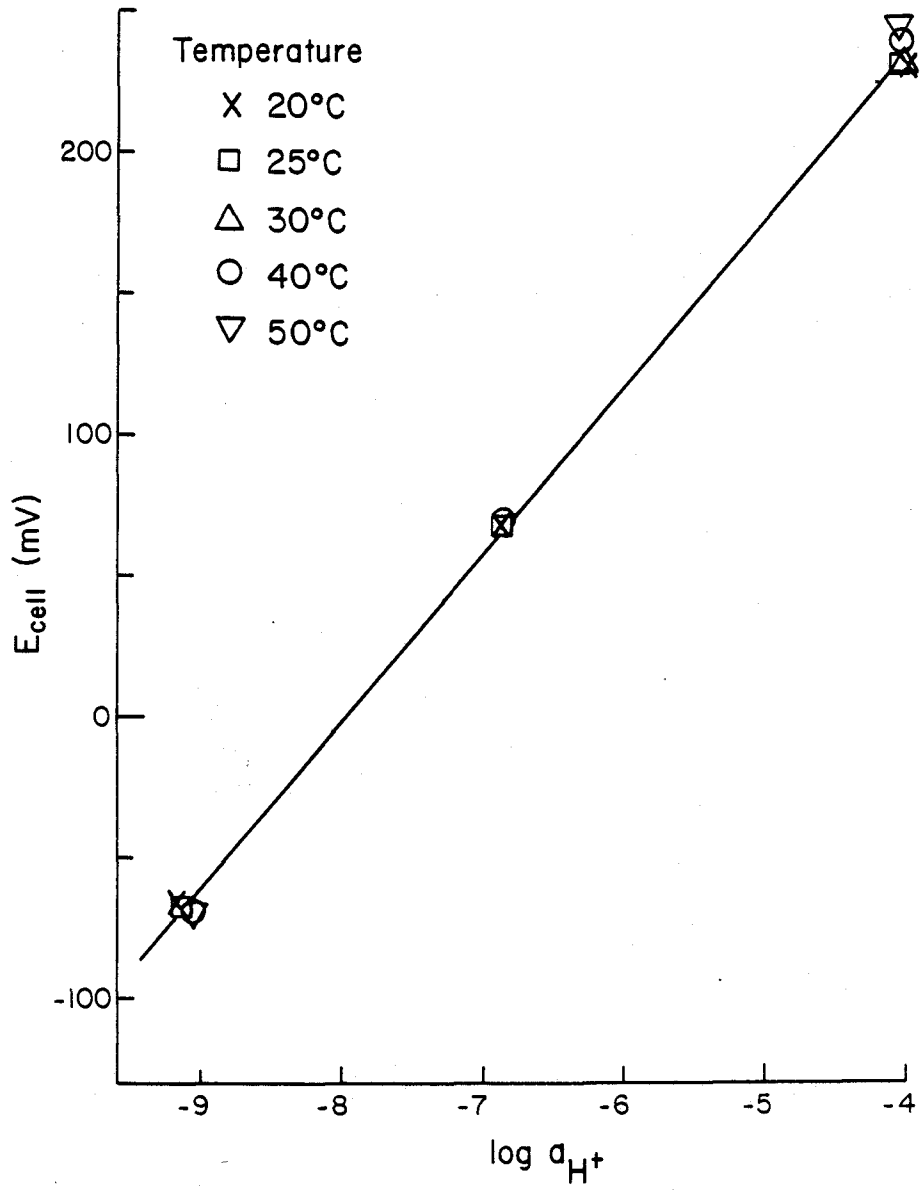

Figure B-4. Calibration Plot for pH Electrode Pair Showing Effect of Temperature.

Table B-II. Effect of Temperature on Calibration.

T (°C)	pH Electrode Pair	
	E_{cell}	s (mV)
20	460	57.0
25	467	58.3
30	476	59.6
40	490	61.6
50	502	63.4
	$\frac{dE^{\circ'}}{dT}$ = 1.41 mV/°C	$\frac{ds}{dT}$ = 0.21 mV/°C

T (°C)	$-\log a_{H^+}$ of Standard (6)		
	0.05 m potassium acid phthalate	0.025 m KH_2PO_4 0.025 m Na_2HPO_4	0.01 m borax
20	4.002	6.881	9.225
25	4.008	6.865	9.180
30	4.015	6.853	9.139
40	4.035	6.838	9.068
50	4.060	6.833	9.011

Standard Test Matrix

The response of the pH electrode pair was monitored in a series of solutions containing components of the standard test matrix. Table B-III lists the cell potential determined for each solution. No significant interference from the constituents of the test matrix with the performance of the glass electrode was anticipated and none were found. The formation of Li^+, Na^+, and cation complexes with borate appear to have caused a slight increase in a_{H^+}, but this cannot be regarded as an interference with the electrode.

Alkaline Error

The pH response of most glass electrodes is imperfect at the alkaline end of the pH scale. The deviation is positive, or in other words, the response of the electrode to changes of pH is less than the ideal response. Hence, the pH value measured will be too low. The response of the electrode to ions other than those for which it is designated is the reason for this deviation. Values range from 0 - 0.5 Δ pH units, but are typically less than 0.2 Δ pH units in magnitude.

Table B-III. Effect of Standard Test Matrix on pH Electrode Pair.

Solution[a]	E (mV)
S1 $B(OH)_3$	189.5
S2 $B(OH)_3$ + fission products	191.8
S3 $B(OH)_3$ + fission products + $LiNO_3$	191.7
S4 $B(OH)_3$ + fission products + $LiNO_3$ + $NaNO_3$	192.6

[a] See Table A-I for concentration of components in solution.

Effect of Radiation

A combination pH electrode was exposed to γ radiation from a ^{60}Co source at the rate of 248 rads/min for 24 hours and 570 rads/min for 206 hours. Cell potential data were obtained for the pH 4, 7, and 10 buffers before and after each radiation exposure to ascertain if $E^{\circ'}_{cell}$ or s is affected by radiation. During exposure, the cell potential from the pH 7 buffers was continually monitored without solution stirring.

The results of the radiation experiments are shown in Table B-IV. Although the electrode shows no permanent damage after removal from the radiation field, cell potentials measured while the electrode was in the field were noisy and subject to drift. Comparison of $E^{\circ'}_{cell}$ and s data indicate that s was little affected by radiation, but that $E^{\circ'}_{cell}$ varied over 50 mV. Without recalibration during the exposure, these shifts in $E^{\circ'}_{cell}$ could cause errors in determining the location of the fixed titration endpoint.

The response of the electrode before and after irradiation appear to rule out the possibility that significant electrolysis of the buffer solution occurred, or that the electrical connection of the electrode to the mV/pH meter was responsible for the noise in the signal. Thus, the non-ideal response of the electrode during

Table B-IV. Exposure of Glass Electrode to Radiation.

Before Exposure:	$E^{\circ'}_{cell}$ = 527 mV s = 57.6 mV
Exposure 1:	1.5×10^4 rads/hr x 24 hr = 3.6×10^5 rads
Maximum Drift Rate	0.5 mV/min (0.01 pH units/min)
Maximum Noise	0.2 mV (0.004 pH units)
After Exposure 1:	$E^{\circ'}_{cell}$ = 363 mV s = 56.9 mV
Exposure 2:	3.4×10^4 rads/hr x 21 hr = 7.2×10^5 rads
Maximum Drift Rate	0.1 mV/min (0.0002 pH units/min)
Maximum Noise	1.0 mV (0.02 pH units)
After Exposure 2:	$E^{\circ'}_{cell}$ = 406 mV s = 57.7 mV

irradiation must be attributed to the radiation field. Of all the possible interferences with glass electrodes, it appears that radiation is potentially the most serious.

APPENDIX C

Program Listing for Flow System Control

Main Program Listing

```
REM     ANALYSIS
REM     DAWN M. MCDANIEL
REM     OREGON STATE UNIVERSITY
REM     SEPTEMBER 1983

REM SET CONSTANTS & DIM VARIABLES
        C1=20997: C2=20998: C3=20999: C4=21000
        MF1=256:  MF2=16:   MF3=2048
        ADS=-6.8287: ADI=0.01167
        D1=10: D2=100: D3=1000: D4=10000
        LOBITE=20995: HIBITE=20996
        PUMP=20480: CLOCK=20512: SIGNAL=20608
        BEEP=21152
        STATUS=40833
        PULSE=21248: PULSE1=21003: PULSE2=21004
        GOSUB 2000: REM INITIALIZE CONTROL PARAMETERS

REM ANALYSIS CONTROL
200     GOSUB 1800: REM ANALYSIS MODE
        INPUT "FILE NAME IS";COLOR$
        FILE COLOR$
        Q=CALL(PUMP): REM INITIALIZE PUMP STATUS
        GOSUB 2100: REM CONTROL SUBROUTINES

REM BEGIN BORON ANALYSIS
400     I=0: D0=-1
      . INPUT "SAMPLE CONCENTRATION (M)=":SC
        GOSUB 1900: REM FLOW SYSTEM CONFIGURATION
        PRINT "*******"
        Q=CALL(CLOCK): REM START  CLOCK & HP PUMP
        PRINT "*********"
        PRINT " ","T(SEC)","ABS(AU)"
        PRINT " "
REM READ TIME
430     POKE 40974,64
        TR=PEEK(C1)+MF1*PEEK(C2)
        TR=TR+MF1*MF1*PEEK(C3)+MF1*MF1*MF1*PEEK(C4)
        POKE 40974,192
        IF TR-INT(TR/SI)*SI=0 THEN GOSUB 500
        IF TR=PS THEN POKE STATUS,11: REM LP PUMP ON
        IF TR=PC THEN POKE STATUS,3: REM LP PUMP OFF
        IF TR=TI THEN POKE STATUS-1,3: REM INJECT SAMPLE
        IF TR=PH THEN POKE STATUS-1,2: REM LOAD POSITION
440     IF TR=PH THEN POKE STATUS,1: REM BOTH PUMPS OFF
        IF TR>TU THEN 1000
        F1=PEEK(40848)
        IF F1=255 THEN 2150
        GOTO 430
```

```
REM READ A/D CONVERTER
500     IF D0=TR THEN RETURN
        D0=TR
        Q=CALL(SIGNAL): REM A/D CONVERTER
        AH=PEEK(HIBITE): AL=PEEK(LOBITE)
        A=(AH*MF2+AL/MF2)-MF3
        A=A*D1/MF3
        A=(A-AD1)/AD5
        A=(INT(A*D4))/D4
        A=A*SE
        IF I=0 THEN PRINT #1;AM
        IF I=0 THEN PRINT #1;SC
        IF I=0 THEN PRINT #1;SI
        PRINT #1;A
        IF A>AU*SE THEN 1000
        IF PF=0 THEN 520
        PRINT I,TR,A
520     I=I+1
        RETURN

REM SOUND BEEPER
1000    PRINT #1;-999
        FOR L7=1 TO 5
        Q=CALL(BEEP)
        NEXT L7
        GOTO 2150

REM ANALYSIS MODE AND CONFIGURATION
1800    PRINT "STOPPED FLOW     :1"
        PRINT "CONTINUOUS FLOW  :2"
        PRINT "FLOW INJECTION   :3"
        INPUT "ANALYSIS MODE=";AM
        IF AM=1 THEN PRINT "STOPPED FLOW ANALYSIS":GOTO 1860
        IF AM=2 THEN PRINT "CONTINUOUS FLOW ANALY":GOTO 1860
        IF AM=3 THEN PRINT "FLOW INJECTION ANALY":GOTO 1860
        GOTO 1800
1860    INPUT "CORRECT MODE CHOOSEN (Y/N)";A$
        IF A$="Y" THEN RETURN
        IF A$="N" THEN 1800
        GOTO 1860

REM FLOW SYSTEM CONFIGURATION
1900    ON AM GOTO 1910,1910,1930
1910    POKE STATUS-1,0: REM POS.A
        RETURN
1930    POKE STATUS-1,2: REM POS.B
        RETURN
```

```
REM INITIALIZE CONTROL PARAMETERS
2000    PF=1
        TU=551
        SI=10
        AU=1.460
        PS=100
        PH=550
        PC=450
        TI=9999
        SE=1
        V1=1
        RETURN

REM CONTROL SUBROUTINES
2100    PRINT "START: START BORON ANALYSIS"
        PRINT "PCP  : PRINT CONTROL PARAMETERS"
        PRINT "CCP  : CHANGE CONTROL PARAMETERS"
        PRINT "NEW  : NEW SAMPLE VALVE POSITION"
        PRINT "TTY  : PREPARE FOR TTY TRANSFER"
        PRINT "CONT : CONTINUE BORON ANALYSIS"
        PRINT "CLOSE: CLOSE FILE "
        PRINT "AGAIN: RUN ANALYSIS AGAIN"
        PRINT "STOP : STOP ANALYSIS AND CLOSE FILE"
2150    PRINT " "
        PRINT "[START],[PCP],[CCP],[CLOSE],[NEW]"
        PRINT "   [CONT],[AGAIN],[TTY],[STOP]   "
        INPUT "*";A$
        IF A$="START" THEN GOTO 400
        IF A$="PCP" THEN GOSUB 3000
        IF A$="CCP" THEN GOSUB 3200
        IF A$="NEW" THEN GOSUB 3500
        IF A$="TTY" THEN GOSUB 3300
        IF A$="CONT" THEN 430
        IF A$="CLOSE" THEN CLOSE 1
        IF A$="AGAIN" THEN 200
        IF A$="STOP" THEN GOSUB 2200
        PRINT " "
        PRINT " "
        GOTO 2150
2200    REM STOP SUBROUTINE
        CLOSE 1
        STOP
```

```
REM PRINT CONTROL PARAMETERS
3000    PRINT "TU: TIME UPPER LIMIT (SEC)   :TU=";TU
        PRINT "AU: ABSORBANCE UPPER LIMIT   :AU=";AU
        PRINT "SI: SAMPLING INTERVAL (SEC)  :SI=";SI
        PRINT "PF: PRINT ALL DATA? (TOGGLE) :PF=";PF
        PRINT "PS: SAMPLE PUMP ON (SEC)     :PS=";PS
        PRINT "PH: PUMPS BOTH HALT (SEC)    :PH=";PH
        PRINT "PC: SAMPLE PUMP CEASE (SEC)  :PC=";PC
        PRINT "TI: TIME FOR SAM.INJECT (SEC):TI=";TI
        PRINT "SE: SENSITIVITY SETTING      :SE=";SE
        PRINT "V1: CURRENT SAMPLE POSITION  :V1=";V1
        PRINT "R : RETURN FROM SUBROUTINE"
        RETURN

REM CHANGE CONTROL PARAMETERS
3200    INPUT "%";A$
        IF A$="AU" THEN INPUT "AU=";AU
        IF A$="TU" THEN INPUT "TU=";TU
        IF A$="SI" THEN INPUT "SI=";SI
        IF A$="PF" THEN PF=1-PF:PRINT "PF=";PF
        IF A$="SE" THEN INPUT "SE=";SE
        IF A$="PS" THEN INPUT "PS=";PS
        IF A$="PH" THEN INPUT "PH=";PH
        IF A$="PC" THEN INPUT "PC=";PC
        IF A$="TI" THEN INPUT "TI=";TI
        IF A$="V1" THEN INPUT "V1=";V1
        IF A$="R"  THEN RETURN
        GOTO 3200

REM PREPARE FOR TTY TRANSFER
3300    POKE 42007,12
        POKE 42008,194
        RETURN
REM NEW SAMPLE
3500    PB=PEEK(STATUS-1)
        POKE PULSE1,8+PB
        POKE PULSE2,PB
        PRINT "CURRENT POSITION=";V1
3550    INPUT "DESIRED POSITION=";V2
        IF V2>6 THEN 3550
        V3=6-V1+V2
        IF V3>6 THEN V3=V3-6
        IF V3=6 THEN RETURN
        FOR L8=1 TO V3
        Q=CALL(PULSE)
        NEXT L8
        V1=V2
        PRINT "CURRENT POSITION=";V1
        RETURN

        STOP
```

Assembly Language Subroutines

```
;PROGRAM SUBROUTINES
;storage locations
COUNT  =       $5200          seconds
;
LOBITE =       $5203          A/D low bite
HIBITE =       $5204          A/D hi bite
;
CLOCK1 =       $5205          C1
CLOCK2 =       $5206          C2
CLOCK3 =       $5207          C3
CLOCK4 =       $5208          C4
;
SPKR   =       $9FBD          speaker port
TONE   =       $520A          tone length location
;
PULSE1 =       $520B          pluse port status on
PULSE2 =       $520C          pluse port status off
PULSE3 =       $520D          length of pulse
;
;
;main program subroutines
;initialize
       *=      $200
       JMP     $5000
;pump
       *=      $5000
       LDY     #255
       STY     $9F83          port A output
       STY     $9F82          port B output
       LDX     #03
       STX     $9F81          initialize pumps
       LDX     #00
       STX     $9F80          initialize valves
       STY     $A003          port A output
       INY
       STY     $A002          port B input
       STY     $9F92          port B input
       RTS
       BRK
;clock
       *=      $5020
       LDX     #02
       LDA     #64
       STA     $A00B          ACR-T1 free running-no PB7
       LDA     #78
       STA     $A004          50 m sec countdown
       LDA     #195
       STA     $A005          start clock
       STX     $9F81          start HP pump
```

```
        LDA     #00
        STA     CLOCK1          initialize clock locations
        STA     CLOCK2
        STA     CLOCK3
        STA     CLOCK4
        LDA     #20
        STA     COUNT           20/50 m sec intervals (1 sec)
        LDA     #00
        STA     $A400           load vectors to interrupt
        LDA     #81
        STA     $A401
        LDA     #192
        STA     $A00E           enable T1 & IER control
        CLI
        RTS
        BRK
        BRK
;signal
;A/D converter
        *=      $5080
        LDX     #01
        STX     $A001           select analog in channel
        LDX     #224
        STX     $A00C           raise CB2
        LDX     #192
        STX     $A00C           drop CB2-start conversion
        LDX     #224
        STX     $A00C           raise CB2-A/D read state
        LDX     #09
        LDA     #16
POLL    BIT     $A00D           mask CB1 flag in IFR
        BEQ     POLL            wait for conversion end
        LDA     $A000           read top 8 bits
        STA     HIBITE          store in HIBITE
        STX     $A001           select low bits
        LDA     $A000           read low 4 bits
        STA     LOBITE          store in LOBITE
        RTS
        BRK
        BRK
;clock interrupt
        *=      $5100
        PHA                     accumulator on stack
        LDA     $A004           clear T1 interrupt flag
        DEC     COUNT
        BNE     EXIT            1 sec elasped, no-exit
        LDA     #20
        STA     COUNT           reload seconds
        INC     CLOCK1          increment clock locations
        BNE     EXIT
        INC     CLOCK2
```

```
        BNE     EXIT
        INC     CLOCK3
        BNE     EXIT
        INC     CLOCK4
EXIT    PLA                     accumulator from stack
        RTI
        BRK
        BRK
;beep
        *=      $52A0
        LDA     #255            tone length
        STA     TONE            duration of beep
L8      LDX     #255            pitch value
L6      DEX
        BNE     L6
        STA     SPKR            toggle speaker
        DEC     TONE
        BNE     L8
        RTS
        BRK
        BRK
;6-way valve
;new sample pulse
        *=      $5300
        LDA     PULSE1
        STA     $9F80           raise port status
        LDA     #64
        STA     $9F8B           ACR-T1 free running-no PB7
        STA     $9F8E           enable T1 interrupt
        LDA     #78
        STA     $9F84           50 m sec countdown
        LDA     #195
        STA     $9F85           start clock
        LDA     #10
        STA     PULSE3          10/50 m sec intervals
P1      BIT     $9F8D           wait for interrupt
        BVC     P1
        LDA     $9F84           clear T1 interrupt flag
        DEC     PULSE3
        BNE     P1              total time elasped?
        LDA     PULSE2
        STA     $9F80           lower port status
        LDA     #20
        STA     PULSE3          20/50 m sec intervals
P2      BIT     $9F8D           wait for interrupt
        BVC     P2
        LDA     $9F84           clear T1 interrupt flag
        DEC     PULSE3
        BNE     P2              total time elasped?
        RTS
        BRK
```

Data Calibration and Unknown Determination

```
REM DATA CALIBRATION
REM SET CONSTANTS AND DIM VARIABLES
       DIM A(1000),X(50),Y(50),Z(50),F(50)
       DIM G(50),XU(50),YU(50),XC(50),YC(50)
       LR=360: UR=460
       PI=10
       TM=1000
       PW=60

REM GET DATA FILE
200    INPUT "FILE NAME:";COLOR$
       FILE COLOR$
       I1=0
       IF END #1 THEN 300
240    READ #1;AM
       READ #1;SC
       READ #1;SI
       I=0
250    READ #1;A(I)
       IF A(I)=-999 THEN 500
       I=I+1
       GOTO 250
300    PRINT "END OF FILE REACHED:I=";I
       CLOSE 1
400    INPUT "CONTINUE [C] OR STOP [S]";A$
       IF A$="C" THEN 500
       IF A$="S" THEN STOP
       GOTO 400

REM CONTROL SUBROUTINES
500    PRINT "[PCP],[CCP],[PRT],[TTY],[CAL]"
       PRINT " [NEW],[NEXT],[DATA],[STOP]"
       INPUT "*";A$
       IF A$="PCP" THEN GOSUB 600
       IF A$="CCP" THEN GOSUB 700
       IF A$="PRT" THEN GOSUB 800
       IF A$="TTY" THEN GOSUB 900
       IF A$="CAL" THEN 5000
       IF A$="NEW" THEN 200
       IF A$="NEXT" THEN 240
       IF A$="DATA" THEN ON AM GOTO 1000,2000,3000
       IF A$="STOP" THEN STOP
       GOTO 500
```

```
REM PRINT CONTOL PARAMETERS
600     PRINT "PI: PRINTING INTERVAL(SEC): 1,2,3 :=";PI
        PRINT "SI: SAMPLING INTERVAL(SEC): FIXED :=";SI
        PRINT "LR: LOWER RANGE LIMIT(SEC): 1,2,3 :=";LR
        PRINT "UR: UPPER RANGE LIMIT(SEC): 1,2,3 :=";UR
        PRINT "TM: TIME MEASUREMENT (SEC): 1     :=";TM
        PRINT "PW: PEAK WIDTH       (SEC):     3 :=";PW
        PRINT "R.: RETURN FROM SUBROUTINE"
        RETURN

REM CHANGE CONTROL PARAMETERS
700     INPUT "@";A$
        IF A$="PI" THEN INPUT "PI=";PI
        IF A$="LR" THEN INPUT "LR=";LR
        IF A$="UR" THEN INPUT "UR=";UR
        IF A$="TM" THEN INPUT "TM=";TM
        IF A$="PW" THEN INPUT "PW=";PW
        IF A$="R"  THEN RETURN
        GOTO 700

REM PRINT DATA
800     IF PI=0 THEN RETURN
        PRINT " "
        PRINT "SAMPLE CONCENTRATION=";SC
        PRINT " "
        PRINT " ","TIME(SEC)","ABS(A.U.)"
        PRINT " "
        FOR P=LR/SI TO UR/SI
        PRINT P,P*SI,A(P)
        NEXT P
        PRINT " "
        RETURN

REM PREPARE FOR TTY TRANSFER
900     POKE 42007,12
        POKE 42008,194
        RETURN

REM STOPPED FLOW [1]
1000    FOR I=1 TO TM/SI
        S=A(I)
        NEXT I
        PRINT " "
        PRINT "SAMPLE CONCENTRATION=";SC
        PRINT "TIME(SEC)=";TM;"    ABS(A.U.)=";S
        XC(I1)=SC
        YC(I1)=S
        I1=I1+1
        GOTO 500
```

```
REM CONTINUOUS FLOW [2]
2000    S=0: S2=0
        FOR I=LR/SI TO UR/SI
        S=S+A(I)
        S2=S2+A(I)*A(I)
        NEXT I
        N=(UR-LR)/SI+1
        S=S/N
        S2=(S2-S*S*N)/(N-1)
        IF S2<1E-20 THEN S1=0 ELSE S1=SQR(S2)
        PRINT " "
        PRINT "SAMPLE CONCENTRATION =";SC
        PRINT "MEAN ABS(A.U.)=";S
        PRINT "VARIANCE ABS(A.U.)=";S2
        PRINT "STD. DEV. ABS(A.U.)=";S1
        XC(I1)=SC
        YC(I1)=S
        I1=I1+1
        GOTO 500

REM FLOW INJECTION [3]
3000    S=0: T2=0: T1=0: T4=0: T5=0
        FOR I=LR/SI TO UR/SI
        IF S<A(I) THEN S=A(I): T=I
        NEXT I
        N=0
        FOR I=LR/SI TO (T-PW/SI)
        T1=T1+A(I)
        T2=T2+A(I)*A(I)
        N=N+1
        NEXT I
        N=N-1
        T1=T1/N
        T2=(T2-T1*T1*N)/(N-1)
        IF ABS(T2)<1E-20 THEN T3=0 ELSE T3=SQR(ABS(T2))
        N=0
        FOR I=(T+PW/SI) TO UR/SI
        T4=T4+A(I)
        T5=T5+A(I)*A(I)
        N=N+1
        NEXT I
        N=N-1
        T4=T4/N
        T5=(T5-T4*T4*N)/(N-1)
        IF ABS(T5)<1E-20 THEN T6=0 ELSE T6=SQR(ABS(T5))
        PRINT " "
        PRINT "TIME(SEC)=";T*SI;"PEAK MAXIMUM(A.U.)=";S
        PRINT "PRIOR ABS(A.U.)=";T1
        PRINT "      VAR(A.U.)=";T2
        PRINT "      STD.DEV. =";T3
        PRINT "POST  ABS(A.U.)=";T4
        PRINT "      VAR(A.U.)=";T5
        PRINT "      STD.DEV. =";T6
```

```
        TA=(T1+T4)/2
        S1=S-TA
        PRINT " "
        PRINT "SAMPLE CONCENTRATION =";SC
        PRINT "PEAK HEIGHT (A.U.)=";S1
        XC(I1)=SC
        YC(I1)=S1
        I1=I1+1
        GOTO 500

REM LINEAR REGRESSION CALIBRATION
5000    I1=I1-1: N=0: J=0
        FOR I=1 TO I1
        IF XC(I)<0 THEN 5040
        N=N+1
        X(N)=XC(I)
        Y(N)=YC(I)
5020    NEXT I
        GOTO 5060
5040    J=J+1
        XU(J)=XC(I)
        YU(J)=YC(I)
        GOTO 5020

5060    PRINT "DELETE [D]"
        PRINT "EDIT   [E]"
        PRINT "STOP   [S]"
        PRINT "INSERT [I]"
        PRINT "GO ON  [G]"
        PRINT "NEW    [N]"
5080    PRINT " "
        PRINT " ","CONC(M)","ABS(A.U.)"
        FOR I=1 TO N
        PRINT I,X(I),Y(I)
        NEXT I
5090    PRINT " "
        INPUT "[D],[E],[S],[I],[G],[N]";A$
        IF A$="D" THEN GOSUB 5100
        IF A$="E" THEN GOSUB 5200
        IF A$="S" THEN STOP
        IF A$="I" THEN GOSUB 5300
        IF A$="G" THEN 6000
        IF A$="N" THEN 500
        GOTO 5080

REM DELETE DATA PAIR
5100    INPUT "INDEX LOCATION TO BE DELETED";IX
        FOR K=IX TO N-1
        X(K)=X(K+1)
        Y(K)=Y(K+1)
        NEXT K
        N=N-1
        RETURN
```

```
REM EDIT DATA PAIRS
5200    INPUT "INDEX LOCATION TO BE EDITTED";IX
        PRINT "ENTER NEW (X,Y) PAIR AFTER THE PROMPT"
        INPUT "*";X(IX),Y(IX)
        RETURN

REM INSERT DATA PAIR
5300    INPUT "INDEX LOCATION FOR NEW DATA PAIR";IX
        FOR K=N+1 TO IX+1 STEP -1
        X(K)=X(K-1)
        Y(K)=Y(K-1)
        NEXT K
        N=N+1
        PRINT "ENTER NEW (X,Y) PAIR AFTER THE PROMPT"
        INPUT "*";X(IX),Y(IX)
        RETURN

REM DETERMINE CALIBRATION CURVE
REM COMPUTE SUMS
6000    U1=0: U2=0
        V1=0: V2=0
        W1=0
        FOR I=1 TO N
        U1=U1+X(I)
        U2=U2+X(I)*X(I)
        V1=V1+Y(I)
        V2=V2+Y(I)*Y(I)
        W1=W1+X(I)*Y(I)
        NEXT I
REM PARAMETERS
        D=N*U2-U1*U1
        A0=(V1*U2-W1*U1)/D
        B0=(N*W1-U1*V1)/D
        U=U1/N
        V=V1/N
        A1=U2/D
        B1=N/D
        C1=-U1/D
REM RECOMPUTE
        S0=0
        FOR I=1 TO N
        F(I)=A0+B0*X(I)
        Z(I)=F(I)-Y(I)
        S0=S0+Z(I)*Z(I)
        NEXT I
        S2=S0/(N-2)
        A2=A1*S2
        B2=B1*S2
        C2=C1*S2
        A3=SQR(A2)
        B3=SQR(B2)
        C3=SQR(ABS(C2))
        S3=SQR(S2)
```

```
REM COVARIANCE
      U3=0: V3=0: W3=0
      FOR I=1 TO N
      U3=U3+(X(I)-U)*(X(I)-U)
      V3=V3+(Y(I)-V)*(Y(I)-V)
      W3=W3+(X(I)-U)*(Y(I)-V)
      NEXT I
      U4=U3/(N-1)
      V4=V3/(N-1)
      W4=W3/(N-1)
      R2=W4*W4/(U4*V4)
      R=SQR(R2)
REM OUTPUT
      PRINT " "
      PRINT " "
      PRINT "*******SUMMATIONS*******"
      PRINT "X",U1
      PRINT "X*X",U2
      PRINT "Y",V1
      PRINT "Y*Y",V2
      PRINT "X*Y",W1
      PRINT "*******MEANS,DETERMINANT*******"
      PRINT "X",U
      PRINT "Y",V
      PRINT "DET",D
      PRINT "*******SUM OF SQUARES,VARIANCE,STD DEV*******"
      PRINT "A+BX-Y",S0,S2,S3
      PRINT "XX",U3,U4,SQR(U4)
      PRINT "YY",V3,V4,SQR(V4)
      PRINT "XY",W3,W4,SQR(ABS(W4))
      PRINT "AA"," ",A2,A3
      PRINT "BB"," ",B2,B3
      PRINT "AB"," ",C2,C3
      PRINT "*******REGRESSION COEFFICIENT*******"
      PRINT "R^2",R2
      PRINT "R",SQR(ABS(R))
      PRINT "*******SLOPE, INTERCEPT*******"
      PRINT "B",B0
      PRINT "A",A0
      PRINT "*******DATA*******"
      PRINT "I","X","Y","A+BX","A+BX-Y"
      FOR I=1 TO N
      PRINT I,X(I),Y(I),F(I),Z(I)
      NEXT I
      PRINT " "
      PRINT " "
```

```
REM USE CALIBRATION CURVE TO DETERMINE UNKNOWN
8000    IF J=0 THEN 9000
        FOR SC=1 TO 10
        M=0
        FOR I=1 TO J
        IF XU(I)=-SC THEN M=M+1:G(M)=YU(I)
        NEXT I
        IF M=0 THEN 8800

8060    PRINT " ","UNK #","ABS(A.U.)"
        FOR I=1 TO M
        PRINT I,-SC,G(I)
        NEXT I
        PRINT " "
8080    PRINT "DELETE [D]"
        PRINT "EDIT   [E]"
        PRINT "STOP   [S]"
        PRINT "INSERT [I]"
        PRINT "UNK    [U]"
        PRINT "NEXT   [N]"
8090    PRINT " "
        INPUT "*";A$
        IF A$="D" THEN GOSUB 9500
        IF A$="E" THEN GOSUB 9600
        IF A$="S" THEN STOP
        IF A$="I" THEN GOSUB 9700
        IF A$="U" THEN 8095
        IF A$="N" THEN 8800
        GOTO 8060

REM UNKNOWN DETERMINATION
8095    T=0: T2=0
        PRINT " "
        FOR I=1 TO M
        T=T+G(I)
        T2=T2+G(I)*G(I)
        NEXT I
        T=T/M
        IF M=1 THEN 8100
        T2=(T2-T*T*M)/(M-1)
        IF T2<1E-20 THEN T1=0 ELSE T1=SQR(T2)
8100    E2=S2/(B0*B0)
        E2=E2*(1/M+1/N+(T-V)*(T-V)*N/(B0*B0*D))
        E1=SQR(E2)
        E=(T-A0)/B0
        PRINT "*******DATA FOR UNKNOWN NUMBER ";-SC;"********"
        PRINT "I","Y"
        FOR I=1 TO M
        PRINT I,G(I)
        NEXT I
        PRINT "*******MEAN, VARIANCE, STD DEV OF UNK*******"
        PRINT "MEAN Y",T
```

```
       IF M=1 THEN 8300
       PRINT "VARIANCE Y",T2
       PRINT "STD DEV Y",T1
8300   PRINT "MEAN X",E
       PRINT "VARIANCE X",E2
       PRINT "STD DEV X",E1
       PRINT " "
       PRINT " "
8800   NEXT SC

9000   PRINT "REPEAT [R]"
       PRINT "STOP   [S]"
       PRINT "DESIGN [D]"
9100   PRINT " "
       INPUT "[R],[S],[D]";A$
       IF A$="R" THEN 9200
       IF A$="S" THEN STOP
       IF A$="D" THEN 5080
       GOTO 9100
9200   INPUT "REPEAT CALIBRATION [C] OR UNKNOWN [U]";A$
       IF A$="C" THEN 6000
       IF A$="U" THEN 8000
       GOTO 9200

REM DELETE UNKNON ABS
9500   INPUT "INDEX LOCATION TO BE DELETED";IX
       FOR K=IX TO M-1
       G(K)=G(K+1)
       NEXT K
       M=M-1
       RETURN

REM EDIT UNKNOWN ABS
9600   INPUT "INDEX LOCATION TO BE EDITTED";IX
       PRINT "ENTER NEW UNKNOW ABS AFTER THE PROMPT"
       INPUT "*";G(IX)
       RETURN

REM INSERT UNKNOWN ABS
9700   INPUT "INDEX LOCATION FOR NEW UNK ABS";IX
       FOR K=M+1 TO IX+1 STEP -1
       G(K)=G(K-1)
       NEXT K
       M=M+1
       PRINT "ENTER NEW UNK ABS AFTER THE PROMPT"
       INPUT "*";G(IX)
       RETURN
       STOP
```